UNIVERSIDADE DE BRASÍLIA

FACULDADE DE TECNOLOGIA

DEPARTAMENTO DE ENGENHARIA CIVIL E AMBIENTAL

ANÁLISE DE FLUXO MULTIFÁSICO E MULTIESCALA EM MEIOS BIMODAIS

SYLVIA REGINA CORRÊA BRANT PEREIRA DE JESUS

ORIENTADOR: MANOEL PORFÍRIO CORDÃO NETO

TESE DE DOUTORADO EM GEOTECNIA
PUBLICAÇÃO: G.TD-132/17

BRASÍLIA-DF, MAIO DE 2017.

UNIVERSIDADE DE BRASÍLIA
FACULDADE DE TECNOLOGIA
DEPARTAMENTO DE ENGENHARIA CIVIL E AMBIENTAL

ANÁLISE DE FLUXO MULTIFÁSICO E MULTIESCALA EM MEIOS BIMODAIS

SYLVIA REGINA CORRÊA BRANT PEREIRA DE JESUS

TESE DE DOUTORADO SUBMETIDA AO DEPARTAMENTO DE ENGENHARIA CIVIL E AMBIENTAL DA UNIVERSIDADE DE BRASÍLIA COMO PARTE DOS REQUISITOS NECESSÁRIOS PARA A OBTENÇÃO DO GRAU DE DOUTORA.

APROVADA POR:

_____

Prof. Manoel Porfírio Cordão Neto, DSc (UnB)
(ORIENTADOR)

_____

Prof. Igor Fernandes Gomes, DSc (UFPE)
(EXAMINADOR EXTERNO)

_____

Prof. João Luiz Armelin, DSc (Furnas Centrais Elétricas S/A)
(EXAMINADOR EXTERNO)

_____

Prof. Márcio Muniz de Farias, PhD (UnB)
(EXAMINADOR INTERNO)

Brasília, 26 de maio de 2017.

FICHA CATALOGRÁFICA

JESUS, SYLVIA REGINA CORRÊA BRANT PEREIRA DE
Análise de Fluxo Multifásico e Multiescala em Meios Bimodais [Distrito Federal] 2017
xx, 122 p., 210x297 mm (ENC/FT/UnB, Doutora, Geotecnia, 2017).
Tese de Doutorado - Universidade de Brasília. Faculdade de Tecnologia.
Departamento de Engenharia Civil e Ambiental.

1. Numerical modeling
2. Homogenization
3. Multiscale media
4. Hydraulic behavior
I. ENC/FT/UnB
II. Título (série)

REFERÊNCIA BIBLIOGRÁFICA

JESUS, S.R.C.B.P. de (2017). Análise de Fluxo Multifásico e Multiescala em Meios Bimodais. Tese de Doutorado, Publicação G.TD-132/17, Departamento de Engenharia Civil e Ambiental, Universidade de Brasília, Brasília, DF, 122 p.

CESSÃO DE DIREITOS

NOME DO AUTOR: Sylvia Regina Corrêa Brant Pereira de Jesus.
TÍTULO DA TESE DE DOUTORADO: Análise de Fluxo Multifásico e Multiescala em Meios Bimodais.
GRAU / ANO: Doutora / 2017.

_____

Sylvia Regina Corrêa Brant Pereira de Jesus
SQS 207 Bl. B Apto. 203
70253-020 - Brasília/DF - Brasil

DEDICATÓRIA

Dedico este trabalho à minha família toda,
pelo amor e apoio incondicionais,
mas especialmente ao meu avô,
Sylvio Pereira de Jesus,
por todo incentivo ao estudo,
pela inspiração e pelo exemplo de vida.

AGRADECIMENTOS

Primeiramente, agradeço a Deus, por todas as oportunidades que me foram dadas.

Agradeço infinitamente à minha mãe, Sandra e meu pai, Sylvio. O carinho, a compreensão, a paciência, as contribuições e, acima de qualquer coisa, o amor incondicional de vocês me fez chegar até esse momento. Quando achei que não ia conseguir, vocês me ajudaram a levantar e a seguir em frente. Sem vocês, eu não seria nada. Obrigada por tudo, sempre! Eu amo vocês!

Agradeço à minha irmã, Sabrina. Você tem um papel essencial na minha vida; é a minha melhor amiga, é a pessoa com quem eu sei que posso contar com a compreensão, com o apoio e que tem as palavras certas, nos momentos certos, da maneira. Obrigada por sempre arranjar um tempinho para mim, seja a milhares de quilômetros de distância, seja depois de muitas horas de trabalho e de estudo. Sou extremamente grata por ter você na minha vida. Não estaria aqui hoje se não fosse por você. Obrigada, Bia! Amo você!

Agradeço muito ao meu namorado Gabriel. Sua compreensão, sua contribuição, sua paciência e seu incentivo me ajudaram a continuar e a ter êxito. Você compartilhou comigo o que é a experiência de fazer essa tarefa. Você colaborou, apoiou, compreendeu e me motivou sempre, em todos os momentos. Se cheguei aqui hoje, devo muito a agradecer a você. Amo você!

Agradeço muito à minha amiga Juliana. Obrigada por me escutar, por me aconselhar, por compartilhar suas experiências com seu próprio trabalho, por ouvir e compreender minhas dificuldades e meus sucessos e, por fim, por me animar para a realização deste trabalho. Suas palavras de incentivo sempre foram importantes e, nesse momento, foram essenciais para eu ter força para continuar! Muito obrigada! Amo muito você! Saudades sempre...

Agradeço imensamente ao meu professor orientador Manoel Porfírio Cordão Neto. Professor, obrigada pelas discussões acadêmicas, pelos aconselhamentos profissionais, por compartilhar suas experiências e por me apoiar ao longo deste trabalho. Você foi essencial para o andamento desta pesquisa. Os mais de 10 anos de convivência que temos são motivo de alegria para mim. Tenho carinho e respeito muito grandes por você!

Agradeço ao auxílio do Professor Igor Gomes pela contribuição durante esta pesquisa. Sua disponibilidade e sua disposição em colaborar foram muito importantes ao longo do processo de elaboração deste trabalho.

Agradeço aos professores Márcio, André Assis, Ennio e aos demais professores do Programa de Pós-graduação em Geotecnia da Universidade de Brasília pelo auxílio, pela inspiração e por todo o trabalho ao longo desse percurso.

Agradeço também aos funcionários do programa pelo apoio dado durante a realização desta pesquisa e à CAPES e ao CNPq pelo apoio financeiro.

Agradeço aos amigos e colegas do Programa de Pós-graduação em Geotecnia. Durante o curso e durante a elaboração deste trabalho, suas contribuições foram sempre muito importantes. O carinho e a gentileza de todos vocês auxiliou muito para que eu pudesse cumprir esta jornada. Vocês marcaram muitos momentos divertidos e importantes durante a realização deste trabalho e que sempre me incentivaram para que tudo desse certo. Destaco em especial os amigos Ewerton, Cristina, Robinson, Jaime, Ivonne, Leonardo, Caroline, Camilla e Bruna.

Agradeço à instituição Universidade de Brasília. Acolhedora desde 2005, quando comecei meus estudos de graduação, e de onde saio hoje doutora, sinto-me plenamente realizada ao finalizar este trabalho. Essa instituição representa para mim um marco de vida; representa parte de quem me tornei. Foram na UnB a maior parte dos melhores dias da minha vida até hoje; espero sempre fazer jus aos conhecimentos que consegui adquirir ao longo da minha caminhada dentro desta belíssima instituição de ensino.

Finalmente este trabalho está concluído. Para mim, esse momento representa muito mais que a obtenção de um título, muito mais que subir mais um degrau na escala acadêmica.

O que importa aqui é realmente o percurso que trilhei. Foram momentos de aprendizado de algumas difíceis lições. Muitas vezes, essas pareceram mais do que poderia alcançar. No entanto, tenho a alegria de dizer que superei tudo, superei a mim mesma e, hoje, cá estou, com um pouco mais de maturidade, um pouco mais de conhecimento. Sei que ainda tenho um caminho grande a trilhar; o curso de doutorado, porém, me oportunizou crescimento moral e intelectual inigualáveis.

Foram inúmeras as experiências de vida pelas quais passei ao longo desse tempo; sou grata por todas elas, pois me fizeram tornar-me mais forte. O que importa é o caminho. Não são os fins, são os meios, diferentemente do que alguns pensam.

Àqueles que estiveram ao meu lado, muito obrigada. Obrigada pela paciência, pelo apoio, pelo amor.

Hoje sou mais forte, sou uma pessoa melhor. Não trocaria essa experiência por coisa alguma.

Assim, a pesquisa aqui apresentada é muito mais que um trabalho acadêmico para cumprir requisitos necessários para a obtenção de um título. É a realização de um sonho, é uma realização pessoal, é o fim de uma difícil tarefa, é a superação de diversos obstáculos. Representa uma série de aprendizados inesquecíveis, que levarei para sempre comigo. Fico muito feliz e muito honrada com a oportunidade de apresentar este trabalho.

Muito obrigada a todos que de alguma forma contribuíram para que esse trabalho pudesse ser feito e que compreendem a importância disso.

RESUMO

A presente pesquisa tem por objetivo avaliar a adequabilidade de uma formulação matemática para representação de problema de fluxo bifásico em meios multiescala. A abordagem utilizada prevê um modelo com dupla porosidade considerando duas escalas, macro e micro, para os problemas analisados. É prevista uma função de transferência para a interação entre a microescala e a macroescala do problema, além de um parâmetro de homogeneização para a adaptação da ordem de grandeza das equações de fluxo de cada uma das escalas avaliadas. Estuda-se a aplicabilidade de tal formulação para meios porosos multiescala como solos com distribuição de poros bimodal e como meios fraturados (maciços rochosos, reservatórios de petróleo). A formulação matemática apresentada foi implementada no *software* FlexPDE, um programa para resolução numérica de equações diferenciais parciais por meio do Método dos Elementos Finitos com sistema de malha auto-adaptativa para um domínio e com dados de entrada definidos pelo usuário. Foram realizados testes da formulação matemática implementada com a simulação de ensaios de permeabilidade, de secagem e de molhagem de uma amostra de solo bimodal teórica. Foram utilizados como dados de entrada do modelo numérico informações referentes à distribuição de poros da amostra, advindas de ensaio de porosimetria por intrusão de mercúrio (MIP). A avaliação dos resultados permite concluir que a formulação matemática utilizada é apropriada para a descrição de fluxo em um meio multiescala. A transferência de massa entre as escalas macro e micro dos problemas avaliados é observada e influencia o fluxo total da amostra de solo nos referidos casos. Foi proposta, ainda, uma metodologia para avaliação do grau de saturação de toda a amostra de solo com base nos resultados do grau de saturação de cada escala do meio. Foi possível calcular com precisão o grau de saturação, provando então ser viável a utilização do ensaio de MIP para a estimativa de relação entre grau de saturação e pressão capilar no solo, implicando em definição da curva característica da amostra.

PALAVRAS-CHAVE: meios multiescala, solos bimodais, fluxo bifásico em meios porosos, homogeneização, *upscaling*.

ABSTRACT

In the present research, a mathematical formulation for representation of biphasic flow problem in multiscale media is tested. The dual-porosity approach is chosen for the referred model, and two scales are considered for simulation purposes, macro and microscale, for a generic porous media. A transfer term is part of the flow equations, and it depicts the interaction of fluid mass between the scales of the medium. Also, a homogenization parameter is defined so as to make possible the adaptation of the flow equations in terms of scale. The suitability of the proposed formulation is assessed for multiscale porous media such as soils with a bimodal pore size distribution and fractured rocks. The mathematical model was implemented on the finite element method solver software FlexPDE. This software provides tools for the solution of differential partial equations with an auto-adaptive generation mesh system for domain of study, problem conditions and input data defined by the user. The formulation was tested with the simulation of permeability tests and drying and wetting trajectory simulations for a theoretical bimodal soil sample. The input data used for the numerical simulations was retrieved from mercury intrusion porosimetry test results. From the results, it is possible to infer that the proposed mathematical model, with the transfer term and homogenization parameter as presented, was appropriate for the description of the flow conditions of a multiscale medium. The mass transfer between the macro and the microscale is proven, and also its influence on the overall hydraulic behavior of the medium is verified. Furthermore, a methodology for determination of the degree of saturation of the entire soil sample based on the results achieved for each scale of the medium is suggested. The accuracy of the results is significant, proving that using the MIP test results as input data for the numerical model is possible. The estimation of the degree of saturation of the entire sample and capillary pressure values is made, and the soil-water characteristic curve of the sample could then be defined via numerical simulation.

KEYWORDS: multiscale media, bimodal soils, biphasic flow in porous media, homogenization, upscaling.

CONTENTS

LIST OF FIGURES

LIST OF TABLES

LIST OF SYMBOLS AND ABBREVIATIONS

a_i	-	Air entry value for the *i* part of the domain.
a_i, m_i, n_i	-	Calibration parameters of the soil-water characteristic curve.
BBM	-	Barcelona Basic Model.
BExM	-	Barcelona Extended Model.
b_α	-	Transfer parameter of the α - fluid phase.
D	-	Diameter of the pores that are intruded with this value of pressure *p*.
DFM	-	Discrete fracture model.
e	-	Total void ratio.
E	-	Elasticity modulus.
E_m^v	-	Microscale volumetric strain for a two-dimensional analysis.
E_{xM}	-	*x*-component of strain.
E_{yM}	-	*y*-component of strain.
E_M^v	-	Macroscale volumetric strain for a two-dimensional analysis.
E_i^v	-	Volumetric strain of *i* part of the domain.
e_{0i}	-	Initial void ratio.
e_{nw}	-	Non-wetting fluid void ratio.
e_w	-	Wetting fluid void ratio.
e_i	-	Void ratio of the *i* part of the domain.
e_M	-	Void ratio parameter of the macroscale.
e_m	-	Void ratio parameter of the microscale.
FDM	-	Finite differences method.
FEM	-	Finite element method.
g	-	Gravity.
G	-	Shear modulus.
$\vec{g}$	-	Gravity vector.
h_α	-	Hydraulic head of the α - fluid.
$h_{\alpha i}$	-	Hydraulic head of the α - fluid phase of the *i* part of the domain.
$\{J\}$	-	Dubbed hydraulic gradient.
i	-	Part of the domain (m is used for microscale; M is used for macroscale)
K	-	Intrinsic permeability of the medium.
$[k]$	-	Hydraulic conductivity tensor.
K_i	-	Intrinsic permeability of the *i* part of the domain.
K_m	-	Intrinsic permeability of the microscale.
K_M	-	Intrinsic permeability of the macroscale.
$k_{r\alpha i}$	-	Relative permeability of the α - fluid phase of the *i* part of the domain.
k_{wt}	-	Equivalent hydraulic conductivity.
$k_{\alpha i}$	-	Hydraulic conductivity of the α - fluid phase (w stands for wetting fluid and nw, for non-wetting fluid) of the *i* part of the domain.
l	-	Size of the side of the cell (local, microscale).
L	-	Size of the side of the entire domain of study (global, macroscale).
m	-	Microscale – micropores or rock matrix.

M	-	Macroscale – macropores or fracture network.
MIP	-	Mercury intrusion porosimetry.
MSR	-	Multiple subregion method.
$m^{v}_{\alpha i}$	-	Coefficient of volume compressibility of the α - fluid phase of *i* part of the domain.
n_e	-	Effective porosity of medium.
n_i	-	Inclination of the curve for the *i* part of the domain.
nw	-	Non-wetting fluid.
p	-	Absolute value of pressure of the non-wetting fluid.
p_c	-	Capillary pressure within the sample.
p_{ci}	-	Capillary pressure of the *i* part of the domain
p_{cM}	-	Capillary pressure of the macroscale.
p_{cm}	-	Capillary pressure of the microscale.
P_{nwi}	-	Pressure of the non-wetting fluid phase of the *i* part of the domain.
PSD	-	Pore size distribution density curve.
p_{wi}	-	Pressure of the wetting fluid phase of the *i* part of the domain.
p_{wM}	-	Wetting fluid pressure of the macroscale.
p_{wm}	-	Wetting fluid pressure of the microscale.
p_{α}	-	Pressure of the α fluid.
$p_{\alpha i}$	-	Pressure of the α - fluid phase of the *i* part of the domain.
$p_{\alpha M}$	-	Pressure of the α - fluid phase acting on the microscale.
$p_{\alpha m}$	-	Pressure of the α - fluid phase acting on the microscale.
$\overline{p}$	-	Average value of fluid pressure acting on the porous medium.
$\frac{p_{\alpha}}{\rho_{\alpha} g}$	-	Piezometric head.
q_{wc}	-	Total fluid flow rate of region 2.
q_{wm}	-	Microscale fluid flow.
q_{wM}	-	Macroscale fluid flow.
q_{wt}	-	Total fluid flow rate of region 1.
$\{q\}$	-	Specific discharge vector.
r	-	Micropore radius average value.
R	-	Macropore radius average value.
r_i	-	Radius of the pore of the i part of the domain.
s	-	Geometric parameter of the transfer term.
S_{nwi}	-	Degree of saturation of the non-wetting fluid of the i part of the domain.
S_{nwM}	-	Degree of saturation of the non-wetting fluid in the macroscale.
S_{nwm}	-	Degree of saturation of the non-wetting fluid in the microscale.
S_{reswi}	-	Residual degree of saturation of the wetting phase in the *i* part of the domain.
S_w	-	Degree of saturation of the wetting fluid phase of the entire domain.
SWCC	-	Soil-water characteristic curve.
S_{wi}	-	Degree of saturation of the wetting fluid of the i part of the domain.
S_{wM}	-	Degree of saturation of the wetting fluid of the macroscale.
S_{wm}	-	Degree of saturation of the wetting fluid in the macroscale.

S_α	-	Saturation degree of the α fluid.
$S_{\alpha i}$	-	Degree of saturation of the α - fluid phase of the i part of the domain.
u_M, v_M	-	Displacements in the x- and the y-direction, respectively (using the macroscale as reference for the analysis).
V	-	Total volume of the medium.
V_e	-	Effective volume.
$\{v_e\}$	-	Effective velocity vector.
$V_{intrusion}$	-	Volume of the non-wetting fluid that intruded the sample during the mip procedure.
V_{solids}	-	Volume of the solids of the studied sample.
$\vec{v}_\alpha$	-	Velocity of the α - fluid phase.
$\vec{v}_{\alpha i}$	-	Velocity of the α - fluid phase of the *i* part of the domain.
w	-	Wetting fluid.
w_M	-	Volume fraction average weight parameter of the macroscale.
w_m	-	Volume fraction average weight parameter of the microscale.
WRC	-	Water retention curve.
x_M	-	Coordinates for the global scale.
x_m	-	Coordinates for the local scale.
y	-	Elevation.
z	-	Altimetric head.
Δe_i	-	Void ratio variation rate.
Δh_{wi}	-	Variation of the hydraulic head for the interval of analysis within the domain.
Ω	-	Cell volume.
Ω_m	-	Matrix block volume.
Ω_M	-	Surrounding fracture volume.
α	-	Fluid phase.
$\delta\Omega_m$	-	Smooth internal boundary piece.
ε	-	Homogenization parameter.
ϕ	-	Porosity of the medium.
ϕ_i	-	Porosity of the *i* part of the domain.
ϕ_M	-	Porosity of the macroscale.
ϕ_m	-	Porosity of the microscale.
γ	-	Specific weight of the soil
γ_α	-	Specific weight of the α - fluid phase.
$\gamma_{x_M y_M}$	-	Distortion component of strain.
λ, 2μ	-	Lamé coefficients.
μ_w	-	Water viscosity.
μ_α	-	Viscosity of the α - fluid phase.
θ_{nw}	-	Contact angle between the porous medium and the non-wetting fluid.
ρ_w	-	Water specific mass.
ρ_α	-	Specific mass of the α fluid.
σ_{nw}	-	Superficial tension of the non-wetting fluid.
$\sigma'_{x_M}, \sigma'_{y_M}$	-	Effective stress components in the indicated directions (using the

		macroscale as reference for the analysis).
$\sigma_{x_M}, \sigma_{y_M}, \tau_{x_M y_M}$	-	Total stress components in the indicated directions (using the macroscale as reference for the analysis).
ν	-	Poisson's ratio.
$\vec{\nabla}$	-	Differentiation operator for the global, macro scale.
$\vec{\nabla}_s$	-	Differentiation operator for the small, local scale.

1 INTRODUCTION

1.1 THEME CONTEXTUALIZATION AND MOTIVATION

The soil formation processes a porous medium undergoes are regulated by different factors, being the climate conditions the most significant of them. The temperature and the pluviometric changes that a certain area are subjected to reflect greatly on the assembly of the particles that composes the soils.

Specifically for tropical climate regions, these considerations must be evaluated when studies of the behavior of the soil are made, so as to take into account the effects that the pedogenetic process has over the porous formation overall structural arrangement.

Tropical soils usually present a bimodal structure, with macropores and micropores. This unique type of assembly of particles affects the hydraulic behavior of these soils. Therewith, the models designed for reproduction of behavior of this specific sort of soil should be able to mathematically incorporate the multimodal distribution of pores that is characteristic of them.

Models with this kind of approach are known as multiscale mathematical models and they can be used not only for the behavior analysis of bimodal soil samples, but also for the assessment of hydraulic behavior of fractured media, such as rock masses.

If one takes into account that a fractured medium presents a dual-porosity, dual-permeability arrangement, with two scales forming it – the macroscale representing the fractures of the medium and the microscale representing the rock matrix, the multiscale numerical model can easily be adapted for the analysis of flow in fractured media.

The study of multiscale numerical models is revealed to be a field of great importance in the assessment of hydraulic behavior in Geotechnics. It is specifically important for regions with porous formations that are notoriously known for their dual-porosity flow conditions, and reproducing this type of behavior with numerical simulation is significant for the enhancement of flow models for porous media.

1.2 RESEARCH OBJECTIVES

The main objective of this research is to define an analysis methodology for the simulation of the hydraulic behavior of multiscale porous media. In the present research, the

focus resides on the evaluation of fluid flow within bimodal soil samples. It is highlighted that the model proposed in the present research is appropriate for application in any type of multiscale porous medium, fractured rocks included. For that purpose, a mathematical model for the representation of the hydraulic behavior of a two-scale porous medium is presented. Some tests are performed in order to verify the validity of the proposed model, as well as the accuracy in terms of reproducing the particular of the two-scale structure of the studied samples.

Considering the latter, the specific objectives of this research are:

- To evaluate the accuracy of the model chosen for flow simulation;
- To verify the effects of the bimodal soil structure in terms of flow prediction;
- To perform analyses of two-phase flow (wetting and non-wetting) in order to verify the implication the bimodal soil structure may cause on the overall hydraulic behavior of the medium;
- To perform sensitivity analyses of the hydraulic parameters for the referred flow simulations.

1.3 OUTLINE OF THE THESIS

This doctorate thesis is divided in 7 chapters, with the outline as follows.

In Chapter 1, the theme of the research is presented with a brief contextualization and motivation of the study. The research objectives are based on this and are also presented in the mentioned chapter.

In Chapter 2, some concepts related to the structure of soils and rocks are presented. Tropical soils are addressed with an overview of their formation process and the implications it has on its particle arrangement, characterizing their bimodal structure. Then, rock masses are presented, with a focus on petroleum reservoir rocks. The importance of flow studies in reservoirs is highlighted in terms of economic feasibility and behavior prediction of the formations on field. For that reason, the multiscale structure of the reservoir rock is presented with a brief discussion on the petroleum reservoir formation process, followed by a description of the shale reservoir main characteristics and considerations regarding petroleum production in fractured formations.

The Chapter 3 is focused on the definition of flow models for porous media. The different approaches one can address to the description of hydraulic behavior of soils and

rock masses are presented, distinguishing the dual continuum models and pointing out their relevance for representation of flow in multiscale media.

The research methodology is presented in Chapter 4, with detailing of the steps for the development of the presented research and the presentation of the numerical tool that will be used for the simulations during the research.

The mathematical model for flow in multiscale media for the analyses proposed for this research is presented in Chapter 5. The chosen model approach for this research is the representation of two scales in the flow problem: macro and microscale. The equations are established following this premise and an upscaling procedure is then performed so as to make the mathematical model solution possible. An adapted homogenization procedure is then shown, with the introduction of a transfer term between macro and microscale that enables coupling between the scales. This formulation is presented in two different forms: one specific for the flow problem, and one for the consolidation problem.

In Chapter 6, the results of the simulations proposed for the development of the research are presented and discussed. Following the methodology steps, the main aspects that are studied related to the hydraulic behavior of bimodal soils and fractured media are verified. Sets of simulations for reproducing permeability tests, drying and wetting trajectories tests are made. At first, the simulations are made with the purpose of validating the numerical model and verifying its accuracy. For that reason, theoretical data is used in this stage of the research. Then, the tests are made with data of real samples for comparison purposes. At this stage, the goal is to verify the possibility of reproduction of the two-scale porous media hydraulic behavior with the proposed numerical model.

The conclusions made from the main results achieved in this research are presented in Chapter 7. Also, a discussion over the topics reported throughout this thesis is proposed. Based on them, some suggestions for further research are proposed.

2 STRUCTURE OF SOILS AND ROCKS: MULTISCALE APPROACH

2.1 BASIC STRUCTURE OF NATURAL POROUS MEDIA

The analysis of behavior of natural porous media is a broad field of study and it requires knowledge and expertise related to their structure. Details of the formation process of rocks and soils could be important so as to justify the cause of the characteristic behavior of different geological formations.

In that matter, some basic concepts regarding soils and rocks are presented in this section for description of the main aspects reported in this research project.

Rocks can be defined as aggregates of minerals consolidated into masses of different sizes and shapes. The minerals found in this type of geologic formation depend on the availability of chemical compounds at the time of its formation process. Different types of rocks can be differentiated not only by the type of minerals they are constituted, but also by their arrangement. This could change depending on the levels of pressure and temperature they are subjected to during the rock formation process (Beavis, 1985). These definitions are important because they could determine the way each rock presents itself and affect significantly the mechanical and the hydraulic behavior of this medium.

The igneous rocks are formed due to the cooling and solidification processes of magma. The sedimentary rocks are formed with the deposition and cementation of material, mostly minerals from the alteration process of other rocks (weathering followed by erosion) and organic matter. The metamorphic rocks are formed with the transformation of existing rocks of any type due to temperature and/or pressure changes that could cause modification in the type and the arrangement of the minerals (Mitchell & Soga, 2005).

The petroleum reservoirs are sedimentary rocks. The study of their hydraulic behavior may be conditioned to its formation process, given the fracture network structure that might have been established within. The hydraulic behavior of this type of geological formation is one of the topics of interest of the present research and it is discussed in Section 2.3.

After going through weathering processes, the rock then is altered to a point that it can be assumed, for engineering studies purposes, as soil. Soil is then defined as a constant-evolving porous medium, formed due to pedogenetic processes. The formation can change its characteristics drastically and significantly differ from its rock of origin. The minerals suffer

physical and chemical transformation over time with the action of factors such as climate, topography, and living organisms (Beavis, 1985).

The climate is one of the most important factors of soil formation specifically for tropical soils. The pluviometric trends and the temperature fluctuation throughout time define characteristics of porosity and permeability particular to this type of soil. Some of these soils tend to present their porosity pattern with a bimodal structure, with a remarkable discontinuity in the distribution of the sizes of its pores. In general, when analyzing the distribution of pores of tropical soils, two distinct sizes of pores are dominant over the sample: the macropores and the micropores.

This type of structure could influence the mechanical and the hydraulic behavior of the porous medium. Therewith, behavior prediction analyses should be performed with different approaches so as to reproduce this peculiarity of the soil (Mitchell & Soga, 2005; Bagherieh et al., 2009; Choo et al., 2016). Bimodal soils and its particularities regarding hydraulic behavior are presented in Section 2.2.

The overall structure of porous media, and the variation of their features, implies on specific studies so as to represent their behavior. When specifically addressing the hydraulic behavior of porous media, there are several models which can be used for depicting what can be observed on the field (Bagherieh et al., 2009; Choo et al., 2016).

The study of the multiscale approach is used in the present research as an alternative for reproduction of hydraulic phenomena observed in both bimodal pore size distribution soils and fractured reservoirs.

2.2 BIMODAL SOILS

As already mentioned, the weathering processes rocks go through gradually transform them into soil. Soil is then defined as being a naturally-formed porous medium. It can go through various processes throughout geological time; nevertheless, its formation process follows the premises already discussed. The soil is composed by a solid skeleton of grains or particles (minerals) with an arrangement that characterizes the porous structure.

The soil voids or pores are filled with fluids, gases and liquids; the studies of behavior prediction of natural porous media are made for verification of the equilibrium and conservation conditions of the solid skeleton and the fluids within the pores (Beavis, 1985).

One of the areas that are explored is the study of tropical soils. Their formation process and all changes they are subjected overtime are extremely specific and this makes the physical behavior of this type of soil quite distinct. Tropical soils are structured soils: the arrangement of the soil particles is organized into, at least, two scales – macro and microstructure – and this influences significantly the physical behavior of the soil (Mitchell & Soga, 2005; Romero & Simms, 2008; Bagherieh et al., 2009; Choo et al., 2016).

Considering the specificities of the compositional and structural characteristics of tropical soils, it is paramount that the main parameters used for the definition of the arrangement conditions of a soil be described.

The soil structure can be defined as the spatial arrangement of the solid particles that compose the soil including the implication the shape, the size, the orientation, the degree of cementation, and the presence of interstitial fluids of the particles may inflict on the overall arrangement of the sample.

When considering the structure of a tropical soil, the main feature pointed out as important for behavior prediction analyses is the size of the pores or voids of the porous medium. This specific characteristic helps the evaluation of the macro and microstructure of soil, making it possible to more appropriately estimate mechanical and hydraulic behavior of the porous medium and, therefore, effort has been made so as to define the distribution of size of the pores of soil sample (Mitchell & Soga, 2005; Romero & Simms, 2008).

Delage & Lefebvre (1984) established the following definition for the soil structure:

- Aggregates: a pack of soil grains or particles; when referring to clays, the soil aggregate is a pack of the minerals that form the solid structure of the soil;
- Interaggregate pores: the void between one aggregate and other; the interaggregate pores are the macropores of the sample;
- Intra-aggregate pores: the void within an aggregate; the intra-aggregate pores are the micropores of the sample.

These definitions help depicting the structure of the soil and better understanding its physical behavior. Many constitutive models are related to pore size and follow it as basis for definition of the premises of the model. The macropore and micropore structural arrangement of some soils may significantly affect the overall behavior of the soil and, therefore, it should be taken into account for an accurate representation of this type of porous medium.

The Barcelona Basic Model – BBM (Alonso et al., 1990) and Barcelona Extended Model – BexM (Alonso et al., 1999) are examples of this. Specifically in BExM, the approach chosen by the authors validates the importance of considering the macro and microstructure of the soil in order to improve the accuracy of the representation of the effects of the soil particle arrangement in the overall physical behavior of the porous medium. Alonso et al. (1999) highlight the significant effect the microstructure inflicts on the macrostructure of the soil samples.

Considering all mentioned, the study of tropical soils requires the measurement of the size of the pores. It is a way of evaluating the type of structural arrangement the soil presents and adapting the models used for representation of its physical behavior. Hence, the study of the soil can be performed with the information related to its microstructure.

There are several techniques that can be used for microstructural analysis of a porous medium. Granulometric distribution curve, water retention curve (WRC), Mercury Intrusion Porosimetry (MIP) are some examples.

The procedure of the MIP test implies on applying a pressurized volume of mercury so as it can intrude the pores of the sample. During the test, the collected data are the pressure of intrusion of the mercury and the volume of mercury intruded for this pressure value. With these data, it is possible to calculate all parameters needed for establishing the relationship between the size of the pores and the permeability of the sample.

The Mercury Intrusion Porosimetry (MIP) technique is cited by Zhang et al. (2006) as one of the alternatives that are the most interesting for studying the microstructure of the soil. The technique simplicity in applying is allied to results that allow a quantitative interpretation of the arrangement of the soil particles.

It is also important to highlight that the MIP technique has been largely employed in research related to the determination of the structure of soils (Delage & Lefebvre, 1984; Prapaharan et al., 1985; Griffiths & Joshi, 1989; Delage et al., 1996; Romero, 1999; Penumadu & Dean, 2000; Simms & Yanful, 2001; Buenfil, 2007; Mascarenha, 2008; Romero & Simms, 2008; Koliji et al., 2010; Sivakumar et al., 2010; Alonso et al., 2011; Alonso et al., 2013) and also as input data for the definition of the Water Retention Curve (Prapaharan et al., 1985; Kosugi & Hopmans, 1998; Romero, 1999; Simms & Yanful, 2002; Mascarenha, 2008; Romero & Simms, 2008; Silva, 2009; Romero et al., 2011; Borges, 2014).

The data collected with the application of the MIP technique treated for the calculation of the diameter of the pores of the sample. This can be mathematically represented as shown

with Washburn's equation (Diamond, 1970; Griffiths & Joshi, 1989), as shown in Equation (2.1) (it is mentioned later in Sections 6.1.1 and 6.2.1).

$$p_c = -\frac{4\sigma_{nw}\cos(\theta_{nw})}{D} \tag{2.1}$$

where: p_c is the absolute value of pressure of the non-wetting fluid (mercury in the case of MIP), σ_{nw} is the superficial tension of the non-wetting fluid (0,484 N/m for mercury), θ_{nw} is the contact angle between the porous medium and the non-wetting fluid (values vary from 139° to 147° for mercury - the value of θ_{nw} used in this research is 140°) and D is the diameter of the pores that are intruded with this value of pressure p_c.

It is also possible to relate the results of the MIP test with the Water Retention Curve for the soil sample. Delage & Lefebvre (1984) describe a procedure for this and it has been chosen for the analyses proposed in the present research. It is thoroughly explained and detailed when results of this research are presented in Section 6.2.1.1.

There are some disadvantages of the MIP technique that are discussed by Romero & Simms (2008) and also mentioned by Simms & Yanful (2004). They are mostly related to difficulties of the operator that performs the tests or to limitations of the technique itself:

- The limitation of pressure of the equipment may represent a difficulty for penetration of the intrusion fluid in the smallest pores of the sample;
- The minimum pressure value for functioning of the equipment may limit the precision of the measurements of the quantity of macropores;
- Isolated pores (surrounded by impermeable solid particles) usually are not intruded by the pressurized fluid and, therefore, are not measured as part of the voids of the sample;
- The quantity of micropores can be overestimated due to a lag in the intrusion of fluid in the small pores: if the micropores are connected to small pores, it takes longer for the firsts to be intruded;
- There are difficulties in the preparation of the samples;
- The pressure of the intrusion fluid may affect the soil structure.

When specifically addressing bimodal structured soils, as is the case of the soil samples studied in the present research, one must take into account the importance of evaluation of the graphic representation of the distribution of the size of the pores. This curve is known as Pore

Size Distribution Density and it represents the quantity of pores related to different diameters for a soil sample. A Pore Size Distribution Density curve (PSD) for a bimodal soil presents itself as depicted in Figure 2.1. The *x*-axis corresponds to the size of the diameter of the pores, measured in micrometers, and the *y*-axis corresponds to the PSD parameter.

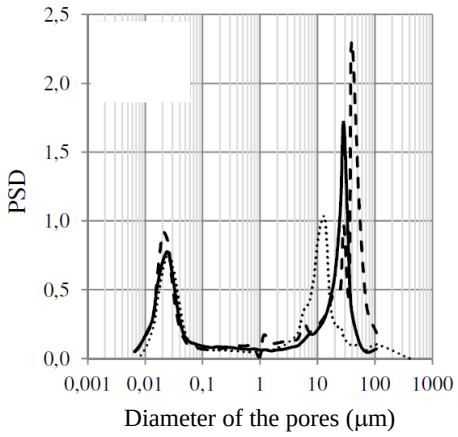

Figure 2.1 - PSD curves of Brasília porous clay in different states (Borges, 2014).

The PSD parameter is calculated as shown in Equation (2.2):

$$PSD = \frac{\Delta e_{nw}}{\Delta \log D_i} \tag{2.2}$$

where: e_{nw} is the void ratio parameter of the sample related to the non-wetting (intruded) volume (non-wetting fluid void ratio) and D is the diameter of the pore of the *i* part of the domain (making reference to the macroscale - subscript *M* - and microscale - subscript *m*).

When observing the format of the pore size density distribution curve (Figure 2.1), the bimodal structure of the referred soil sample is clearly seen. The soil studied in this research (Section 6.2) has had its samples collected in the same region of study of Borges (2014) and, therefore, it presents the same structural characteristics.

The results of the MIP test are used for description of the pore distribution of the sample, and, consequently, its microstructure. It could be interesting to employ these data for definition of other parameters that could help in the description of the hydraulic behavior of bimodal soil samples. The void ratio should then be addressed, given it is related to the arrangement of the solid particles and volume of the pores of the sample. It is a parameter that can directly correlate the microstructure to the overall hydraulic behavior of the medium.

With that, the relationship between the non-wetting fluid and the wetting fluid void ratio is established so as to define the total void ratio value as shown in Equation (2.3):

$$e_{nw} + e_w = e \tag{2.3}$$

where: e_w is the wetting fluid void ratio - the void ratio parameter related to the wetting fluid volume within the entire sample, e_{nw} is the non-wetting fluid void ratio - the void ratio parameter related to the non-wetting fluid volume within the entire sample and *e* is the total void ratio of the sample.

Also, the determination of the non-wetting fluid void ratio can be made with the results of the MIP test. This parameter could be employed for later definition of the quantity of wetting fluid within the sample. The non-wetting fluid void ratio is determined as shown in Equation (2.4):

$$e_{nw} = \frac{V_{\text{int}rusion}}{V_{solids}} \tag{2.4}$$

where: e_{nw} is the void ratio parameter of the sample related to the non-wetting fluid volume (non-wetting fluid void ratio), $V_{\text{int}rusion}$ is the volume of the non-wetting fluid that intruded the sample during the MIP procedure and V_{solids} is the volume of the solids of the studied sample.

In addition, the calculation of the quantity of wetting fluid within the voids of the sample can be related to the values of the wetting void ratio and the capillary pressure within the sample, as shown in Equation (2.5):

$$e_w = \frac{e_M}{\left\{1+\left[\frac{p_c}{a_M}\right]^{n_M}\right\}^{m_M}} + \frac{e_m}{\left\{1+\left[\frac{p_c}{a_m}\right]^{n_m}\right\}^{m_m}} \tag{2.5}$$

where: p_c is the capillary pressure within the sample, a_i is the air entry value for the *i* part of the domain (*i*=*m*, *M*; *m* is used for microscale; *M* is used for macroscale) and n_i is the inclination of the curve for the *i* part of the domain.

The parameter m_i can be calculated as shown in Equation (2.6):

$$m_i = 1 - \frac{1}{n_i} \tag{2.6}$$

where: n_i is the inclination of the curve for the *i* part of the domain.

The void ratio parameter can be defined in terms of the two scales the hydraulic behavior of the medium is described. This is shown in Equation (2.7):

$$e_M = e - e_m \tag{2.7}$$

where: e_M is the void ratio parameter of the macroscale, e is the total void ratio parameter of the sample (total void ratio) and e_m is the void ratio parameter of the microscale.

Then, the degree of saturation of the soil sample can be determined with the relationship established between the void ratio values as expressed in Equation (2.8):

$$S_w = \frac{e_w}{e} \tag{2.8}$$

where: e_w is the wetting fluid void ratio and e is the total void ratio parameter of the sample (total void ratio) and e_m is the void ratio parameter of the microscale.

Finally, considering there is an association established between the size of the pores and its distribution, and the permeability of the soil sample, this should be discussed so as to accurately define all parameters that interfere in the hydraulic behavior of the bimodal medium. With that, García-Bengochea et al. (1979) suggest that the hydraulic conductivity of the medium can be calculated based on the premises as shown in Equation (2.9):

$$k_{\alpha i} = K_i \frac{\gamma_\alpha}{\mu_\alpha} = \frac{\gamma_\alpha}{\mu_\alpha}\left[\phi_i \frac{1}{8}\sum_1^i f\left(r_i\right) r_i^2\right] \tag{2.9}$$

where: $k_{\alpha i}$ is the hydraulic conductivity of the α - fluid phase (*w* stands for wetting fluid and *nw*, for non-wetting fluid) of the *i* part of the domain (*m* stands for microscale and *M*, macroscale), K_i is the intrinsic permeability of the *i* part of the domain, γ_α is the specific

weight and μ_α is the viscosity of the α-fluid phase, ϕ_i is the porosity of the *i* part of the domain and r_i is the radius of the pore of the *i* part of the domain.

The $f(r_i)$ term of Equation (2.9) is a function that mathematically represents the distribution of the size of the pores of the sample. This function is assumed as the pore size distribution density (PSD), already shown in Equation (2.2).

The $\sum_1^i f(r_i) r_i^2$ term of Equation (2.9) statistically represents the second moment of the referred data (size of the pores of the sample).

The porosity of soil sample can be calculated based on the values of void ratio as depicted in Equation (2.10):

$$\phi_i = \frac{e_i}{1+e_i} \tag{2.10}$$

where: e_i is the void ratio of the *i* part of the domain.

As to proceed to the specific calculation of the intrinsic permeability of each scale for the soil sample, only part of the terms that define Equation (2.9) are considered for calculation purposes. This rearrangement of Equation (2.9) is shown in Equation (2.11).

$$K_i = \phi_i \frac{1}{8} \sum_1^i f(r_i) r_i^2 \tag{2.11}$$

where: K_i is the intrinsic permeability of the *i* part of the domain, ϕ_i is the porosity of the *i* part of the domain and r_i is the radius of the pore of the *i* part of the domain.

Besides from the hydraulic implication the microstructure has on the overall hydraulic behavior of bimodal soils, Borges (2014) also reports the importance evaluating the microstructural mechanical behavior of the soil for the verification of the effects of void ratio changes and distortions of the soil samples. Given there is a degree of influence the microstructure exerts on the macrostructure of the soil, this may help better understanding the macroscopic mechanical and hydraulic behavior of the medium.

The study of the microstructure of the soil is extremely relevant for a more comprehensive approach of the occurring physical phenomena of the porous medium. The microstructure of the soil may influence significantly the overall behavior of bimodal soils and, therefore, the techniques employed for the definition of pore size and pore size distribution are essential for an accurate approach in the models designed for this type of soil.

Specifically referring to the importance of the microscale influence on the overall behavior of the medium, it should be pointed out that the multiscale approach involves the definition of a model for the mathematical description of the each scale of the medium with a different equation. Given the hydraulic behavior of the medium comprises both scales and their respective phenomena simultaneously, it is essential that the mathematical model addresses this particularity.

Also, a coupling term is used for the interaction between scales, referred to as a transfer term; this consideration leads to the verification of influence of the hydraulic behavior of the microscale on the macroscale and on the overall flow conditions of the porous medium.

Different mathematical model approaches are presented in Chapter 3, and the model specifically chosen for the study proposed in the present research is presented in Chapter 5.

2.3 FRACTURED ROCKS

The geologic formation process of rocks is mainly affected by pressure and temperature conditions and availability of minerals. This combination of factors implies on specific features that may influence the mechanical and hydraulic behavior of this porous medium.

The heterogeneity of the rocks due to its formation process reflects on their features; most rocks have natural fractures. A natural fracture is a macroscopic planar discontinuity in a rock due to its deformation or to physical diagenetic processes. The natural fractures could influence the hydraulic behavior of the rock, given their porosity and permeability characteristics. In some cases, the natural fractures could be a preferential path for fluid flow within this porous medium. Therewith, it is important to evaluate their influence on the physical behavior of the rock (Salimi, 2010).

In terms of fluid flow, it can be established that this type of geologic formation presents dual porosity, with distinct types of flow behavior in each of them, one referring to the rock matrix, another referring to the fractures (Rosa et al., 2006). The natural fractures represent, in terms of hydraulic behavior, a flow network already established in the rock formation.

Natural fractures are identified with different investigation methods depending on the scale of the fracture. Large-scale fractures are detected with seismic methods, whereas small-scale fractures are identified in wellbores extracted on field (Borbiaux et al., 2005). This classification of fractures is shown in a fractured sedimentary rock mass in Figure 2.2.

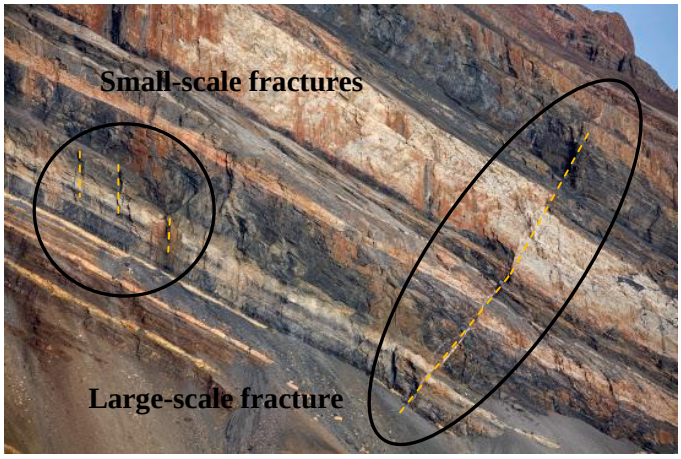

Figure 2.2 - Fractured rock mass (with sedimentary geological formation).

In many cases, the model of geological fracture network is reproduced based only on the data retrieved from investigation. Nevertheless, interpolation and extrapolation of data are required in order to cover areas where there is less information (Borbiaux et al., 2005).

Large-scale fractures are usually easier to be identified. Small-scale fractures are often more difficult to be observed due to their geometric characteristics. Despite of any difficulties, a model with great accuracy should include both types of fractures, characterizing a multi-scale fracture network. Considering the complexity regarding reproduction of both scales of fracturing of the medium should influence significantly fluid flow simulation.

This characterizes the rocks as naturally fractured porous media, with multiscale features regarding its hydraulic behavior. Simultaneously, any transformation processes the rocks may undergo can alter its initial condition and affect the hydraulic behavior of the medium. The deformation the rock may suffer affects its solid matrix and, therefore, the porosity and permeability patterns of the medium.

This subject is specifically addressed by Arson & Pereira (2013) and Pereira & Arson (2013). These authors show that damaged porous rocks present PSD curves with two distinct modes, as represented in Figure 2.3. The format of these curves resembles the PSD curve of bimodal soils (Figure 2.1). This could justify the fact that a multiscale hydraulic model is appropriate for depicting the fluid flow within fractured rocks.

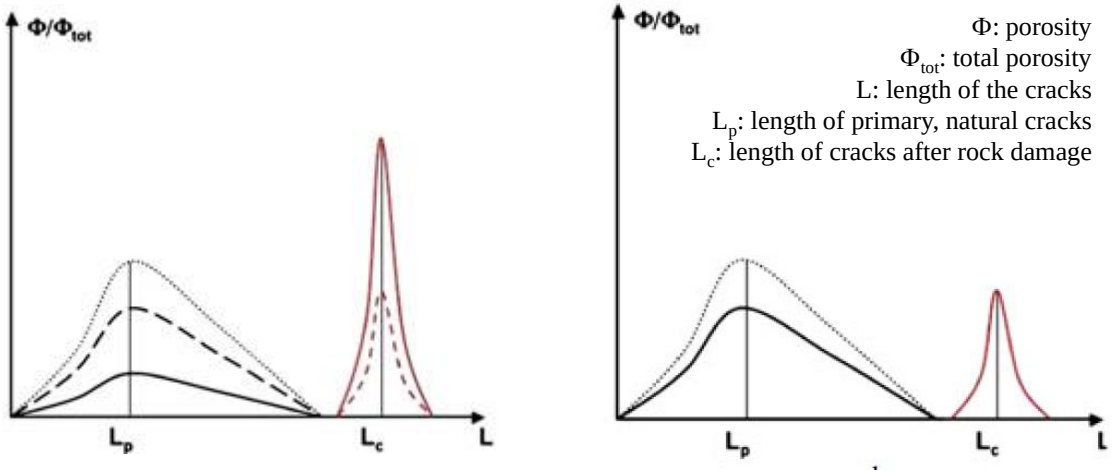

Figure 2.3 - Pore size distribution curves for damaged materials (Arson & Pereira, 2013).

To sum up, the main idea is that rocks are naturally fractured media that present a structure with distinct overall hydraulic behavior depending on their porosity and permeability characteristics. So as to address these singularities, the hydraulic mathematical model should take into account the multiscale features observed in this type of medium.

The assessment of the hydraulic behavior of rocks is particularly important in the petroleum industry. The evaluation of the fluid flow within reservoir rocks helps with the estimates of petroleum production and also verification of its profitability, with suggestions of the most adequate methods for petroleum recovery in such reservoirs (Chen et al, 2006). Therewith, some aspects related to petroleum reservoirs, shale reservoirs, and petroleum production are addressed in Sections 2.3.1, 2.3.2 and 2.3.3.

2.3.1 BASIC CONCEPTS REGARDING PETROLEUM RESERVOIRS

A petroleum reservoir is created from the sedimentation process of organic matter and minerals. These compounds form sedimentary rocks when subjected to appropriate conditions of pressure and temperature over geologic time. Moreover, the decomposition of the organic matter within the sediments produces a mixture of gas and oil composed by hydrocarbons and metals known as petroleum.

At first, these fluids stay within the pores of this layered geological formation. The rock in which the petroleum is produced is known as source rock (Dake, 1978). Given its low density, petroleum has the tendency of migrating overtime from its generation zone (source rock) to other porous regions of the geological formation (reservoir rock). In a typical

geological formation of a petroleum reservoir, petroleum stays confined in a region due to the existence of low permeability rocks (cap rocks) that overlain the reservoir rock, as shown in the scheme portrayed in Figure 2.4.

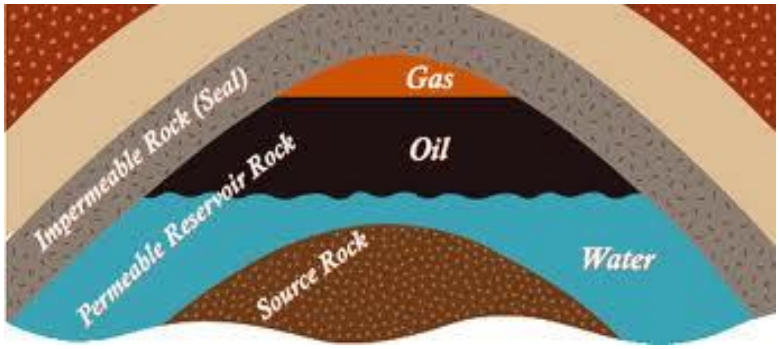

Figure 2.4 - Petroleum reservoir scheme.

Masses of sedimentary rock are usually highly inhomogeneous due to its formation process: each layer may have different types of compounds. Also, this type of rock is known to have bedding planes, the boundaries or contact surfaces between layers of sediment. The bedding planes are usually tightly closed, but they might also contain filling material (Beavis, 1985). Examples of sedimentary rocks are sandstones and shales, depicted in Figure 2.5.

(a) (b)

Figure 2.5 - (a) Sandstone formation; (b) Shale formation.

2.3.2 SHALE RESERVOIRS

The process of layering of minerals and other compounds in a region with proper temperature and pressure provide the optimum condition to the formation of sedimentary rocks. When the geological formation is composed by clayey minerals in its majority, it is

known as mudstone. There are several types of mudstones and shales may be pointed out as the most important for petroleum industry.

The black shales, with this color due to the presence of organic matter during their formation process, are known for being source of oil and gas. Usually, petroleum migrates from the shale (source rock) to an overlying rock unit, such as sandstone (reservoir rock). Oil and gas deposits in sandstones are referred to as conventional reservoirs. Sandstones are highly permeable (in comparison to other rocks) and, therefore, it is expected that the oil and the gas can flow easily through the reservoirs in these cases. Petroleum industry typically focuses on the exploration of these conventional reservoirs (King, 2014).

Nevertheless, not all petroleum migrates from the source rock to the reservoir rock. There is still remaining oil and gas within the shale. In cases like this, the shale formation is considered source, reservoir and cap rock at the same time (Stephenson, 2013). An example of formation with a shale reservoir is shown in Figure 2.6.

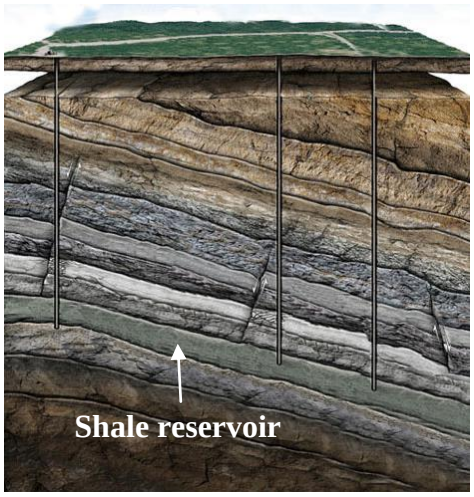

Figure 2.6 - Shale reservoir.

Considering that one of the main goals of petroleum industry is combining high production rates with economic feasibility of the exploration alternatives, efforts are being made for shale oil and, mostly, shale gas exploration.

There are some difficulties regarding petroleum exploration in shales. The arrangement of the minerals in shales distinguishes them from other mudstones for being fissile and laminated. Also, the pores of this type of rock are extremely small. Therewith, the permeability of a shale formation is much lower than in conventional reservoirs.

The extremely low permeability of shales makes flow difficult within these rocks. This characteristic motivated the development of alternative methods for increasing petroleum production in this type of rock. The use of the hydraulic fracturing procedure has been seen as one of the most appropriate solution for enabling petroleum exploitation in shale reservoirs. The induced fractures form a fracture network in which fluid flow is established, enabling oil and gas production in this type of reservoir (Stephenson, 2013).

The fracture network established within the shale reservoir may significantly affect its overall hydraulic behavior. A different porosity and permeability pattern is formed within the reservoir with even, in some cases, a preferential direction or path of fluid flow. This specific type of hydraulic behavior characterizes this medium as multiscale.

The formulation presented in this research (Section 5) could be used for the study of fluid flow within the reservoir rock in the referred condition. The permeability of each scale within the medium could be modified so as to appropriately represent the condition of flow inherent to the verified hydraulic behavior of the formation, with not only scale consideration, but also anisotropy representation for each given situation.

The versatility of this formulation is of great importance, given it can enhance the accuracy and representativeness of hydraulic behavior simulation for multiscale media.

2.3.3 PETROLEUM PRODUCTION IN FRACTURED FORMATIONS

As previously defined, petroleum reservoirs are rocks formed from the deposition and the lithification of organic and inorganic sediments, followed by a decomposition process in which petroleum is produced. Like other rocks, the reservoirs undergo physical diagenetic processes and deformation over time and this could result in macroscopic planar discontinuities through the rock defined as natural fractures.

In some cases, there are reservoirs that do not have the referred fractures. Instead, the crystals that form the rock matrix are tightly arranged, and, as a result, the rock formation has low porosity and low permeability, making flow within the reservoir more difficult, keeping the fluids trapped in the voids of the rock matrix.

For that reason, the importance of addressing the fractures for evaluation of the hydraulic behavior of reservoirs is emphasized. The fractures form a preferential path for fluid flow within the reservoir and their influence should then be evaluated (Salimi, 2010).

When studying fractures in reservoirs, one should also take into account not only the influence of the natural fractures, but also the effects of hydraulic induced fractures in the behavior of reservoirs. The hydraulic fracturing technique has been largely used as a procedure to enable fluid flow for petroleum production in shale reservoirs. If we consider the procedure of hydraulic fracturing in a homogeneous, non-fractured reservoir rock, one should expect to have preferential flow of fluids within the induced fractures.

The study of the relationship between natural and induced fractures within the reservoir is essential, considering that the preferential path flow may be changed with the induced fractures. A new flow network may be established, greatly influencing the hydraulic behavior of the medium. The numerical modeling of naturally and hydraulically fractured reservoirs, as well as the fluid flow models for understanding the physics of the problem and for performing numerical simulation could help in advances in this study field.

2.4 SUMMARY

The formation process of a soil or a rock, being that related to the availability of minerals, climate conditions or in situ stress conditions, affects significantly the porous formation in regards to the arrangement of its solid matrix.

The size of the pores of the sample is the main focus for that matter. This feature is of great importance for studies of behavior prediction. When specifically addressing soil and rock conditions in tropical climate areas, this topic is a main concern, given the porous formation in these regions are mainly known for their bimodal structural arrangement, with macropores and micropores being distinguished within the samples.

For that reason, the main objective in this chapter was to present the basic concepts related to the structural arrangement of porous media. Some aspects regarding bimodal soils and fractured rocks formations are presented, given the importance of a comprehensive understanding of the structure of the multiscale porous media for the proposed study of evaluation of hydraulic behavior of the present research.

3 STUDY OF HYDRAULIC BEHAVIOR OF MULTISCALE MEDIA

3.1 STANDARD APPROACH OF FLOW STUDIES IN POROUS MEDIA

The hydraulic behavior analysis of porous media takes into consideration the principle of conservation of mass. So as to represent what occurs in terms of fluid percolation within porous media, the balance of mass is the basis for the models of this type of phenomenon.

The most typical approach for the representation of flow models takes into account the balance of fluid mass in a representative control volume. The control volume is chosen according to the specifics characteristics of the analyzed problem, so as to properly depict the conditions on which fluid flow takes place. The scale of analysis for the fluid flow problem is the main discussion topics of the present research and it is addressed in Section 3.2.

The conservation of mass is used to mathematically express the hydraulic behavior of porous medium and it is shown in Equation (3.1):

$$-\vec{\nabla}\cdot\left(\rho_\alpha \vec{v}_\alpha\right) = \frac{\partial\left(\phi\rho_\alpha S_\alpha\right)}{\partial t} \tag{3.1}$$

where: ρ_α is the specific mass of the α fluid [ML^{-3}], $\vec{v}_\alpha$ is the velocity of the α fluid [LT^{-1}], ϕ is the porosity of the medium, S_α is the saturation degree of the α fluid and *t* is time.

The velocity of the α fluid is assumed to follow Darcy's law and it can be represented as shown in Equation (3.2):

$$\vec{v}_\alpha = \left[K\right]\frac{\rho_\alpha g}{\mu_\alpha}\vec{\nabla}h_\alpha \tag{3.2}$$

where: $\left[K\right]$ is the intrinsic permeability of the medium tensor [L^2], g is gravity, μ_α is the dynamic viscosity of the α fluid [$ML^{-1}T^{-1}$] and h_α is the hydraulic head of the α fluid [L].

The formulation presented in Equation (3.1) is representative of general models of fluid flow in porous medium. Some adjustments could be made in order to make this mathematical approach more appropriate for particularities of the porous medium.

Depending on the observed structure of the soil or rock, it may be necessary to represent the medium with a multiscale approach, as mentioned in Chapter 2. The different types of multiscale approach for fluid flow models are presented in Section 3.2, followed by a discussion on the methodology chosen for this research in Chapter 4.

3.2 FLOW SIMULATION IN MULTISCALE MEDIA

Flow simulations for porous media fluid flow are based on the conservation of mass principle and follow the mathematical models presented in Section 3.1. Depending on the characteristics of the medium, the model may be adapted so as to accurately represent the medium and its behavior conditions in specific situations.

As mentioned in Chapter 2, bimodal soils and fractured rocks present features that classify them as multiscale media, requiring an appropriate approach for hydraulic behavior analyses. It is important to study these characteristics in order to properly adapt the mathematical models used for fluid flow in this type of porous medium.

The hydraulic behavior of bimodal soils or fractured reservoirs may be greatly influenced by their flow and storage capacities. These characteristics are related to the porosity and the permeability of the medium. Depending on how the flow network is established within the soil or the rock, it is possible to identify its hydraulic features in order to classify it. Nelson (2001) defines four different categories for reservoirs rocks:

- Type-I reservoir: fractures (macroscale) provide the essential reservoir storage capacity and permeability;
- Type-II reservoir: fractures (macroscale) provide the essential permeability, but the matrix (microscale) provides the essential porosity;
- Type-III reservoir: the matrix (microscale) permeability is relatively high, with the fractures (macroscale) acting to further increase flow capacity;
- Type-IV reservoir: the fractures (macroscale) are filled with minerals and provide no additional porosity or permeability.

This categorization of reservoirs is appropriate for evaluating the behavior of multiscale media. Considering that the fractures of a reservoir comprehend the macroscale of the medium and the matrix rock, the microscale, one can define an accurate approach for the mathematical model so as to represent the hydraulic behavior of the studied medium. The

distinction made among the available methods of hydraulic behavior modeling is based on the storage and flow capabilities of the microscale and the macroscale (Diodato, 1994).

Hence, it can be inferred that the choice of the most adequate model depends not only on the type of soil or reservoir, but also on the scale used for study and designing purposes.

Scaling of the medium should be evaluated in order to verify in which degree of detail the problem is being treated in comparison to field observations. The scaling of the problem can vary, going from a totally zoomed-in approach to the most zoomed-out approach.

Using the parallel made by Hoek & Brown (1997) for the scaling of fractured media to evaluate the scale of the problem, one can verify the type of analysis is being suggested for the simulation of the hydraulic behavior of the multiscale in study. These scale levels are represented in Figure 3.1.

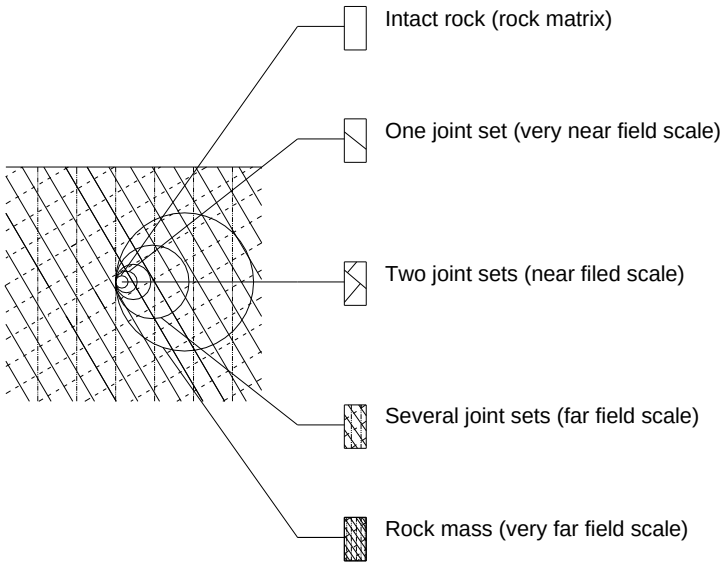

Figure 3.1 - Field scale for treatment of problems in fractured media (modified Hoek & Brown, 1997).

When using the *very near field* scale approach for rocks, flow is considered to occur in a single fracture and porous medium exchange is possible. If a bimodal soil is being studied, this scale could represent the case in which the microscale flow and storage contribution is considered almost insignificant, being the macroscale flow and storage the focus of the analysis. Nevertheless, it is possible to have microscale exchange.

For the *near field* scale approach for rocks, flow occurs in a fractured porous medium and each fracture is described in detail, with a well-defined flow network. For bimodal soils, the same analysis can be made, with the main flow established through the macroscale.

In the *far field* scale, flow occurs in two overlapping continua, with interaction between macro and microscale. Finally, for the *very far field* scale, flow occurs on an equivalent porous medium, with a calculated average of the behavior of the macro and the microscale.

It can be seen that the scale definition proposed by Hoek & Brown (1997) can be used for both soils and rocks. The scale used for treating the flow problem in porous media is what differentiates the chosen mathematical approach and, consequently, the numerical model that could reproduce the studied hydraulic behavior.

Considering all mentioned, the classification of the different models for flow simulation in multiscale media can be made into three main types, depending on the scale of the problem and its representativeness to the simulations: discrete fracture network model, dual continuum models and single equivalent continuum model. Also, alternative conceptual models can be employed. These models are briefly discussed in Sections 3.2.1, 3.2.1, 3.2.3 and 3.2.4.

3.2.1 DISCRETE FRACTURE NETWORK MODELS

The Discrete Fracture Model (DFM) is used in cases in which the very near scale is considered or when there are clear and distinct fractures in the reservoir.

Given the characteristics of this model, one can infer it could be more appropriate to represent the hydraulic behavior of specific parts of a rock mass. Therewith, its usage in bimodal soils is not recommended.

With that, one can evaluate the specificities of this type of model for rock masses. It can be defined that each fracture of the rock mass has its geometry well-defined, providing enough information for explicit modeling of the flow within them. With this definition of the flow in each fracture, it is possible to predict the flow network that will take place within the rock mass. Also, matrix flow may be represented if it is significant to the overall flow within the medium. In that case, the Darcy law is valid for this portion of the fractured medium.

In general, the Finite Element Method (FEM) and the Finite Differences Method (FDM) have been employed for the solution of the flow problem with this type of model. Solutions for single and two-phase flow have been presented, with both bi-dimensional and tri-dimensional approaches (Baca et al., 1984; Juanes et al., 2002; Borbiaux et al., 2005; Matthai et al., 2005). An example of discrete fracture network is depicted in Figure 3.2.

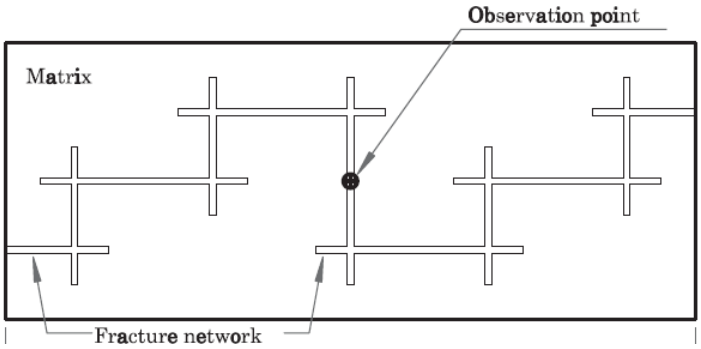

Figure 3.2 - Model of fracture network (Juanes et al., 2002).

It is important to highlight that softwares developed with DFM allow explicit representation of the fractures, guaranteeing thorough description of the fracture flow network within the medium. The combination of this model with other types, such as dual-porosity and dual-porosity/dual-permeability, may provide improved simulation results. Also, when combined with other types of models, the discrete fracture flow network simulation results provide data for the simulation of flow between fractures and porous media with minimal non-physical parameterization. However, one must take into account that using DFM may have extremely high computational costs (Diodato, 1994).

3.2.2 DUAL CONTINUUM MODELS

The dual continuum models preview an interpretation of the medium consisting of a primary porosity and a secondary porosity (Diodato, 1994).

When specifically verifying the characteristics of bimodal soils, one can say that the primary porosity is formed by the pores of largest diameter of the sample, with the secondary porosity being the pores with smallest diameter, as defined by Delage & Lefebvre (1984).

At the same time, the dual continuum approach can be applied for rock masses. The primary porosity is created by deposition and lithification of sediments, establishing a highly interconnected geological formation. The secondary porosity is created by fracturing, jointing, or dissolution, as defined by Warren & Root (1963). Therewith, the two types of porosity are envisioned as two separate but overlapping continua, forming the medium.

There are two different types of dual continuum approaches: dual-porosity, and dual-porosity/dual-permeability. This multiscale type of approach for flow simulations is usually applied in media such as rocks and rock masses. Considering that, the basic concepts of the

models presented in Sections 3.2.2.1 and 3.2.2.2 have an approach based on studies made for this type of geologic formation. Nevertheless, the understanding of these concepts is extended for bimodal soils, so as to comprise the topics of discussion of the present research.

3.2.2.1 DUAL-POROSITY MODELS

Barenblatt & Zheltov (1960) introduced the studies of fluid flow in fractured medium. These authors presented a physical model based on the premise that the flow inside the fracture network (macroscale flow) and the matrix (microscale flow) are dissociated, with a set of equations for slightly compressible single-phase flow developed for both scales. Also, the authors assumed there might be some exchange between these two media, represented on the model by a transfer function, being the transfer assumed to occur at a pseudo-steady state.

Extending this approach, Warren & Root (1963) presented the dual-porosity model concept applied specifically for petroleum reservoirs. The fractured medium representation followed an idealized geometry, with a set of identical rectangular parallelepipeds representing the matrix blocks, separated by fractures, as depicted in Figure 3.3.

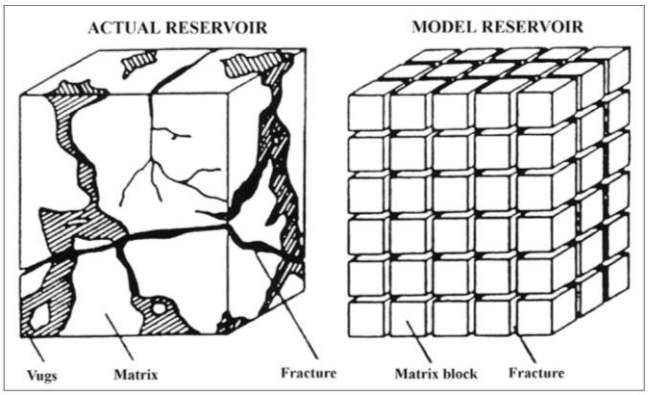

Figure 3.3 - Idealized geometry of the dual-porosity model (Warren & Root, 1963).

There are some hypotheses considered for the dual-porosity model developed by Warren & Root (1963):

- The fracture network is completely interconnected;
- The matrix blocks are not connected to one another;
- Most of the fluid resides in the rock matrix, but most of the flow occurs in the fractures;

- There is fluid transfer from the matrix to the fractures (matrix is source or sink to the fracture), mathematically represented by a transfer function.

These hypotheses are valid for all dual-porosity models. Nevertheless, the flow model suggested by Warren & Root (1963) is only applicable to single-phase flow simulations, and other considerations should be made for its extension to multiphase flow situations.

Research and further investigation as to broaden the proven limitations of this model have been performed. Focusing specifically on the evaluation of the transfer functions, the assessment of different flow mechanisms between matrix and fracture could be studied and enhanced. Also, changes on the shape of the matrix block could be taken into account in order to represent more accurately the hydraulic behavior in fractured media.

Thomas et al. (1983) presented a three-dimensional, three-phase model for simulation of the flow of water, oil, and gas in naturally fractured reservoirs. The transfer function used in this model is based on an extension of the equation developed by Warren & Root (1963), and it takes into account the effects of capillary pressure, gravity and viscous forces.

It is important to highlight that dual-porosity models are representative of Type-II reservoirs (Nelson, 2001), in which the fractures provide the essential permeability of the medium and the matrix, the essential porosity. One must take this into account for choosing this type of approach when studying fractured media fluid flow.

With adequate definition of parameters, the dual-porosity or the extended dual-porosity models may provide accurate results. One may observe the physical and numerical simplicity in these models if compared to others, preserving, however, the accuracy of results and representativeness of the phenomena taking place at the studied fractured medium. That is the main reason for having this type of model being currently the most applied in the petroleum industry. Nevertheless, some difficulties regarding the definition and the application of the transfer functions may represent a barrier for its broader utilization.

The dual-porosity models have been developed and established for rocks, namely petroleum reservoirs. However, when analyzing the hydraulic behavior of bimodal soils, the macro and microscale structure could be interpreted as dual-porosity. For that reason, this model approach could be also implemented for the solution of hydraulic behavior problems in soils with this specific, as mentioned in Section 3.2.2.

3.2.2.2 DUAL-POROSITY/DUAL-PERMEABILITY MODELS

The main difference between the dual-porosity and the dual-porosity/dual-permeability models is that in the latter, matrix-matrix interblock flow is significant. Matrix to matrix connection is used in the hydraulic model of the fractured medium, and the matrix blocks are no longer considered isolated. The matrix contribution to the overall fluid flow is not only the transfer of fluid from the matrix to the fracture, but also within blocks (Gong, 2007).

This type of model provides a more accurately representation of Type-III reservoirs (Nelson, 2001), in which the matrix permeability is relatively significant and must be included in the physical representation of the model. This consideration enables the model to being employed in a much broader variety of fractured media problems.

It must be emphasized that the main difference between matrix-fracture transfer functions in dual-porosity and dual-porosity/dual-permeability models is the level of complexity of them. For the dual-porosity models, the transfer functions are based on empirical evidence or with much simplification, whereas for the dual-porosity/dual-permeability models, they are established with a physical background, based on the mathematical model defined for the problem (Simunek et al., 2003).

Also, it is pointed out that this approach could be extended to bimodal soils if one considers the micropores are interconnected, with a fully-established flow network within.

One of the first models with the dual-porosity/dual-permeability approach was proposed by Kazemi et al. (1976). They introduced Warren & Root's model into a numerical model for application on large-scale problems with extension of the governing equations to a two-phase flow situation. A three-dimensional, compressible, water-oil reservoir simulator has been developed for the solution of the problem, with FDM application.

Then, other models have been developed with two-scale homogenization procedures (Arbogast et al., 1990; Arbogast, 1992), considering that the dual-porosity description of the fractured medium is recovered via homogenization. Homogenization is a specific mathematical technique of upscaling applied to this type of fluid flow analysis, in which there are two scales: scale of the fracture and scale of the rock matrix.

After the studies of Arbogast et al. (1990) and Arbogast (1992), effort has been made towards the evaluation of the transfer phenomena in fractured media. Uleberg & Kleppe (1996) discussed physical characteristics of the fractured medium and established fluid flow mechanisms that influence matrix-fracture transfer, such as capillary continuity, reinfiltration or reimbibition, diffusion and matrix block shape and size, as depicted in Figure 3.4.

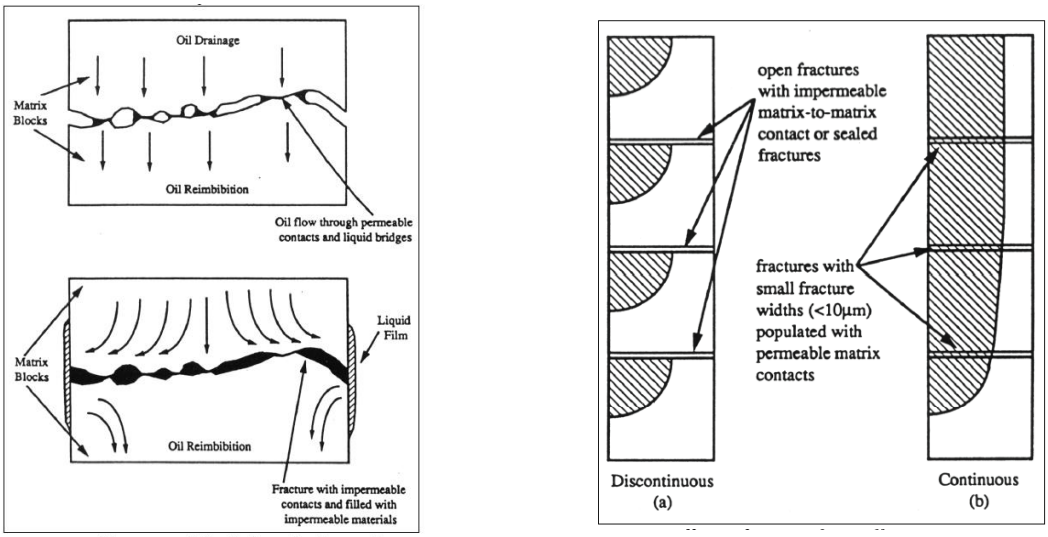

(a) (b)

Figure 3.4 - (a) Reinfiltration; (b) Capillary continuity (Uleberg & Kleppe, 1996).

An enhanced version of the Arbogast et al. (1990) and Arbogast (1992) model was proposed by Gong (2007), which results on the development of a procedure for upscaling a fine-scale fracture description to a large-scale, continuum flow simulation model, similarly to the technique employed by Arbogast et al. (1990) and Arbogast (1992) were presented. Nevertheless, the upscaling methodology used in Gong's research differs from the Arbogast's approach. Here, the applied procedure is known as Multiple Subregion Method (MSR), rather than the standard homogenization procedure. With that, the MSR approach used by Gong (2007) could be interpreted as a generalized dual-porosity/dual-permeability representation.

Also, Salimi (2010) has employed the homogenization procedure to Arbogast et al. (1990) and Arbogast (1992)'s approach for fractured media flow cases with more than one fluid (oil and water, e.g.).

The dual-porosity/dual-permeability models seem to be adequate to represent fluid flow in fractured media, considering their degree of detailing of the hydraulic characteristics of the medium. At the same time, these models are satisfactory in terms of computational performance in comparison to the discrete fracture models and they can be an adequate alternative for representation of fluid flow in fractured reservoirs.

As mentioned before, these models could also be satisfactory for the representation of the hydraulic behavior of bimodal soils when considering the connection of the smallest pores of the medium (interconnection within the microscale). In this case, these models could be used so as to simulate the flow and storage conditions of this type of soil with an enhanced approach of what happens within the microscale, when compared to dual-porosity models.

3.2.3 SINGLE EQUIVALENT CONTINUUM MODEL

As seen, the verification of suitability of a type of model for fluid flow analysis in multiscale media depends on the scale of the problem. In cases of *very far or very near field* scale, the level of detailing for the description of the problem is reduced.

In these situations, it can be assumed the medium is supposed to have average hydraulic characteristics and properties, and, therefore, the flow simulation may proceed with the simplified assumptions of classical continuum mechanics. This approach, known as single equivalent continuum model, is used for simplifying the representation of the medium at its fullest, providing information valid for the entire domain of study, making no distinction between rock matrix and fractures properties, when dealing with rock masses representation, or macro and micropores, when representing bimodal soils. In either way, the model is conceived for an homogeneous hydraulic behavior approach of the medium.

Assuming the continuity of the medium, a pseudo-continuum medium is established. This pseudo-continuity of the medium replaces the real discontinuous condition of the multiscale medium for an equivalent hydraulic behavior medium.

It is recommended to have the pseudo-continuous system separated into smaller subsystems, each of them with their hydraulic properties and adequate formulation of governing flow equations. These subsystems are separated according to their similar characteristics in terms of their hydraulic properties. The size of the subsystem and the number of subsystems that will be used in the model depend on the desired level of detailing of the output and computational cost, and, therefore, they should be cautiously defined. Also, the calibration of the model should be made, if possible, with real data from field investigation, given the need to verify the accuracy of the model (Franciss, 2010).

A pseudo-continuous model for one-phase fluid has two basic physical quantities within the flow domain: dubbed hydraulic gradient, $\{J\}$, and specific discharge, $\{q\}$.

The hydraulic gradient refers to the measurement of spatial decay rate of energy during percolation of a fluid particle. The dubbed hydraulic gradient is an average value of the hydraulic gradient for the entire system or subsystem. The specific discharge is defined with base on Darcy velocity, with the consideration of the effective porosity (n_e) of medium (Equation (3.4)). The definition of effective porosity comes from the term effective volume (V_e), which is used to refer to the volume of voids, excluding the volume occupied by adherent liquid fluid (Equation (3.3)).

$$n_e = \frac{V_e}{V} \tag{3.3}$$

where: V_e is the effective volume [L^3] and V is the total volume of the medium [L^3].

$$\{q\} = n_e \{v_e\} \tag{3.4}$$

where: $\{q\}$ is the specific discharge vector and $\{v_e\}$ is the effective velocity vector [LT^{-1}].

Another parameter, hydraulic conductivity, [k], is considered so as to interconnect this assembling of variables. The hydraulic conductivity is a parameter that describes the hydraulic properties of the medium. When assembling all the referred parameters in mathematical terms, one can imagine the following relation (Equation (3.5)) for the description of the hydraulic behavior of the medium:

$$\{q\} = [k]\{J\} \tag{3.5}$$

where: $[k]$ is the hydraulic conductivity tensor and $\{J\}$ is the dubbed hydraulic gradient.

This is a simple mathematical approach for flow in porous media and it can be used in general for many types of flow problems in porous media. Nevertheless, specifically for the studies of flow through a fractured medium, it is necessary to consider the effect of transmissivity of the fractures and its effect in terms of permeability of the medium, given the characteristics of the problem. Therewith, the calculation of the hydraulic conductivity tensor is based on the transmissivity assumptions made for the medium.

In an overall analysis, it can be inferred that the usage of a single equivalent continuum model could neglect specific phenomena in fluid flow in fractured media, given the many simplifications and assumptions made to make the model viable. Nevertheless, it could be an appropriate alternative for preliminary analyses of hydraulic behavior of fractured media.

3.2.4 ALTERNATIVE CONCEPTUAL MODELS

The alternative conceptual models have been in development so as to enhancing the techniques already used for fractured media flow model representation. They could also be extended for bimodal soils hydraulic behavior analyses.

Bai et al. (1993) introduced a unified multiporosity/multipermeability approach for the modeling of flow in fractured media. According to the authors, the single equivalent continuum and the dual continuum models are specific cases of their generalized approach.

In addition, Bear (1993) pointed out that geological and environmental processes might have an impact on the fractured medium, and the rock mass may seem to have multiple domains. This interpretation resembles the principles proposed by Gong (2007), with the possibility of subdomains being defined within the same medium.

Borbiaux et al. (2005) extended research on the field of combining approaches, using DFN and dual-porosity models and representing the detailed geometry of the fracture network together with the matrix-fracture transfer evaluation. This combination of fractured media flow models results in an alternative method of solution of the flow problem.

Given the degree of detailing and, consequently, computational cost and time-consuming difficulties of the mentioned methods, these alternative conceptual models should be employed in more specific studies of fluid flow in fractured media, in which it might be essential to develop the research with approaches that differ from the standard procedures.

3.3 SUMMARY

The present study main focus is the hydraulic behavior of multiscale media. For that matter, mathematical models that represent the phenomena occurring within the porous media and affected by the multiscale structure they present are addressed.

There are cases of analyses made for the evaluation of hydraulic behavior patterns in which the size of the pores can be an aspect that dictates the changes on the overall response of the medium. Therewith, the consideration of the multiscale structure in hydraulic behavior mathematical models is of paramount importance.

Different approaches can be used for that purpose. Four main groups of mathematical models are presented and discussed in this chapter: discrete fracture network models, dual continuum models (sub-divided into dual-porosity and dual-porosity/dual-permeability models), single equivalent continuum model and alternative conceptual models.

The mathematical approach shown in Chapter 3 is base for the definition of the model for the simulations proposed for the achievement of the objectives of the present research.

4 RESEARCH METHODOLOGY

4.1 METHODOLOGY OUTLINE

In this thesis, fluid flow simulations in multiscale media were executed for attaining the proposed research objectives. Different hydraulic behavior conditions for multiscale media were represented so as to allow the previewed analyses. The research methodology was organized in stages in order to appropriately describe the outline proposed for the performed steps. The overall methodology scheme is represented in Figure 4.1.

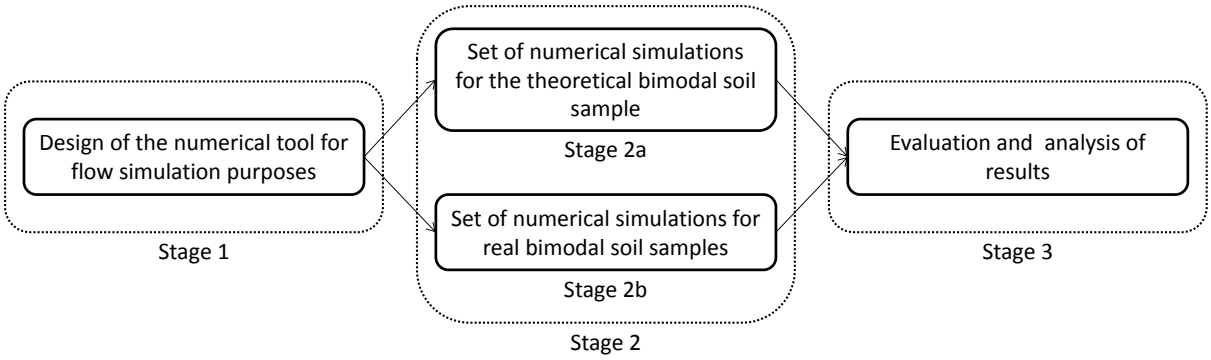

Figure 4.1 - Overall research methodology scheme.

The Stage 1 of the research methodology corresponds to the implementation of the mathematical model on the numerical tool chosen for performing the proposed simulations, FlexPDE (described in Section 4.2), and all steps required for the appropriate functioning of the numerical model. This is represented in Figure 4.2.

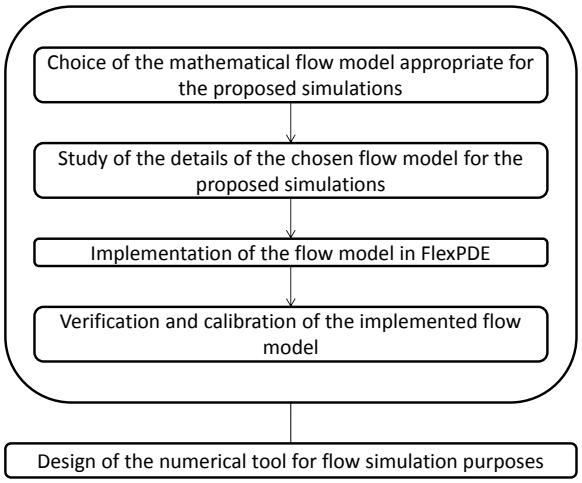

Figure 4.2 - Scheme for the Stage 1 of the research.

Then, two sets of simulations were performed for the assessment of the hydraulic behavior of multiscale media. They were divided into tests for a theoretical bimodal soil sample (Stage 2a), and numerical simulation tests for a real bimodal soil samples (Stage 2b).

At first, a set of simulations in a theoretical bimodal soil sample was performed so as to verify the effectiveness of the proposed mathematical and numerical models. The following guideline was proposed in this step of the research (Stage 2a):

- Definition of total and microscale void ratio values for the theoretical bimodal soil sample;
- Definition of parameters for the soil-water characteristic curve (SWCC) of the theoretical bimodal soil sample;
- Estimation of the size (diameter) of the pores of the theoretical soil sample;
- Definition of the pore size distribution density curve;
- Definition of the intrinsic permeability of the macro and microscale;
- Homogenization parameter sensitivity analysis;
- Drying and wetting simulations for the theoretical bimodal soil sample;
- Sensitivity analyses for the parameters of the SWCC.

The definition of the total and microscale void ratio values is based on typical values of this parameter for tropical soils reported by Otálvaro (2013) and Otálvaro et al., (2016).

Then, the parameters of the soil-water characteristic curve are defined. The main goal in this step is to provide a format to the curve that not only allows the performance of the drying and wetting simulations appropriately, but also the sensitivity analyses for all evaluated parameters. Therewith, the validation of the model is provided, with verification of applicability of the numerical model for various analysis conditions of flow simulation.

The next proposed steps are made based on the theoretical data defined for void ratio and SWCC for this bimodal soil sample. The estimation of the size of the pores and, consequently, definition of the pore size distribution density curve can be mathematically made with Washburn's equation (Diamond, 1970; Griffiths & Joshi, 1989), as shown in Equation (2.1), and the PSD parameter, calculated with Equation (2.2).

The intrinsic permeability of the macro and microscale is defined and, with this information, it was possible to proceed to the sensitivity analysis of the homogenization parameter. Details about its importance for the model are addressed in Chapter 5.

The procedure chosen for this set of analysis is based on the simulation of a one-direction, single-phase fluid flow through a medium divided into two different regions, one with a bimodal-type soil and another with a monomodal soil. This problem configuration simulates a permeability test, and the values of hydraulic conductivity of each part of the domain, as well as the equivalent hydraulic conductivity, ought to be defined.

The domain of simulation is divided as follows:

- Region number 1: blue-colored, squared region (1 meter high, 1 meter wide); it represents a sample with bimodal soil characteristics correspondent to the theoretical bimodal soil sample intrinsic permeability parameters;
- Region number 2: yellow-colored, squared region (1 meter high, 1 meter wide); it represents a soil with only one scale of size of pores. The value of intrinsic permeability used for this set of simulation is K=1,00·10^{-9} m². This value was arbitrarily chosen and it is greater than the values of intrinsic permeability of the bimodal soil sample so as to not interfere in the flow conditions through the bimodal soil sample (flow through region 1).

The software used for the simulation (FlexPDE, see Section 4.2) automatically generates the finite element mesh (triangular elements) used for the solution of the problem. Specifically for this problem, the domain is initially discretized into 130 elements, with a total of 291 nodes. This domain is represented in Figure 4.3. The software used for the simulations has a scheme of auto-adaptation of the finite element mesh; for that reason, the number of elements and nodes varies as needed throughout the simulation.

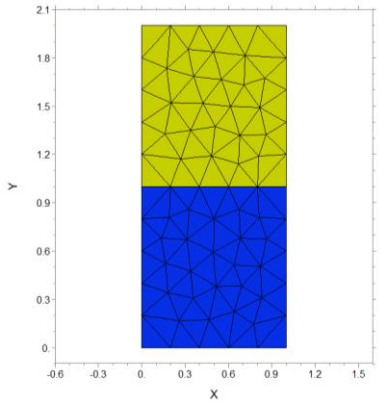

Figure 4.3 - Initial domain geometry and mesh definition for calibration of ε.

The boundary conditions for this problem are given so that flow is established only in the vertical direction (y) due to a hydraulic head gradient. The value of hydraulic head is assumed to be 10 m on the bottom of Region 1 and zero on the top of Region 2.

Then, the sensitivity analysis was performed for the homogenization parameter ε. Its initial value was 0,1, being known that this parameter should be lower than 0,1 so as to make the multiscale approach recommended for the solution of the problem (Warren & Root, 1963; Arbogast et al., 1990; Arbogast, 1992; Salimi, 2010).

The comparison of values of fluid flow rate and hydraulic conductivity between regions is used for analysis of the results. For that purpose, the following data should be collected:

- Fluid flow rate in Region 1 in the macroscale;
- Fluid flow rate in Region 1 in the microscale;
- Total flow rate in Region 2;
- Hydraulic head in the beginning of Region 2 ($y=1{,}0001\ m$).

The fluid flow rate is calculated with Equation (4.1):

$$q_{wi} = -K_i \frac{\rho_w g}{\mu_w} \Delta h_{wi} \tag{4.1}$$

where: K_i is the intrinsic permeability of the i part of the domain (m is used for microscale, M is used for macroscale and c is used for Region 2) and Δh_{wi} is the variation of the hydraulic head for the interval of analysis within the domain (from $y=0$ to $y=1{,}0001\ m$).

For this set of simulations, the fluid flow is assumed to be with only one fluid phase (water). The values of its specific mass and viscosity, and gravity are defined in Table 4.1.

Table 4.1 - Values of ρ_w, μ_w and g for the homogenization parameter calibration simulations.

Property/characteristic	**Value**
Water specific mass (ρ_w)	1,00 g/cm³
Water viscosity (μ_w)	$1{,}00 \cdot 10^{-6}$ kPa.s
Gravity (g)	10,00 m/s²

The analyses of calibration of the homogenization parameter of the theoretical bimodal soil sample followed these steps:

- Step 1: Calculation of the equivalent hydraulic conductivity parameter for Region 1 (calculated with the total porosity and intrinsic permeability values and fluid properties);
- Step 2: Determination of fluid flow rate of the macroscale portion (q_{wM}) and the microscale portion of Region 1 (q_{wm}) (data collected from the numerical simulation);

- Step 3: Calculation of the total fluid flow rate of Region 1 (q_{wt});
- Step 4: Determination of total fluid flow rate of Region 2 (q_{wc}) and hydraulic head value at $y=1,0001\ m$ ($h_{y=1,0001m}$) – immediately in the beginning of the referred region of the domain (data collected from the numerical simulation);
- Step 5: Calculation of the hydraulic conductivity parameter for Region 2 (k_{wc}).

The calculation proposed in Step 1 is made with the direct application of Equation (2.9) for the total intrinsic permeability value for each soil sample.

In Step 3, the calculation of the total fluid flow rate for Region 1 is made by adding up both macro and microscale fluid flow rates. The microscale fluid flow is considered in the same scale of the macroscale by dividing the value of the microscale fluid flow rate by the square value of the homogenization parameter (ε^2).

With these simulations, the fluid flow rate of Region 1 and Region 2 are expected to be the same (no fluid loss or storage). Considering this, in Step 4, the value of the total fluid flow rate is collected from the simulations for comparison purposes.

Finally, in Step 5, the hydraulic conductivity is calculated for Region 2. The total fluid flow rate (q_{wc}) and the hydraulic head at $y=1,0001m$ ($h_{y=1,0001m}$) data collected at Step 4 and the hydraulic head at the bottom of the sample (fixed value at $y=0$; $h=10m$) are used for this purpose, as shown in Equation (4.2).

$$k_{wc} = \frac{q_{wc}}{\Delta h_{wc}} = \frac{q_{wc}}{\left(10 - h_{y=1,0001m}\right)} \tag{4.2}$$

The results of the homogenization parameter sensitivity analysis are presented in Section 6.1.2 for the theoretical soil sample and in Section 6.2.1 for the real soil samples.

Then, drying and wetting simulations were conducted for the theoretical soil sample. In this step, the effects of drying and wetting are studied with parametric analyses.

When addressing drying and wetting simulations, the expected result is following the drying and wetting trajectories over the SWCC for the studied soil sample. The drying and wetting tests simulated with the numerical model are a representation of experimental tests performed in laboratory with the same purpose.

The definition of the SWCC of a soil sample can be made using different experimental approaches. Nevertheless, the main goal is to establish the relationship there is between an

index for measurement of water content within the soil and fluid pressure values, expressed by matric suction or capillary pressure.

At this stage of the present research, the objective was to reproduce the experimental procedure for drying and wetting trajectories. For that purpose, a domain was defined for the numerical modeling of the problem, with specific boundary conditions to represent what happens with a soil sample subjected to drying and wetting tests on laboratory. Specifically for this situation, the chosen approach is the simulation of two-dimensional flow in a sample 1 meter wide and 0,9 meter high. At the bottom of the sample, a region of the domain (0,1 meter high) is used for the representation of the porous disk at the base of the cell. Therewith, the entire domain is divided into two regions; one correspondent to the soil sample (blue-colored region), and the other correspondent to the porous, high air-entry value, disk (yellow-colored region).

The initial discretization of the domain of this problem is made into 228 elements, with a total of 497 nodes and it is shown in Figure 4.4. The simulation was run so as to depict 6 hours of drying or wetting test. The chosen time step was 120 seconds.

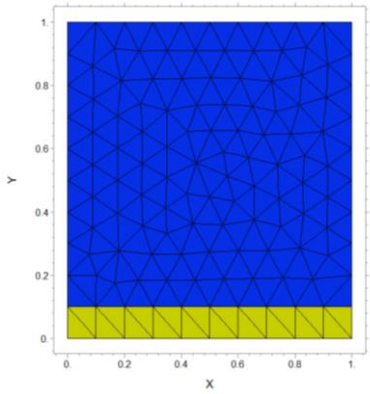

Figure 4.4 - Initial domain geometry and mesh definition for drying and wetting.

The values of initial conditions of this set of simulations are defined based on the type of trajectory being evaluated. At the beginning of the simulation of the drying trajectory simulation, the highest value of degree of saturation of the theoretical soil sample must be encountered for both scales, whereas for the wetting trajectory simulation, the lowest possible value for the degree of saturation should be used. With these considerations, the sample is taken to its limit and the extents of validity of the model are appropriately verified.

It is important to take into account that in both cases, the limit value for the degree of saturation is established with the simultaneous analysis of the macro and microscale SWCC

of the theoretical bimodal soil sample. This means that the values used for simulation purposes must be evaluated so as to avoid situations in which one of the scales of the bimodal soil sample is either completely dry (in case of the drying trajectory) or saturated (in case of the wetting trajectory). The equilibrium between what happens in the macroscale and in the microscale must be evaluated and guaranteed based on the capillary pressure values verified as appropriate for both scales as an initial condition for the simulated problem.

In what concerns the boundary conditions of the problem, these premises are followed:

- The bottom part of the domain represents the portion of the cell correspondent to the high air-entry value, porous disk placed on the bottom of the cell. Then, the essential, Dirichlet boundary condition is used, with imposition of values for the wetting fluid pressure and degree of saturation of the wetting fluid correspondent to the initial conditions of the simulation;
- The left and the right sides of the domain represent an impermeable material, such as the stainless steel case that holds the soil sample, is represented; For that purpose, the natural, Neumann boundary condition is used, with imposition of the value of the normal derivate of wetting fluid pressure being zero;
- In the upper part of the domain a condition that simulates the effect of drainage or wetting of the sample with the wetting fluid is imposed. For that purpose, the natural, Neumann boundary condition is used, with value correspondent to the normal derivate of wetting fluid pressure being equivalent to a reference value of wetting fluid flow rate. The degree of saturation is assumed to remain constant throughout the simulation.

The defined boundary conditions are correspondent to the macroscale of the problem. There is no need to address the microscale boundary conditions, given there is a transfer function in the simulations that previews interaction between the scales.

Mathematically, this should suffice in terms of representing what happens with the fluid flow between scales. Therewith, all variables of the microscale are assigned a natural Neumann boundary condition equals zero. The boundary conditions for the macroscale are schematically represented in Figure 4.5 and are summarized in Table 6.7.

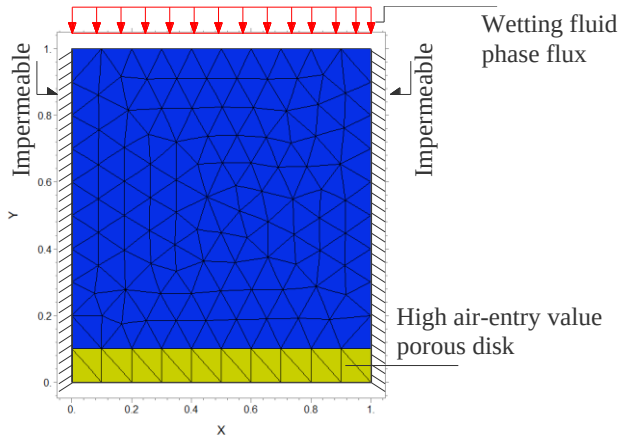

Figure 4.5 - Boundary conditions scheme for the drying and wetting simulations.

The values of degree of saturation for each scale, as well as the values of capillary fluid pressure are retrieved from the simulation results; they are used as basis for determination of the value of degree of saturation for the entire sample after it goes through drying or wetting.

The calculation of the degree of saturation of the entire sample is made with an averaging procedure based on the approach suggested by Szymkiewicz (2013) using volume fraction average weight parameters.

The volume fraction average weight parameters of the macro and microscale are determined with the solution of the system of equation formed by Equations (4.3) and (4.4).

$$\phi = w_M \phi_M + w_m \phi_m \tag{4.3}$$

$$\phi S_w = w_M \phi_M S_{wM} + w_m \phi_m S_{wm} \tag{4.4}$$

where: w_M is the volume fraction average weight parameter of the macroscale and w_m is the volume fraction average weight parameter of the microscale; ϕ_M, ϕ_m and ϕ are the porosity values for the macroscale, the microscale, and the entire domain, respectively; S_{wM}, S_{wm}, and S_w are degree of saturation values of the wetting fluid phase for the macroscale, the microscale, and the entire domain, respectively.

The porosity and the degree of saturation of the wetting fluid phase are known for both scales and also for the entire domain for the initial condition of the analyzed problem. For that reason, they are suitable for the calculation of w_M and w_m. Then, w_M and w_m values are employed in the calculation of the degree of saturation of the entire sample. The calculation is made via Equation (4.4), with the macro and microscale degree of saturation final values, retrieved from the simulation results.

This calculation procedure for the degree of saturation of the entire sample considering the values found for each scale of the sample is interesting as it represents a way of reproducing the hydraulic behavior of bimodal media. This gives the possibility of addressing MIP tests results to determine parameters that could be used for the definition of degree of saturation of the sample, and, consequently, the SWCC of the soil sample.

This contribution is pointed out as one of the most significant of this research. The procedure methodology proposed here, with input data coming from MIP tests resolving into the definition of the SWCC is unique for bimodal soils and should be emphasized.

The results of the drying and wetting trajectories simulations are presented in Section 6.1.3 for the theoretical soil sample and in Section 6.2.2 for the real soil samples.

Finally, a set of sensitivity analyses for the parameters of the SWCC was proposed. The residual degree of saturation, the parameter *a* (non-wetting fluid entry pressure value), and the parameter *n* (inclination of the curve) for the macro and microscale had their influence verified and analyzed in this step of the research; the influence of each parameter on the hydraulic behavior of each scale of the soil and on the overall hydraulic behavior of the theoretical soil sample were assessed. In total, 13 different formats for the SWCC of the theoretical soil sample were evaluated, and 6 drying trajectory test simulations were carried out to reproduce the behavior of the sample in the referred conditions. The procedure used for the tests and the correspondent results are presented in Section 6.1.4.

To sum up, the Stage 2a of the research correspond to the sets of simulations followed with the purpose of assessing the validity of the numerical model. Different situations were verified and the applicability of the proposed model was thoroughly tested, providing enough information to assure the adequacy of the model for the purposes of the present research.

Furthermore, it is important to highlight that the methodology here tested relates MIP test results of a bimodal soil sample with the model used for the simulations carried out throughout this research. This procedure enables the possibility of acquiring data from the sample experimentally and reproducing its bimodal hydraulic behavior accurately numerically. The validity of this procedure is one of the main contributions of this research.

The summary with all steps required for the set of simulations related to the theoretical bimodal soil sample (Stage 2a) is represented in Figure 4.6.

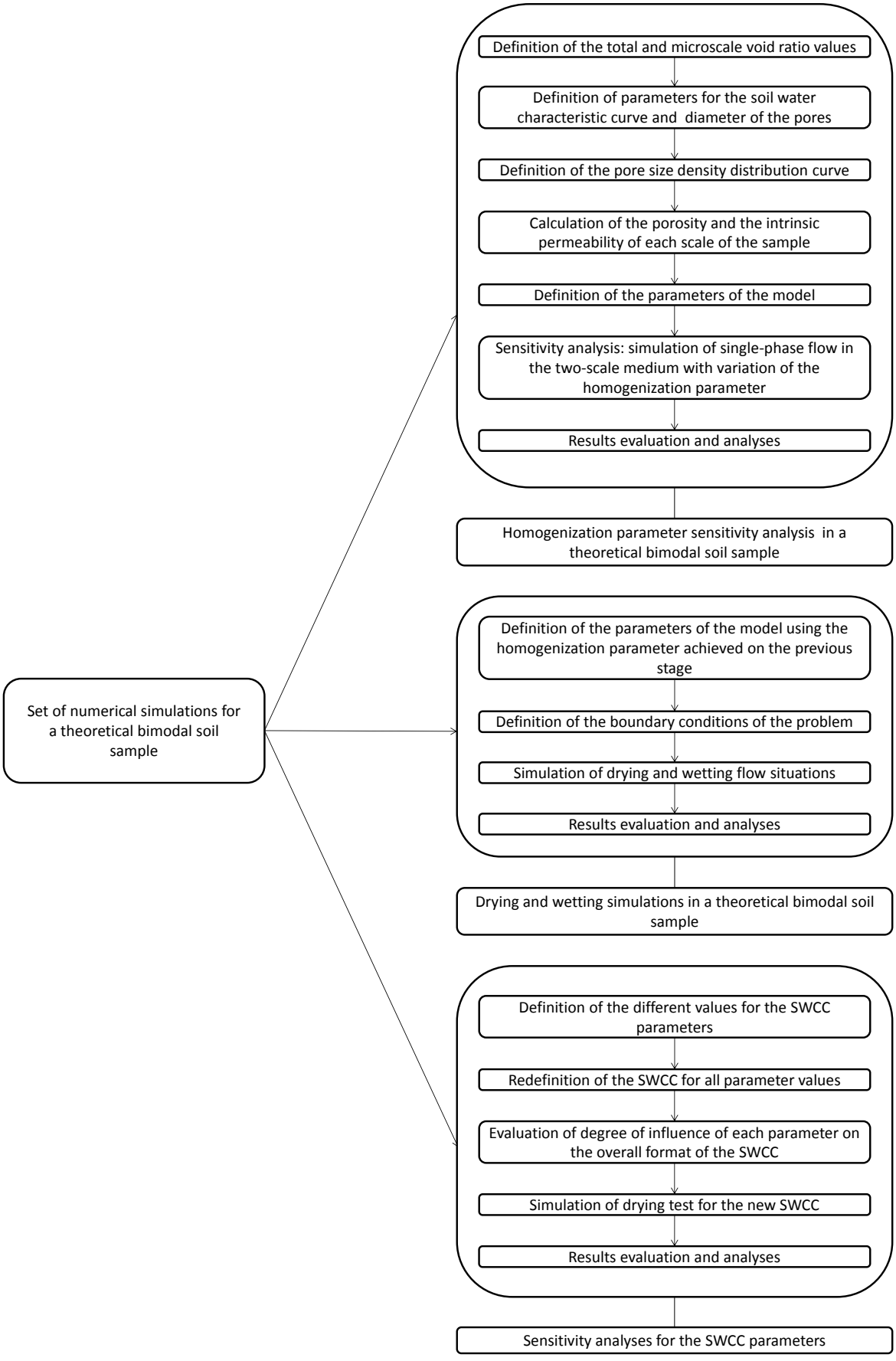

Figure 4.6 - Scheme for the Stage 2a of the research.

Then, the research followed up to Stage 2b of simulations. The tests made here were conducted with the experimental data of two bimodal soil samples provided by Otálvaro (2013). At first, it was necessary to adjust the data from the MIP tests, with definition of the distribution of the diameter of the pores (pore size density distribution curve); then, the limit of macro and microscale was established. Finally, the porosity and the intrinsic permeability of each scale for the two studied soil samples were defined.

With the information of porosity and intrinsic permeability of each scale of the soil samples, it was possible to perform the sensitivity analysis of the homogenization parameter, following the same procedure described for the theoretical bimodal soil sample in Stage 2a.

Then, a drying simulation analysis was made for the two soil samples. Again, the same simulation conditions described for the theoretical bimodal soil sample in Stage 2a were used.

The summary with all steps required for the set of simulations related to the bimodal soil samples (Stage 2b) is represented in Figure 4.7.

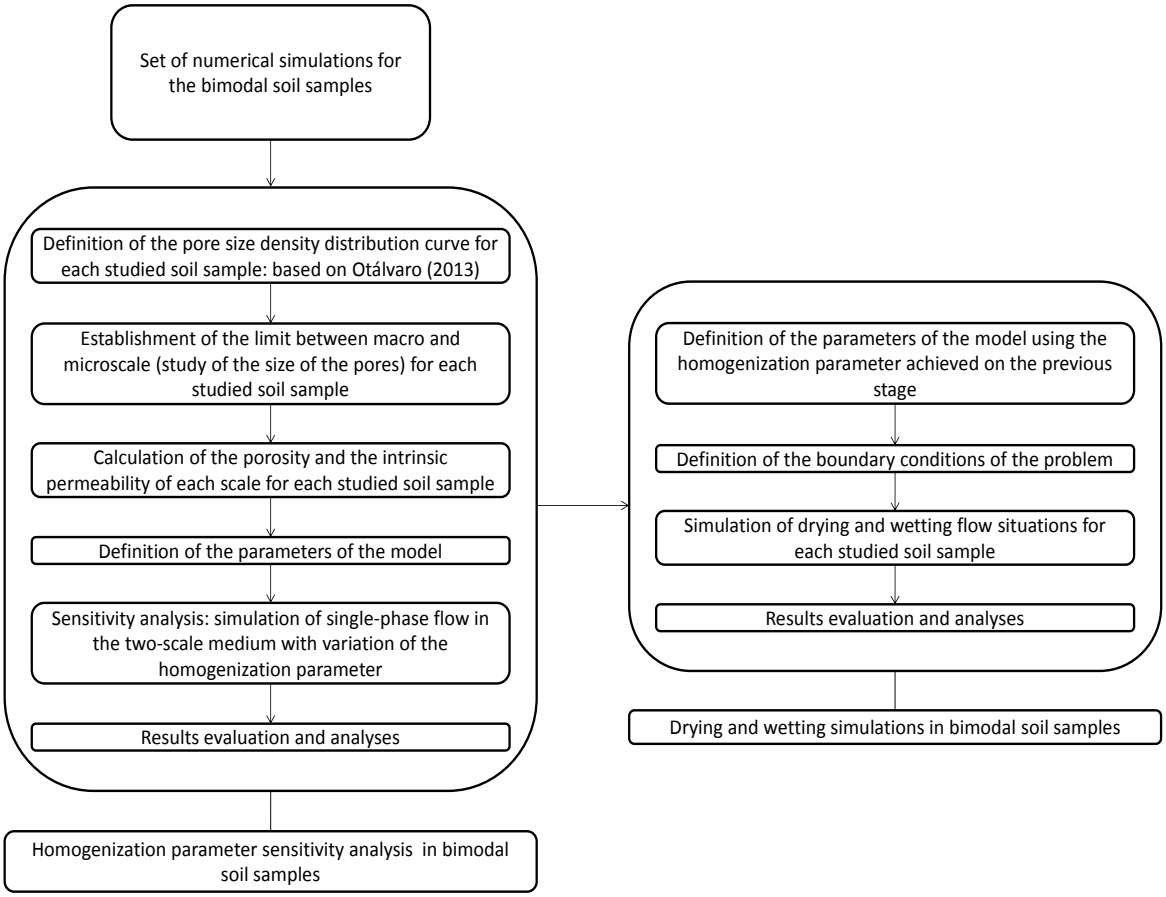

Figure 4.7 - Scheme for the Stage 2b of the research.

The Stage 3 of the research methodology corresponds to the evaluation and the analyses of the results of each set of simulations. The discussion of the achieved results is based on the literature review made for the present research, combined with verification of the hypotheses proposed with this work. All considerations made and the inferences projected from the achieved results are presented throughout Chapter 6.

4.2 NUMERICAL TOOL: FLEXPDE

In this research, the use of a numerical tool for solution of the problem is required for the simulation of fluid flow in multiscale media.

The numerical tool chosen for the mathematical solution of these problems is the software FlexPDE. This software has been developed by PDE Solutions Inc., with the main purpose of providing support to the solution of different problems in engineering and science. It is a processing tool for the numerical solution of various problems, including stress analysis and fluid mechanics.

The numerical solution the software provides is obtained with the application of the Finite Element Method. A single equation, or a coupled set of equations, are written by the user on the interface of the software, with the appropriate boundary conditions and prescribed initial values of variables, if necessary, and also information related to the geometry of the domain, giving a complete description of the problem. The data the user provides the software with forms a script for the solution of the problem. The following items should be filled out by the user, according to the characteristics of the problem (FlexPDE, 2006):

- Variables;
- Definitions: the parameters of the model, constitutive relations, e.g., should be informed;
- Equations: the equations that are going to be solved by the software should be informed. For each variable of the problem, there should be an equation;
- Boundaries: the boundary conditions of the problem should be defined;
- Plots: the user chooses which graphic are going to be plotted in order to monitor and verify the results of the problem.

An example of script of a problem implemented on FlexPDE is shown in Figure 4.8. This example is part of the samples that are available in the software.

```
{ POROUS.PDE }
{
 This problem describes the flow through an anisotropic porous foundation.
 It is taken from Zienkiewicz, "The Finite Element Method in Engineering Science",
 p. 305. }

title 'Anisotropic Porous flow'

variables
 pressure

definitions
 ky = 1
 kx = 4

equations
 dx(kx*dx(pressure)) + dy(ky*dy(pressure)) = 0

boundaries
 region 1
    start(0,0)
     natural(pressure)=0     line to (5,0) to (5,5)
     value(pressure)=0       line to (2,2)
     natural(pressure)=0     line to (2.5,2) to (2.5,1.95) to (1.95,1.95)
     value(pressure)=100     line to close
monitors
 contour(pressure)
plots
 contour(pressure)
 surface(pressure)
end   142486866
```

Figure 4.8 - Example of script implemented in FlexPDE (FlexPDE, 2006).

FlexPDE provides solution of the problem described in the script with an auto-iterative solution processing. The Finite Element mesh and time steps are updated according to need throughout the processing of the problem. For that reason, the number of elements and nodes, as well as the time step size, may vary during each simulation, becoming constant as the problem solution eventually stabilizes.

Given the flexibility FlexPDE provides to the user in terms of implementation of equations, boundary conditions and prescribed values of the variables, it seems to be a numerical tool suitable for the solution of the problem of flow in multiscale media. It is appropriate for simulating the conditions that are ought to be tested. Hence, it was chosen as the numerical tool for the numerical simulations proposed.

The formulation described in Chapter 5 was implemented on FlexPDE and used as model for the sets of simulations performed throughout the research efforts made for this doctorate thesis.

4.3 SUMMARY

As already mentioned, the main goal of this research is to study the hydraulic behavior of multiscale porous media. A numerical model is proposed for that purpose, and several

simulations are made in order to verify if the accuracy of the model in regards of representation of phenomena within multiscale samples.

In this chapter, the methodology of the research is presented. Each proposed simulation is thoroughly described, with an appropriate definition of the stages of the adopted research procedure.

Also, there is a description of the numerical tool used for simulation purposes, the software FlexPDE. The pre-processing procedure, with determination of all required information on the script is explained; the processing method of the software is described; and the post-processing tools are addressed, as well as any specificities the software may present that are significant for the purposes of the research.

5 DEFINITION OF THE MATHEMATICAL MODEL FOR FLOW SIMULATION IN MULTISCALE MEDIA

For the definition of an accurate model for representation of fluid flow in multiscale reservoir, one must verify the permeability and the storage conditions of the macro and the microscales. In many cases, a preferential path for fluid flow is observed in the interconnected fractures or macropores of the medium, as consequence of the difference of the order of magnitude between the permeability values of the macro and the microscale.

These particularities of the macro and microscale are significant in terms of hydraulic behavior and they should be taken into account in the formulation of the flow model.

The mathematical description of this type of medium can be accurate when using a dual continuum approach, where the matrix or the micropores and the fractures or the macropores are envisioned as two separate but overlapping continua, forming the multiscale medium (Diodato, 1994).

One of the main concerns related to the consideration of separate equations for each domain – microscale and macroscale – is the fact that the problem is treated in different scales. Therewith, there should be a coupling term in order to enable the solution of both equations at the same time.

The approach proposed by Arbogast et al. (1990) and Arbogast (1992) is an extension of Warren & Root's model with enhancements in the mathematical description of the problem, with the introduction of a homogenization procedure for the rock matrix and the fracture network's flow equations.

The formal two-scale homogenization procedure proposed by Arbogast et al. (1990) and Arbogast (1992) consists of introducing a term related to the scale in the formulation of the problem. This term is appropriate to allow the coupling between the fracture network flow equation and rock matrix flow equation in terms of scale, determining the correct form of interaction between the rock matrix and the fractures.

The homogenization is a specific type of upscaling procedure. Upscaling procedures can be applied when properties of the medium (porosity, permeability, *e.g.*), defined at the finest scale of the problem, must be scaled up, in order to both systems give results at the same scale. The use of the homogenization procedure is appropriate considering it allows deriving the exchange rate between micro and macroscale based on the principle of

conservation of mass, making this approach physically rigorous and adequate for description of the referred problem (Salimi, 2010).

The formal homogenization upscaling procedure is based on a rigorous mathematical deduction of the transfer term between the micro and the macroscale of the domain. Even though it may be an interesting alternative for representation of the hydraulic behavior of the medium, there are limitations in the numerical tool employed for the research (Section 4.2) that make the computational costs of the simulation expressive with this kind of approach.

So as to optimize the simulations and keep the physical consistency of the mathematical model, an adaptation of the transfer term is made for the model used in this thesis. The adapted homogenization upscaling used in the present research is, therefore, based on the assumptions made by Salimi (2010), and includes an adaption of the transfer term, as interpreted by the author of the present thesis.

This transfer term is used for mathematical representation of the transfer of mass between the micro and macroscale. It is assumed that this term is equivalent to an inlet/outlet term, with mass coming out of the microscale and flowing into the macroscale void space (pores or fractures, depending on the medium it is being studied at the time). This approach characterizes this mathematical formulation as a dual-porosity model. The specific representation of the term is presented later in Section 5.1, Equation (5.12).

Foremost, for better understanding of the physics of the studied phenomenon, the multiscale medium is represented as a model that is idealized as being periodic, *i.e.* it is divided in blocks, or cells, each of them with the same size and pattern, repeated periodically through the entire domain of study, as shown in Figure 5.1.

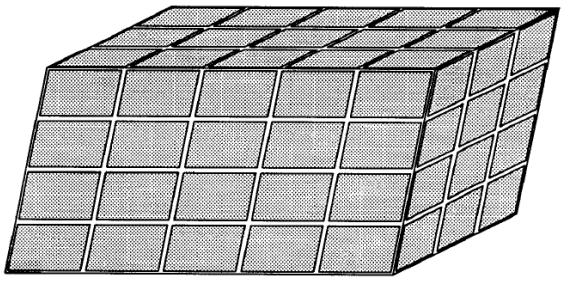

Figure 5.1 - The idealized periodic medium (Arbogast, 1992).

When analyzing this idealized medium, it can be established that there are three scales in this system (Arbogast, 1992):

- The scale of fracture thickness (microscale; finest, local scale);

- The scale of average distance between fracture planes (intermediate/coarse scale);
- The scale of the entire porous medium (macroscale; largest, global scale).

In this model, fluid flow takes place in the global scale of the problem (entire domain of study). This represents the macroscale flow: flow within the interconnected macropores (bimodal soils) or within the interconnected fractures (rock masses). Nevertheless, it is influenced by the local flow scale: the transfer of fluids between the micro and macroscale takes place. Hence, the governing equations of the problem must be written with the scale effect taken into consideration. As mentioned, the adapted homogenization procedure is the mathematical tool chosen for the solution of this problem, validating the relationship between the different scales so as to accurately represent the hydraulic behavior of a fractured medium.

5.1 UPSCALING: ADAPTED HOMOGENIZATION PROCEDURE FOR MULTISCALE FLOW MATHEMATICAL MODEL DEFINITION

The governing equations of the flow model for the micro and the macroscale are based on the principle of conservation of mass (Arbogast, 1992). Two different equations must be defined, each of them being valid for a specific part of the domain. Herein, it has its scale peculiarities: the flow through the macropores or fractures represents the effects on the global scale (macroscale) and the flow through the micropores or rock matrix is considered only on the local scale (microscale). Both equations should be in the same scale in order to make the solution of the problem possible. In order to solve the incompatibility of scales, the adapted homogenization procedure is used to adequately describe the equations.

The solution of the problem is presented in a generalized form, with the consideration of a two-phase fluid flow, based on the approach presented by Salimi (2010).

At first, it is necessary to define the geometry and the conditions of the problem. With that purpose, the domain of study is defined and adequately subdivided. The division of the medium follows the premises already depicted in Figure 5.1, with cells of the same size and repeated periodically throughout the medium.

For the study of bimodal soils, the cells are shaped with sets of soil grains, arranged in such way that macro and micropores are formed. The macropores are interconnected, establishing flow paths within the sample. This model is defined to characterize the structure

of the soil and it is the basis of definition of the domain for the analyses. The representation of the cells of the bimodal soil sample is made in Figure 5.2. Each cell includes macropores and micropores, as to best represent the characteristics of the medium. The coordinates are denoted by x_M for the global scale and x_m for the local scale.

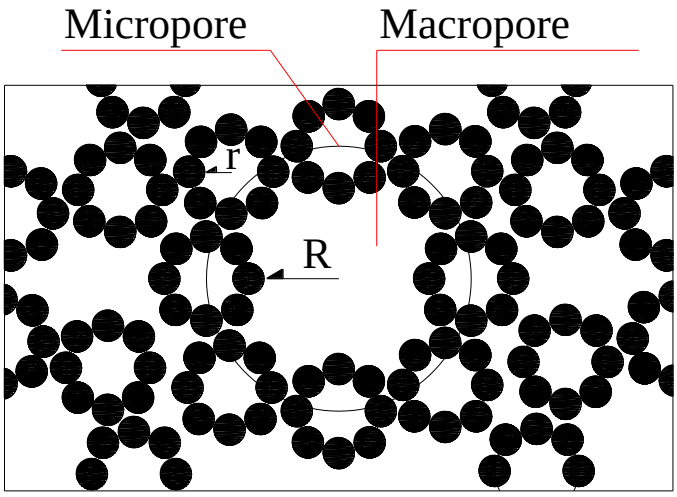

Figure 5.2 - Cell of the domain discretization for bimodal soils.

This choice of pattern for representation of the bimodal soil sample could denote certain limitation in terms of representativeness of the hydraulic behavior of real soil samples; nonetheless, it is considered sufficient for the study of the overall influence of the microstructure on the fluid flow and storage of this porous medium.

For the study of fractured media, such as reservoir rocks and rock masses, the cells are cubes with sides of size *l*, representing the local scale, and the entire domain of study is of size *L*, representing the global scale. This is depicted in Figure 5.3.

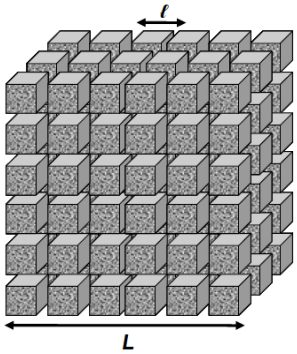

Figure 5.3 - Schematic representation of the medium with local and global scale side measurements (Salimi, 2010).

The representation of one of the cells of the fractured medium (rock mass or reservoir rock) is made in Figure 5.4. Each cell includes fractures and rock matrix portions, as to best represent the characteristics of the medium. The coordinates are denoted by x_M for the global scale and x_m for the local scale, following the same logic used for bimodal soils.

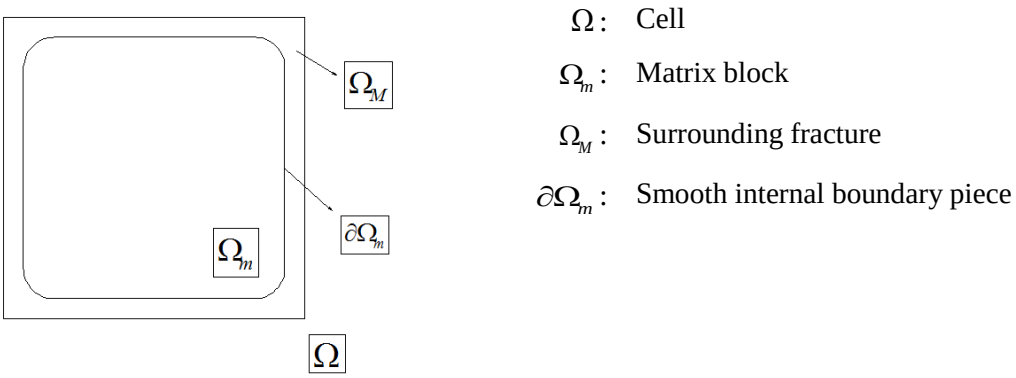

Figure 5.4 - Cell of the domain discretization for rocks.

Based on the geometry of the cells, a scaling parameter is defined so as to establish the relation between macro and microscale. For each type of porous medium (soil or rock), a different correlation for this parameter is made, in order to best represent the characteristics of the cell and the entire domain into the parameter. Nevertheless, the relationship of each part of the medium to the overall flow contribution must be respected (Arbogast, 1992).

For the bimodal soils, the measurements of the average value of micropore radius r and the mean value of macropore radius R are used as basis for calculation of the scaling. For the rock masses or reservoir rocks, the measurements of the side l of the cell and side L of the entire domain of study are the values used for the calculation of the homogenization parameter ε. Then, the homogenized model is conceived with the discretization of the domain into the referred individual cells (Figure 5.2 and Figure 5.4). The homogenization parameter for bimodal soils is calculated with the Equation (5.1).

$$\varepsilon = \frac{r}{R} \tag{5.1}$$

where: r represents the micropore radius average value (local, microscale) and R represents the macropore radius average value (global, macroscale).

The homogenization parameter for rock masses and reservoir rocks is calculated with the Equation (5.2):

$$\varepsilon = \frac{l}{L} \tag{5.2}$$

where: l represents the size of the side of the cell (local, microscale) and L represents the size of the side of the entire domain of study (global, macroscale).

The second step of the adapted homogenization procedure is to describe the governing equations of the problem. They are based on the principle of conservation of mass, for both macro and microscale. Equation (5.3) depicts this principle and it is used for the development of the mathematical model used in the present research.

$$-\vec{\nabla} \cdot \left(\vec{v}_{\alpha i} \right) = \phi_i \frac{\partial S_{\alpha i}}{\partial t} + S_{\alpha i} \frac{\partial \phi_i}{\partial t} \tag{5.3}$$

where: $\vec{v}_{\alpha i}$ is the velocity of the α - fluid phase of the i part of the domain, ϕ_i is the porosity of the i part of the domain and $S_{\alpha i}$ is the degree of saturation of the α - fluid phase of the i part of the domain.

The subscript i and α are used throughout the present research to represent the part of the domain (subscript i) or the type of fluid is being evaluated (subscript α). For the representation of each part of the domain, it is defined that $i=m, M$; m is used for microscale – micropores or rock matrix; M is used for macroscale – macropores or fracture network. For the representation of the type of fluid, it is defined that $\alpha = w, nw$; w is used for the wetting fluid; nw is used for the non-wetting fluid.

Also, it is taken into consideration that two fluid phases are studied in the present research, wetting and non-wetting phases. The non-wetting fluid phase is assumed to be continuous, with the range of values of capillary pressure comprising the conditions of continuity of both wetting and non-wetting fluid phases in the performed simulations. Therewith, there are no cases addressed for the situations in which bubbles of the wetting (low values of capillary pressure) or the non-wetting (high values of capillary pressure) fluid are formed. Moreover, regardless the type of fluid that percolates through the studied porous medium, the α-fluid phase is considered incompressible and, therefore, the density and the viscosity of the α - fluid phase are assumed constant.

The physical representativeness of Equation (5.3) can be evaluated: the first term of the equation (term of the left side of the referred equation) mathematically represents the flow portion of the overall hydraulic behavior in analysis. The other two terms (right side of the referred equation) mathematically represent the storage of fluids within the porous medium for each scale in analysis.

The velocity of the α - fluid phase of the *i* part of the domain is described following Darcy's law, as shown in Equation (5.4):

$$\vec{v}_{\alpha i} = -K_i k_{r_{\alpha i}} \frac{\rho_\alpha g}{\mu_\alpha} \vec{\nabla} h_{\alpha i} \tag{5.4}$$

where: K_i is the intrinsic permeability of the *i* part of the domain, $k_{r_{\alpha i}}$ is the relative permeability of the α - fluid phase of the *i* part of the domain, ρ_α is the specific mass of the α - fluid phase, g is the gravity, μ_α is the viscosity of the α - fluid phase and $h_{\alpha i}$ is the hydraulic head of the α - fluid phase of the *i* part of the domain.

The intrinsic permeability should be mathematically expressed as a tensor, whereas it could be arranged so as to take into consideration the anisotropy of the specific addressed part of the domain. In the present research, the medium is assumed to be homogeneous and isotropic for both scales. With that, a simplification in the representation of the tensor is made, and it is reduced to its scalar form, as shown in Equation (5.4).

The relative permeability can be defined as shown in Equations (5.5) and (5.6):

$$k_{r_{wi}} = \left(S_{wi}\right)^2 \tag{5.5}$$

$$k_{r_{nwi}} = \left(1 - S_{wi}\right)^2 \tag{5.6}$$

where: S_{wi} is the degree of saturation of the wetting fluid phase of the *i* part of the domain.

The hydraulic head can be mathematically defined as expressed in Equation (5.7):

$$h_{\alpha i} = \frac{p_{\alpha i}}{\rho_\alpha g} + y \tag{5.7}$$

where: $p_{\alpha i}$ is the pressure of the α - fluid phase of the *i* part of the domain and *y* indicates the elevation. The first term of the hydraulic head is the pressure or piezometric head and the second term of the hydraulic head is the elevation head.

The derivative in the third term of Equation (5.3) should be treated as to accurately represent the hydraulic behavior of the studied problems of the present research. Then, the porosity of the *i* part of the domain can be expressed in terms of void ratio, as shown in Equation (2.10).

The volumetric strain for porous media is defined as expressed in Equation (5.8):

$$E_i^v = \frac{\Delta e_i}{1 + e_{0i}} \tag{5.8}$$

where: Δe_i is the void ratio variation rate and e_{0i} is the initial void ratio.

Also, one can assume that the volumetric strain and the porosity of the studied porous medium are related as shown in Equations (5.9) and (5.10):

$$d\phi_i = dE_i^v \tag{5.9}$$

$$\frac{\partial \phi_i}{\partial t} = \frac{\partial E_i^v}{\partial t} \tag{5.10}$$

where: E_i^v is the volumetric strain of *i* part of the domain.

One of the premises assumed by Biot (1941) in the general theory of consolidation behavior of porous media is that any variation in the void ratio of the sample is proportional to the effective stress increment to which this sample is subjected. Also, the effective stress increment is related to the fluid pressure, and a relationship between porosity and fluid pressure can be expressed as shown in Equation (5.11).

$$\frac{\partial \phi_i}{\partial t} = \frac{\partial E_i^v}{\partial p_{\alpha i}} \frac{\partial p_{\alpha i}}{\partial t} = m_{\alpha i}^v \frac{\partial p_{\alpha i}}{\partial t} \tag{5.11}$$

where: $m_{\alpha i}^v$ is the coefficient of volume compressibility of the α - fluid phase of *i* part of the domain.

Moreover, the transfer term must be included in the presented formulation. The conservation of mass equation must be redefined with the addition of the term that physically represents the exchange of fluids between the micro and macroscale of the domain.

For the present research, it is assumed that transfer occurs from the local, microscale to the global, macroscale. This accurately defines the flow direction within the domain. The format of the transfer function is based on the research work presented by Sabathier et al. (1998), Lemonier & Borbiaux (2010) and Szymkiewicz (2013). Also, this assumption makes the interpretation of the transfer flow using the hydraulic parameters of the microscale appropriate for the description of the phenomenon. Also, it is assumed that the transferring occurs only within the same α - fluid phase. This form of expressing the contribution of the microscale stored fluids to the macroscale corresponds to a dual-porosity model approach. The transfer term is mathematically defined as shown in Equation (5.12):

$$T_\alpha = -K_m k_{r_{\alpha m}} \frac{\rho_\alpha g}{\mu_\alpha} \frac{\left(h_{\alpha m} - h_{\alpha M}\right)}{s^2} = -b_\alpha \left(h_{\alpha m} - h_{\alpha M}\right) \tag{5.12}$$

where: K_m is the intrinsic permeability of the microscale, $k_{r_{\alpha i}}$ is the relative permeability of the α-fluid phase of the microscale; ρ_α is the specific mass and μ_α is the viscosity of the α - fluid phase, g is the gravity, and $h_{\alpha i}$ is the hydraulic head of the a-fluid phase of the i part of the domain. b_α is defined as the transfer parameter of the α-fluid phase.

s is a geometric parameter that varies according to the type of problem is being analyzed. The assumed values are based on the geometric representation of the medium, following the premises already shown in Figure 5.2 and Figure 5.4. They are mathematically expressed in Equation (5.13) – valid for bimodal soils – and Equation (5.14) – valid for fractured rocks:

$$s = r \tag{5.13}$$

$$s = \frac{l}{2} \tag{5.14}$$

where: r represents the micropore radius average value of the bimodal soil sample and l represents the size of the side of the cell of the rock mass or reservoir rock analyzed.

Finally, the problem can be mathematically represented for the two scales that are envisioned in the present study: micro and macroscale. Since there are terms of each equation in different scales, it is necessary to assemble the system of equations and redefine the equations in the same scale in order to maintain physical consistency of the model.

The next step of the adapted homogenization procedure is the differentiation in the equations of the model in macro and microscale terms. The terms involved in the representation of the conservation of mass within the microscale need to be revised. Therewith, it is made the consideration of the homogenization parameter ε as mathematical tool to transform the small scale terms and make the equations appropriate for the evaluation of the overall flow and storage conditions of the studied medium. After the adapted homogenization procedure, the equations should be in the same scale. The differentiation operator (nabla) is adapted for the small scale terms as shown in Equation (5.15):

$$\vec{\nabla}_s = \varepsilon^{-1}\vec{\nabla} \tag{5.15}$$

where: $\vec{\nabla}_s$ is the differentiation operator for the small (*s*), local scale, ε is the homogenization parameter and $\vec{\nabla}$ is the differentiation operator for the global, macro scale.

After all the mentioned assumptions and procedures are made, the final form of the transport equations for the studied problem can be achieved, as depicted in Equation (5.16) for the macroscale and Equation (5.17) for the microscale hydraulic behavior.

$$\vec{\nabla}\cdot\left(K_M k_{r_{\alpha,M}}\frac{\rho_\alpha g}{\mu_\alpha}\vec{\nabla}h_{\alpha,M}\right) = \phi_M\frac{\partial S_{\alpha M}}{\partial t} + S_{\alpha M}m^{v}_{\alpha M}\frac{\partial p_{\alpha M}}{\partial t} - b_\alpha\left(h_{\alpha m} - h_{\alpha M}\right) \tag{5.16}$$

$$\frac{1}{\varepsilon^2}\vec{\nabla}\cdot\left(K_m k_{r_{\alpha m}}\frac{\rho_\alpha g}{\mu_\alpha}\vec{\nabla}h_{\alpha m}\right) = \phi_m\frac{\partial S_{\alpha m}}{\partial t} + S_{\alpha m}m^{v}_{\alpha m}\frac{\partial p_{\alpha m}}{\partial t} + b_\alpha\left(h_{\alpha m} - h_{\alpha M}\right) \tag{5.17}$$

In these equations, it is possible to physically evaluate the terms that explain the hydraulic behavior of the medium.

The term of the left side of the equations represents the net flow balance of the α - fluid phase of *i* part of the domain. The right side of the equation is related to the storage conditions of the medium. Its first term, regulated by the saturation degree of the α - fluid phase of *i* part of the domain, represents the storage capacity within the *i* part of the domain.

The second term of the right side of the equations, regulated by the pressure of the α - fluid phase of *i* part of the domain, represents the variation of the amount of fluid within the *i* part of the domain given the straining of the porous medium. The third term represents the transferring of the α - fluid phase from the microscale to the macroscale, contributing to the overall flow within the medium.

5.2 ASSEMBLING OF THE SYSTEM OF UPSCALED TWO-PHASE FLOW EQUATIONS AND REDUCTION OF VARIABLES OF THE PROBLEM

The mathematical approach shown in Section 5.2 is appropriate for the description of the problem of fluid flow in multiscale media. For the assembling of the problem, the transport equations have been arranged so as to adequately represent the hydraulic behavior of the studied problem. The adapted homogenization procedure has been employed for the transformation of the equations, solving the difficulties related to the scale of the problem.

There are, however, some specificity of the equations and the variables that must be verified in order to make the solution of the problem feasible.

After the homogenization procedure, the mathematical model is presented as follows. There are six independent variables: two phase pressures (wetting pressure and non-wetting pressure), two hydraulic heads (wetting hydraulic head and non-wetting hydraulic head) and two saturations (wetting saturation and non-wetting saturation). However, there are only four equations for description of the problem: macroscale flow of the wetting fluid (Equation (5.18)), microscale flow of the wetting fluid (Equation **Erro! Fonte de referência não encontrada.**), macroscale flow of the non-wetting fluid (Equation (5.20)) and microscale flow of the non-wetting fluid (Equation (5.21)). These are the upscaled two-phase flow equations, already transformed and properly presented to describe the problem, as shown in Section 5.1.

$$\vec{\nabla}\cdot\left(K_M k_{r_{wM}}\frac{\rho_w g}{\mu_w}\vec{\nabla}h_{wM}\right)=\phi_M\frac{\partial S_{wM}}{\partial t}+S_{wM}m_{wM}^{v}\frac{\partial p_{wM}}{\partial t}-b_w\left(h_{wm}-h_{wM}\right) \tag{5.18}$$

$$\frac{1}{\varepsilon^2}\vec{\nabla}\cdot\left(K_m k_{r_{wm}}\frac{\rho_w g}{\mu_w}\vec{\nabla}h_{wm}\right)=\phi_m\frac{\partial S_{wm}}{\partial t}+S_{wm}m_{wm}^{v}\frac{\partial p_{wm}}{\partial t}+b_w\left(h_{wm}-h_{wM}\right) \tag{5.19}$$

$$\vec{\nabla}\cdot\left(K_M k_{r_{nwM}}\frac{\rho_{nw}g}{\mu_{nw}}\vec{\nabla}h_{nwM}\right)=\phi_M\frac{\partial S_{nwM}}{\partial t}+S_{nwM}m^{v}_{nwM}\frac{\partial p_{nwM}}{\partial t}-b_{nw}\left(h_{nwm}-h_{nwM}\right) \quad (5.20)$$

$$\frac{1}{\varepsilon^2}\vec{\nabla}\cdot\left(K_m k_{r_{nwm}}\frac{\rho_{nw}g}{\mu_{\alpha}}\vec{\nabla}h_{nwm}\right)=\phi_m\frac{\partial S_{nwm}}{\partial t}+S_{nwm}m^{v}_{nwm}\frac{\partial p_{nwm}}{\partial t}+b_{nw}\left(h_{nwm}-h_{nwM}\right) \quad (5.21)$$

This number of equations is not sufficient for the solution of the problem, given the number of variables there are. Therefore, it is essential to use strategies for reducing the number of variables of the problem, so as to make the solution of the problem possible.

The approach chosen for the final form of the equations is to present the results in terms of the variables of pressure of the wetting phase ($p_{\alpha M}$ and $p_{\alpha m}$) and saturation degree of the wetting phase ($S_{\alpha M}$ and $S_{\alpha m}$). Three assumptions can be made in order to reduce the number of variables. At first, the pressures are defined as function of the hydraulic head (Equation (5.7)). With that, one can consider that the two variables of pressure are the calculated values when the analyses are performed. In terms of the numerical model, the hydraulic head of the α - fluid phase of the *i* part of the domain is expressed on the DEFINITIONS section of the written script for the studied model in the software FlexPDE (Section 4.2).

The second step is to eliminate one of the saturations when the volume-balance relation is established. The volume-balance relation is depicted in Equations (5.22) and (5.23).

$$S_{wM}+S_{nwM}=1\rightarrow S_{nwM}=1-S_{wM} \quad (5.22)$$

$$S_{wm}+S_{nwm}=1\rightarrow S_{nwm}=1-S_{wm} \quad (5.23)$$

where: S_{wM} and S_{nwM} are the degree of saturation of the wetting and the non-wetting fluid in the macroscale, respectively; and S_{wm} and S_{nwm} are the degree of saturation of the wetting and the non-wetting fluid in the microscale, respectively.

In addition, the relationship that exists between the pressure of the wetting and the non-wetting fluid phases is defined. The capillary pressure is the variable employed for that purpose, as shown in Equations (5.24) and (5.25).

$$p_{c_M}=p_{nw_M}-p_{w_M}\rightarrow p_{nw_M}=p_{c_M}+p_{w_M} \quad (5.24)$$

$$p_{c_m} = p_{nw_m} - p_{w_m} \rightarrow p_{nw_m} = p_{c_m} + p_{w_m} \tag{5.25}$$

where: p_{c_M} is the capillary pressure of the macroscale and p_{c_m} is the capillary pressure of the microscale.

It is important to highlight that there is also an established relationship between the capillary pressure and the degree of saturation of the wetting phase. It is known as the soil-water characteristic curve (SWCC) or water retention curve (WRC), as defined by van Genuchten (1980). It is mathematically expressed as shown in Equation (5.26):

$$p_{c_i} = a_i \left[\left(\frac{1 - S_{res_{wi}}}{S_{wi} - S_{res_{wi}}} \right)^{\frac{1}{m_i}} - 1 \right]^{\frac{1}{n_i}} \tag{5.26}$$

where: p_{c_i} is the capillary pressure of the *i* part of the domain, $S_{res_{wi}}$ is the residual degree of saturation of the wetting phase in the *i* part of the domain, a_i, m_i and n_i are calibration parameters of the curve (adjusted to the provided data).

The derivative form of the SWCC is necessary for the calculation proposed in the mathematical model used in the present research. This is defined in Equation (5.27):

$$\frac{\partial}{\partial S_{wi}} \left(p_{c_i} \right) = - \frac{a_i \left[\left(\frac{1 - S_{res_{wi}}}{S_{wi} - S_{res_{wi}}} \right)^{\frac{1}{m_i}} - 1 \right]^{\frac{1}{n_i}} \left(\frac{1 - S_{res_{wi}}}{S_{wi} - S_{res_{wi}}} \right)^{\frac{1}{m_i}}}{n_i m_i \left(S_{wi} - S_{res_{wi}} \right) \left[\left(\frac{1 - S_{res_{wi}}}{S_{wi} - S_{res_{wi}}} \right)^{\frac{1}{m_i}} - 1 \right]} \tag{5.27}$$

With all the assumptions made so as to reduce the number of variables of the presented formulation, the equations of the studied phenomenon must be rearranged. The final form of the transport equations after the procedure of reduction of variables is depicted in Equations (5.28), (5.29), (5.30) and (5.31). Each equation refers to part of the multiscale medium hydraulic behavior problem:

- Equation (5.28): final form of the wetting phase macroscale equation;

- Equation (5.29): final form of the wetting phase microscale equation;
- Equation (5.30): final form of the non-wetting phase macroscale equation;
- Equation (5.31): final form of the non-wetting phase microscale equation;

$$\nabla \cdot \left(K_M k_{r_{wM}} \frac{\rho_w g}{\mu_w} \nabla h_{wM} \right) = \phi_M \frac{\partial S_{wM}}{\partial t} + S_{wM} m_{wM}^{v} \frac{\partial p_{wM}}{\partial t} - b_w \left(h_{wm} - h_{wM} \right) \tag{5.28}$$

$$\frac{1}{\varepsilon^2} \nabla \cdot \left(K_m k_{r_{wm}} \frac{\rho_w g}{\mu_w} \nabla h_{wm} \right) = \phi_m \frac{\partial S_{wm}}{\partial t} + S_{wm} m_{wm}^{v} \frac{\partial p_{wm}}{\partial t} + b_w \left(h_{wm} - h_{wM} \right) \tag{5.29}$$

$$\begin{aligned} \nabla \cdot \left(K_M k_{r_{nwM}} \frac{\rho_{nw} g}{\mu_{nw}} \nabla h_{nwM} \right) = -\phi_M \frac{\partial S_{wM}}{\partial t} + \left(1 - S_{wM}\right) m_{nwM}^{v} \frac{\partial p_{c_M}}{\partial S_{wM}} \frac{\partial S_{wM}}{\partial t} \\ + \left(1 - S_{wM}\right) m_{nwM}^{v} \frac{\partial p_{wM}}{\partial t} - b_{nw} \left(h_{nwm} - h_{nwM} \right) \end{aligned} \tag{5.30}$$

$$\begin{aligned} \frac{1}{\varepsilon^2} \nabla \cdot \left(K_m k_{r_{nwm}} \frac{\rho_{nw} g}{\mu_\alpha} \nabla h_{nwm} \right) = -\phi_m \frac{\partial S_{wm}}{\partial t} + \left(1 - S_{wm}\right) m_{nwm}^{v} \frac{\partial p_{c_M}}{\partial S_{wm}} \frac{\partial S_{wm}}{\partial t} \\ + \left(1 - S_{wm}\right) m_{nwm}^{v} \frac{\partial p_{wm}}{\partial t} + b_{nw} \left(h_{nwm} - h_{nwM} \right) \end{aligned} \tag{5.31}$$

The set of equations assembled for the solution of the problem are satisfactory for the purposes of flow simulation of the presented research and, therefore, they were used for the detailing of the problem in FlexPDE, allowing its numerical solution, as previewed in the research methodology (Chapter 4). The variables and the input data of the proposed mathematical model are organized in Figure 5.5 and Figure 5.6.

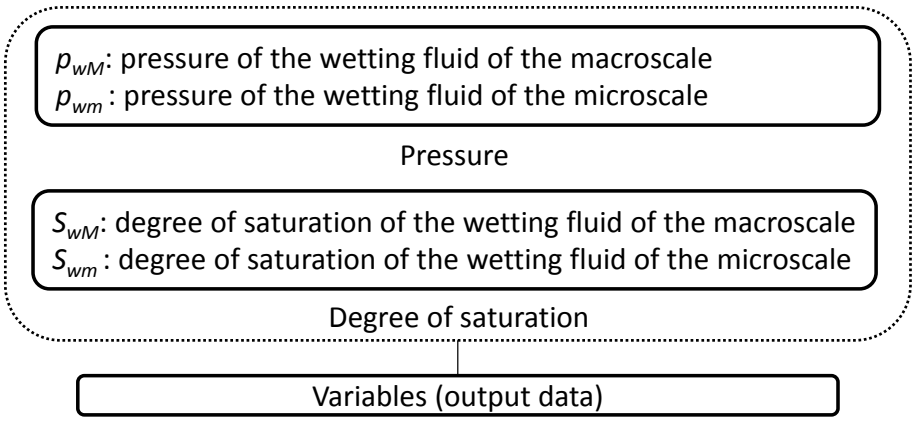

Figure 5.5 - Schematic representation of the variables (output) of the proposed mathematical model.

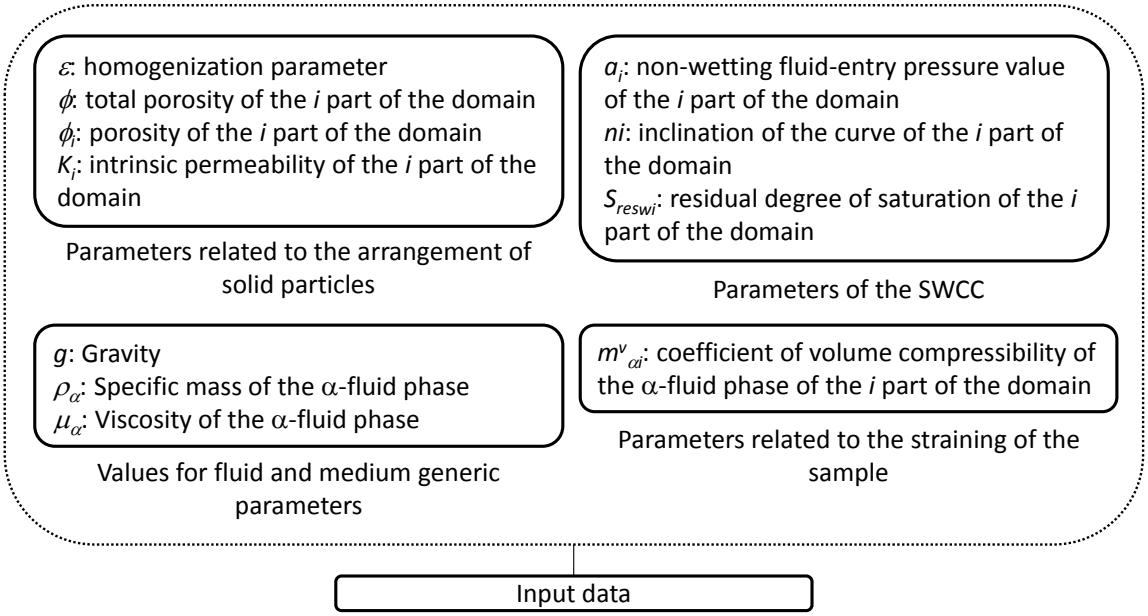

Figure 5.6 - Schematic representation of the input data for the proposed mathematical model.

5.3 ASSEMBLING OF THE SYSTEM OF EQUATIONS FOR THE MULTISCALE APPROACH OF THE CONSOLIDATION PROBLEM SIMULATION

The consolidation problem is a combination of the mechanical and the hydraulic behavior of the porous medium. The imposition of load implies on straining of the sample, with reduction of the voids. This reduction of volume of the pores has an effect over the hydraulic behavior of the sample, with flow being induced.

In the present research, the consolidation analyses proposed take into consideration the multiscale assumption made for the hydraulic behavior verifications. Therewith, the governing equations for the flow portion of the problem follow the same premises presented on Sections 5.1 and 5.2.

An additional equation must be established for the mechanical part of the overall behavior of the medium when representing the consolidation process in porous media.

At first, the equations for the hydraulic behavior of the medium are rearranged so as to comprise the conditions of flow during the consolidation process in the multiscale medium. They are based on the principle of conservation of mass, for both macro and microscale.

As already shown, Equation (5.3) depicts this principle and it is used for the development of the multiscale flow mathematical model used in the present research, with the assumption of incompressibility of the fluid phases maintained for this part of the research

(density and viscosity are assumed constant). Also, it is important to highlight that the transfer term must be kept in fluid equations so as to accurately represent the specificities of the multiscale media flow behavior, as already discussed in Section 5.1.

The velocity and the porosity, part of Equation (5.3) must be evaluated for consolidation mathematical model purposes. The velocity of the α - fluid phase of the *i* part of the domain is described following Darcy's law, as shown in Equation (5.4).

For the assessment of the porosity term in the model, the relationship established between volumetric strain and void ratio of the medium is assumed valid. In Equation (5.10), it is shown that the time derivative of the porosity is equivalent to the time derivative of the volumetric strain. Therefore, it is possible to rearrange the flow mathematical model with this consideration, as depicted in Equations (5.32) and (5.33).

$$\vec{\nabla}\cdot\left(K_M k_{r_{\alpha M}}\frac{\rho_\alpha g}{\mu_\alpha}\vec{\nabla}h_{\alpha M}\right)=\phi_M\frac{\partial S_{\alpha M}}{\partial t}+S_{\alpha M}\frac{\partial E_M^v}{\partial t}-b_\alpha\left(h_{\alpha m}-h_{\alpha M}\right) \tag{5.32}$$

$$\frac{1}{\varepsilon^2}\vec{\nabla}\cdot\left(K_m k_{r_{\alpha m}}\frac{\rho_\alpha g}{\mu_\alpha}\vec{\nabla}h_{\alpha m}\right)=\phi_m\frac{\partial S_{\alpha m}}{\partial t}+S_{\alpha m}\frac{\partial E_m^v}{\partial t}+b_\alpha\left(h_{\alpha m}-h_{\alpha M}\right) \tag{5.33}$$

The volumetric strain E_i^v of *i* part of the domain (*i*=*m*, *M*; *m* is used for microscale; *M* is used for macroscale) can be defined for a two-dimensional analysis as shown in Equation (5.34):

$$E_M^v=E_{x_M}+E_{y_M}+E_m^v \tag{5.34}$$

where: E_M^v is the macroscale volumetric strain for a two-dimensional analysis, E_m^v is the microscale volumetric strain for a two-dimensional analysis, E_{x_M} is the x-component of strain and E_{y_M} is the y-component of strain.

The *x* and the *y*-component of strain are shown in Equations (5.35) and (5.36):

$$E_{x_M}=\frac{\partial u_M}{\partial x_M} \tag{5.35}$$

$$E_{y_M} = \frac{\partial v_M}{\partial y_M} \tag{5.36}$$

where: u_M and v_M are the displacements in the *x*- and the *y*-direction, respectively (using the macroscale as reference for the analysis).

The component of strain indicated by E_m^v is exclusively related to the volumetric straining behavior of the microscale and it is used as the mathematical way to represent the effect of straining of the microscale affecting the macroscale. The approach chosen for this purpose follows the premises already discussed and shown in Equation (5.11). Then, the time derivative of this strain component is defined as shown in Equation (5.37):

$$\frac{\partial E_m^v}{\partial t} = \frac{\partial E_m^v}{\partial p_{\alpha m}} \frac{\partial p_{\alpha m}}{\partial t} = m_{\alpha m}^v \frac{\partial p_{\alpha m}}{\partial t} \tag{5.37}$$

where: $m_{\alpha i}^v$ is the coefficient of volume compressibility of the α - fluid phase acting on the microscale and $p_{\alpha m}$ is the pressure of the α - fluid phase acting on the microscale.

Finally, the equations for the mechanical part of the overall behavior of the porous medium are established. This mathematical model is based on the principle of conservation of linear momentum and can be depicted by Equations (5.38) and (5.39):

$$\frac{\partial \sigma_{x_M}}{\partial x_M} + \frac{\partial \tau_{x_M y_M}}{\partial y_M} = 0 \tag{5.38}$$

$$\frac{\partial \sigma_{y_M}}{\partial y_M} + \frac{\partial \tau_{x_M y_M}}{\partial x_M} = -\gamma \tag{5.39}$$

where: σ_{x_M} , σ_{y_M} and $\tau_{x_M y_M}$ are total stress components in the indicated directions (using the macroscale as reference for the analysis) and γ is the specific weight of the soil.

The normal components of total stress σ_{x_M} and σ_{y_M} are defined in terms of effective stress and fluid pressure, as shown in Equations (5.40) and (5.41):

$$\sigma_{x_M} = \sigma'_{x_M} + \bar{p} \tag{5.40}$$

$$\sigma_{y_M} = \sigma'_{y_M} + \bar{p} \tag{5.41}$$

where: σ'_{x_M} and σ'_{y_M} are the effective stress components in the indicated directions (using the macroscale as reference for the analysis) and $\bar{p}$ corresponds to an average value of fluid pressure acting on the porous medium.

The definition made for the calculation of the average value of fluid pressure acting on the porous medium corresponds to the simultaneous effect of the macro and microscale fluid pressure of the wetting and non-wetting fluid phases, as defined by Choo et al. (2016). The mathematical representation used in the present research of this definition is an adaptation of the approach shown by Choo et al. (2016) so as to appropriately address the variables and the parameters used throughout this thesis. The average value of fluid pressure acting on the porous medium is shown in Equation (5.42).

$$\bar{p} = \sum_{i=M,m} \left[\left(e_i e S_{wi} \right) p_{wi} + \left(e_i e S_{nwi} \right) p_{nwi} \right] \tag{5.42}$$

where: e_i is the void ratio parameter of the i part of the domain; e is the total void ratio parameter of the sample; S_{wi} and S_{nwi} are the degree of saturation of the wetting and the non-wetting fluids of the i part of the domain, respectively; p_{wi} and p_{nwi} are the pressure of the wetting and the non-wetting fluids of the i part of the domain, respectively.

It is important to highlight that the approach shown in Equation (5.42) is valid for continuous fluid phases and for any values of pressure, including the values different from zero for the non-wetting fluid phase. This is significant for the generalization of the proposed formulation, considering that if the mathematical model were only suitable for air, the value of the non-wetting fluid phase would be considered zero and all equations would have this simplification. This makes the formulation appropriate for the simulation of problems with the non-wetting fluid phase of any kind.

Then, it is necessary to establish the relationship between strain and stress components. This depends on the constitutive model chosen for the proposed analyses. In the case of the linear elastic model being used, the effective stress components can be related to the straining components as depicted in Equations (5.43) and (5.44):

$$\sigma'_{x_M} = \lambda \varepsilon_M^v + 2\mu E_{x_M} \tag{5.43}$$

$$\sigma'_{y_M} = \lambda \varepsilon_M^v + 2\mu E_{y_M} \tag{5.44}$$

where: λ and 2μ are the Lamé coefficients.

The Lamé coefficients can be defined as shown in Equations (5.45) and (5.46):

$$\lambda = \frac{\nu E}{(1+\nu)(1-2\nu)} \tag{5.45}$$

$$2\mu = \frac{E}{1+\nu} \tag{5.46}$$

where: E is the modulus of elasticity and ν is the Poisson's ratio.

The definition of the relationship between stress and strain must also be made for the shear component of stress. If the linear elastic model is assumed for simulation purposes, this is established as shown in Equation (5.47):

$$\tau_{x_M y_M} = G\gamma_{x_M y_M} \tag{5.47}$$

where: G is the shear modulus and $\gamma_{x_M y_M}$ is the distortion component of strain.

The distortion component of strain is defined as shown in Equation (5.48):

$$\gamma_{x_M y_M} = \frac{\partial u_M}{\partial y_M} + \frac{\partial v_M}{\partial x_M} \tag{5.48}$$

where: u_M and v_M are the displacements in the x- and the y-direction, respectively (using the macroscale as reference for the analysis).

Given the assumptions made in terms of representation of the principle of conservation of linear momentum, and considering they are valid for the study proposed in the present research, the set of equations presented in this section of the thesis is adequate for the simulation of the consolidation problem of the multiscale samples.

5.4 SUMMARY

The main focus of this research is the definition of a mathematical model capable of representing the effects of a multiscale approach on the hydraulic behavior prediction analysis. Therewith, the developed mathematical model is presented in this chapter.

Following the approach mentioned in Chapter 3, a dual-porosity model is proposed based on the principle of conservation of mass and including an adaption of the transfer term as interpreted by the author of the present thesis.

The flow equations are defined for two scales within the medium: a macroscale, physically represented by the larger pores of a bimodal soil sample, or the fractures of a fractured rock medium, and a microscale, correspondent to the smaller pores of a bimodal soil sample, or the rock matrix of a fractured rock medium.

The equations of the macroscale and the microscale should be in the same scale in order to enable the solution of the problem. In order to solve the incompatibility of scales, the adapted homogenization procedure is used. This is the chosen method for upscaling the equations that mathematically represent the addressed problem.

Also, two fluid phases are considered within the porous medium: a non-wetting and a wetting fluid phase. With two scales and two types of fluids within the porous sample, four equations are defined for the reproduction of the hydraulic behavior of the medium.

Finally, the assembling of these equations into a system for numerical solution is addressed for two different cases: upscaled two-phase flow simulation, and multiscale approach of the consolidation problem.

The mathematical model assembled and shown in Chapter 5 was implemented on the FlexPDE software and used for the simulations proposed in the present research.

It is important to highlight that the referred mathematical model is appropriate for evaluation of the hydraulic behavior of any multiscale media. When addressing porous media, both soils and rocks may present multiscale hydraulic characteristics with distinct patterns of porosity and permeability. This implies on specific fluid flow distribution within the medium among the scales.

Evaluating the proposed formulation altogether, it can be noticed it is appropriate for the description of any multiscale hydraulic behavior approach for porous media, regardless of being a soil or a rock. The versatility of this mathematical model is one of its main advantages and therefore, it is assessed in the present research.

6 FLOW SIMULATION FOR MULTISCALE MEDIA

The validity of the proposed mathematical model was assessed with simulations on a theoretical and on real bimodal soil samples.

The main goal with the theoretical sample simulations was verifying the model representativeness in terms of the specificities of the hydraulic behavior of a bimodal medium and also the range of values that could be used for providing accurate results. The results of the performed tests are presented in Section 6.1.

Then, the simulations were made based on the experimental data of Otálvaro (2013) for bimodal soil samples. The results for this set of simulations are presented in Section 6.2.

6.1 SIMULATION OF FLOW IN A THEORETICAL BIMODAL SOIL SAMPLE

For this stage of the research, the main focus was on understanding the limits of the model in what concerns the hydraulic behavior of a bimodal soil sample. The simulations made with that purpose are addressed in Sections 6.1.1, 6.1.2, 6.1.3 and 6.1.4.

6.1.1 DEFINITION OF PARAMETERS FOR THE THEORETICAL SOIL SAMPLE

The first step was the definition of the total and microscale void ratio values for this theoretical bimodal soil sample. Afterwards, the microscale void ratio value was determined. The total void ratio was set as 1,000, followed by the microscale void ratio, 0,750. These choices were based on the values observed for the samples tested by Otálvaro (2013).

Using these values, it was possible to determine the macroscale void ratio with Equation (2.7), followed by the definition of the curve that establishes the relationship between the capillary pressure and wetting fluid void ratio values using Equation (2.5). The coefficients of the curve are calibrated so as make it appropriate for this simulation stage.

Finally, the degree of saturation of the sample is calculated with the values of wetting fluid void ratio acquired in the previous step. This is made with Equation (2.8). After this, it is possible to define the SWCC for the theoretical bimodal soil sample. It presents a format typical for bimodal soil samples, with two plateaus corresponding to the non-wetting fluid entry values for the macro and micropores, as shown in Figure 6.1.

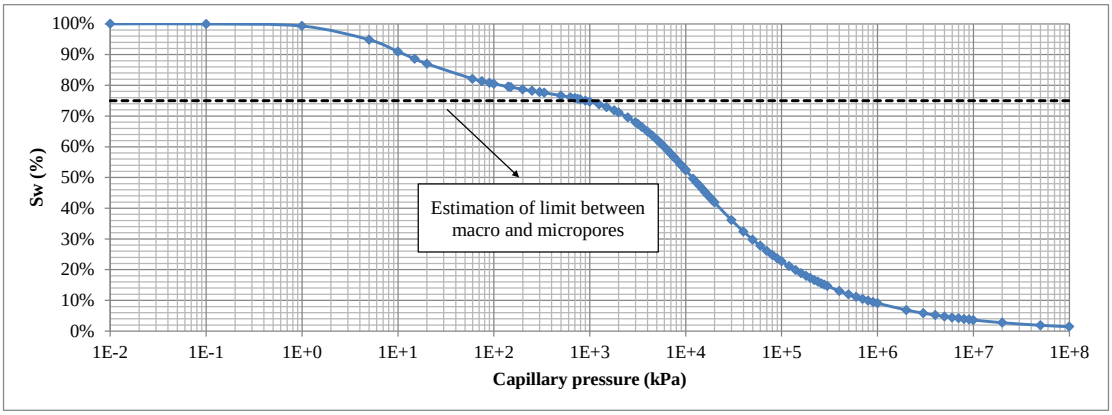

Figure 6.1 - Soil-water characteristic curve for the theoretical bimodal soil sample.

With the preceding calculated information, the diameter of the pores of the theoretical soil sample is determined. The capillary pressure is related to the size of the pores with Washburn's equation (Diamond, 1970; Griffiths & Joshi, 1989), as shown in Equation (2.1).

The size of the pores is essential information for the definition of the Pore Size Distribution Density curve. The *x*-axis corresponds to the size of the diameter of the pores, and the *y*-axis corresponds to the PSD parameter, calculated with Equation (2.2). The PSD curve for the theoretical bimodal soil sample is then defined, and it can be seen in Figure 6.2.

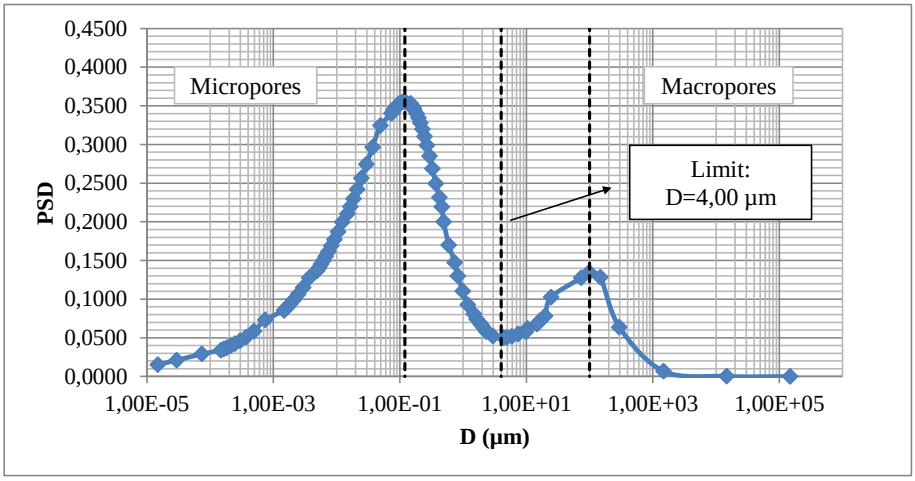

Figure 6.2 - PSD curve for the theoretical bimodal soil sample.

The PSD curve is used as input data for the estimation of permeability and void ratio of each scale. This is the methodology proposed in this research: the data from the PSD curve are employed in the model, and the values of fluid pressure and degree of saturation of each scale of the problem can then be determined. From the results, the SWCC of the entire sample is defined. This is pointed out as one of the main contributions of this research.

It was possible to determine the average values of diameter of the macro and micropores and the limit between the macro and the micropores from the PSD curve:

- Macropore diameter average value: 100,00 µm
- Micropore diameter average value: 0,12 µm
- Limit diameter between the macro and the micropores: 4,00 µm

Finally, with all the properly analyzed and arranged data, the intrinsic permeability of each scale can be calculated as shown in Equation (2.11). The values used for the calculation and the final value of intrinsic permeability for the theoretical bimodal soil sample are organized for each scale and for the entire sample in Table 6.1.

Table 6.1 - Intrinsic permeability calculation parameters for the theoretical soil sample.

Calculation parameter	**Macroscale**	**Microscale**	**Total**
Porosity (ϕ_i)	20,00%	42,86%	50,00%
$\sum_{1}^{i} f(r_i) r_i^2$	$1{,}93 \cdot 10^{-8}$	$7{,}00 \cdot 10^{-13}$	$1{,}93 \cdot 10^{-8}$
Intrinsic permeability (K_i)	$4{,}83 \cdot 10^{-10}$ m²	$3{,}75 \cdot 10^{-14}$ m²	$1{,}29 \cdot 10^{-9}$ m²

6.1.2 HOMOGENIZATION PARAMETER SENSITIVITY ANALYSIS

After defining the parameters required for the numerical model, the first set of simulations is arranged. The homogenization parameter is calibrated with a permeability test, made with the simulation of a one-dimensional, single-phase fluid flow analysis for the theoretical bimodal soil sample.

The value of hydraulic conductivity of the medium is used as basis for the hydraulic behavior evaluation and proper adjustments of the homogenization parameter ε. The conditions of this simulation are described in Section 4.1.

6.1.2.1 RESULTS OF THE NUMERICAL ANALYSES

The sensitivity analysis procedure described in Section 4.1 was employed for the calibration of the homogenization parameter of the theoretical bimodal soil sample. The parameter ε was varied for precise determination of the hydraulic conductivity of Region 2.

The first step was the calculation of the equivalent hydraulic conductivity for Region 1. In order to consider both macro and microscales, the equivalent hydraulic conductivity is calculated using Equation (2.9) with the value of total intrinsic permeability (Table 6.1). The equivalent hydraulic conductivity value is $1{,}20 \cdot 10^{-2}$ m/s and it is used as basis for ε sensitivity analysis. The results of this analysis are summarized in Table 6.2.

Table 6.2 - Homogenization parameter calibration data for the theoretical soil sample.

ε	q_{wM} [m³/s]/[m]	q_{wm} [m³/s]/[m]	q_{wt} [m³/s]/[m]	q_{wc} [m³/s]/[m]	$h_{y=1,0001m}$ [m]	k_{wc} [m/s]
0,1000	$3{,}22 \cdot 10^{-2}$	$2{,}50 \cdot 10^{-4}$	$3{,}25 \cdot 10^{-2}$	$3{,}25 \cdot 10^{-2}$	3,273236	$4{,}82 \cdot 10^{-3}$
0,0100	$2{,}58 \cdot 10^{-2}$	$2{,}00 \cdot 10^{-2}$	$4{,}58 \cdot 10^{-2}$	$4{,}58 \cdot 10^{-2}$	4,616945	$8{,}50 \cdot 10^{-3}$
0,0090	$2{,}46 \cdot 10^{-2}$	$2{,}36 \cdot 10^{-2}$	$4{,}82 \cdot 10^{-2}$	$4{,}82 \cdot 10^{-2}$	4,860184	$9{,}37 \cdot 10^{-3}$
0,0080	$2{,}31 \cdot 10^{-2}$	$2{,}81 \cdot 10^{-2}$	$5{,}12 \cdot 10^{-2}$	$5{,}12 \cdot 10^{-2}$	5,165568	$1{,}06 \cdot 10^{-2}$
0,0075	$2{,}23 \cdot 10^{-2}$	$3{,}07 \cdot 10^{-2}$	$5{,}30 \cdot 10^{-2}$	$5{,}30 \cdot 10^{-2}$	5,347046	$1{,}14 \cdot 10^{-2}$
0,0074	$2{,}21 \cdot 10^{-2}$	$3{,}13 \cdot 10^{-2}$	$5{,}34 \cdot 10^{-2}$	$5{,}34 \cdot 10^{-2}$	5,385964	$1{,}16 \cdot 10^{-2}$
0,0073	$2{,}19 \cdot 10^{-2}$	$3{,}19 \cdot 10^{-2}$	$5{,}38 \cdot 10^{-2}$	$5{,}38 \cdot 10^{-2}$	5,425807	$1{,}18 \cdot 10^{-2}$
0,0072	$2{,}17 \cdot 10^{-2}$	$3{,}25 \cdot 10^{-2}$	$5{,}42 \cdot 10^{-2}$	$5{,}42 \cdot 10^{-2}$	5,466595	$1{,}20 \cdot 10^{-2}$
0,0071	$2{,}15 \cdot 10^{-2}$	$3{,}31 \cdot 10^{-2}$	$5{,}46 \cdot 10^{-2}$	$5{,}46 \cdot 10^{-2}$	5,508351	$1{,}22 \cdot 10^{-2}$
0,0070	$2{,}13 \cdot 10^{-2}$	$3{,}37 \cdot 10^{-2}$	$5{,}50 \cdot 10^{-2}$	$5{,}50 \cdot 10^{-2}$	5,551097	$1{,}24 \cdot 10^{-2}$

As seen from the results, the value of the homogenization parameter ε is 0,0072. The homogenization parameter had already been mathematically defined as depicted in Equation (5.1). Based on this equation, the homogenization parameter was calculated. This allows a comparison of the numerical and the theoretical approaches of the homogenization parameter. The calculation for the theoretical value of the homogenization parameter ε for the theoretical bimodal soil sample uses the values of macro and micropore radius average. These data are collected from the PSD curves of the sample, as shown in Section 6.1.1. The calculation parameters and the theoretical homogenization parameter ε are depicted in Table 6.3.

Table 6.3 - Theoretical homogenization parameter ε for the theoretical bimodal soil sample.

Calculation parameter	
Macropore diameter average value (μm)	100,00
Micropore diameter average value (μm)	0,12
ε	0,0012

The value of ε=0,0072 achieved with the simulations is compared to the theoretical, calculated with Equation (5.1) (ε=0,0012). The observed difference may be justified by the fact that the calculated value is based on a specific circular geometry for the pores. This geometry pattern may differ from the actual geometry of the pores within the sample, and this could imply on the difference verified between the referred values of ε. Nevertheless, the two values are in the same order of magnitude and, therefore, the calibration of the homogenization parameter is valid and appropriate for the goals of this research.

6.1.3 PARAMETRIC ANALYSES FOR DRYING AND WETTING TRAJECTORIES SIMULATIONS FOR THE THEORETICAL BIMODAL SOIL SAMPLE

For the evaluation of the performance tendency of the proposed model in terms of hydraulic behavior, a set of simulations of drying and wetting tests were made on the theoretical bimodal soil sample. The objective was to verify the accuracy of the model and any specific effects the used approach could have on the hydraulic behavior of the sample.

6.1.3.1 DEFINITION OF THE MACRO AND MICROSCALE PARAMETERS

At first, it was necessary to define the parameters that were used as input of the numerical model. For this set of simulations, the following parameters are required:

- Fluid characterization parameters (for each α-fluid phase): density and viscosity;
- Porosity and intrinsic permeability of the macroscale and the microscale of the sample;
- Coefficient of volume compressibility;
- SWCC parameters for the macroscale and the microscale of the sample.

The values for the fluid characterization parameters used in all simulations proposed in the research are shown in Table 6.4:

Table 6.4 - Density and viscosity values for the wetting and non-wetting fluid phases.

Fluid characterization parameter	**Wetting fluid phase**	**Non-wetting fluid phase**
Density (ρ_α)	1,00 g/cm³	0,95 g/cm³
Viscosity (μ_α)	$1{,}00 \cdot 10^{-6}$ kPa.s	$5{,}00 \cdot 10^{-6}$ kPa.s

The porosity and the intrinsic permeability of the macro and the microscale of the theoretical bimodal soil sample used in this stage of the research are shown in Table 6.1.

The coefficient of volume compressibility is a parameter that is part of the formulation presented in Section 5. It is employed to show the relationship between the compressibility of the pores of the soil sample and the fluid pressure acting on them.

The values of coefficient of volume compressibility defined for this set of simulations are $1{,}00 \cdot 10^{-5}$ kPa^{-1}, being the same value used for both scales. Even though the coefficient of volume compressibility has an effect on the term of the equation related to the straining of the solid matrix of the soil, the overall evaluation of the response of the numerical model is focused on isolating the hydraulic behavior of the sample with no significant influence from the compressibility of solid particles arrangement. Given that, the value considered for the referred coefficient was defined so as to not compromise the verification made at this stage of the research, with its order of magnitude being correspondent to very low compressibility soils (Carter & Bentley, 1991). This is appropriate for the goals of this set of simulations.

Finally, the parameters of the SWCC are presented (Table 6.5). Each scale of the sample had a SWCC associated to it, defined by Equation (5.26) and shown in Figure 6.3.

Table 6.5 - Parameters of the macro and microscale SWCC of the theoretical soil sample.

SWCC parameters	**Macroscale**	**Microscale**
Residual degree of saturation ($S_{res_{wi}}$)	1,00%	4,00%
Parameter a_i	5 kPa	5000 kPa
Parameter n_i	1,50	1,40
Parameter m_i	0,33	0,29

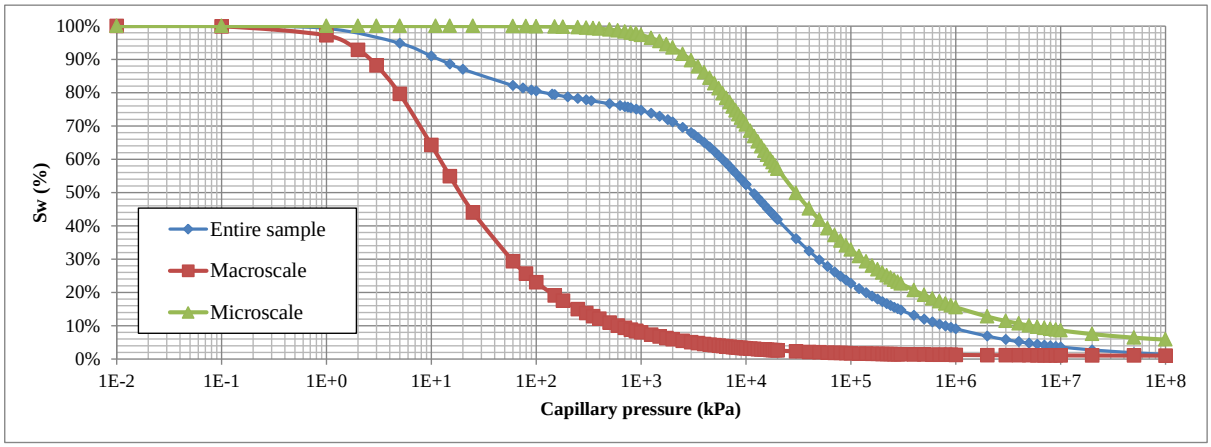

Figure 6.3 - SWCC for the macro and the microscale of the theoretical bimodal soil sample.

It is important to highlight that the SWCC of each scale of the theoretical soil sample, with the definition of their correspondent parameters, were designed specifically for simulation purposes. Then, the SWCC of the macroscale and the SWCC of the microscale should reproduce the behavior pattern expected for a bimodal soil sample, with the effects of the macroscale and microscale affecting the overall hydraulic behavior of the medium.

In order to maximize the range of values that could be used for providing accurate results, the suggested SWCC had its parameters adjusted so as to comprise the research objectives. The low values of residual degree of saturation were chosen specifically for allowing the widest range of values of capillary pressure applied to the studied sample.

With these parameters define, it is possible to proceed to the sets of drying and wetting trajectories simulations that are previewed for the theoretical bimodal soil sample. These simulation results are presented in Section 6.1.3.2.

6.1.3.2 DRYING AND WETTING TRAJECTORIES NUMERICAL SIMULATIONS FOR THE THEORETICAL BIMODAL SOIL SAMPLE

Using the parameters already defined as shown in Section 6.1.3.1, the model was employed for the simulation of drying and wetting tests on the theoretical soil sample.

The relationship between the capillary pressure and the degree of saturation for each scale and the starting values for each type of trajectory are represented in Figure 6.4 and the initial conditions for the problem variables are defined as shown in Table 6.6. The boundary conditions for this set of simulations are summarized in Table 6.7.

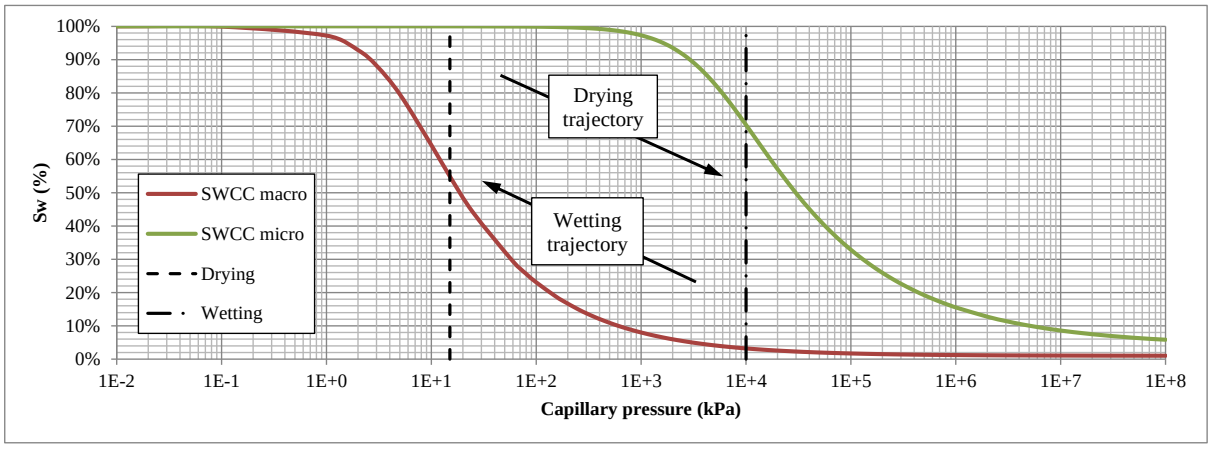

Figure 6.4 - SWCC study for definition of initial condition of the drying and wetting simulations on the theoretical bimodal soil sample.

Table 6.6 - Initial conditions for drying and wetting simulations for the theoretical sample.

Variable	Drying simulation	Wetting simulation
Wetting fluid pressure of the macroscale (p_{wM})	100 kPa	100 kPa
Wetting fluid pressure of the microscale (p_{wm})	100 kPa	100 kPa
Capillary pressure of the macro and microscale (p_{cM} and p_{cm})	15 kPa	10000 kPa
Degree of saturation of the wetting fluid of the macroscale (S_{wM})	54,90%	3,21%
Degree of saturation of the wetting fluid of the microscale (S_{wm})	99,99%	70,37%

Table 6.7 - Boundary conditions for the drying and wetting simulations for the theoretical bimodal soil sample analyses.

Variable	Boundary	Condition	Drying	Wetting
Wetting fluid pressure (p_{wM})	Bottom	Essential (Dirichlet)	p_{wM}=100 kPa	p_{wM}=100 kPa
Degree of saturation of the wetting fluid (S_{wM})			S_{wM}=54,90%	S_{wM}=3,21%
Wetting fluid pressure (p_{wM})	Right side	Natural (Neumann)	$\frac{\partial p_{wM}}{\partial n}=0$	$\frac{\partial p_{wM}}{\partial n}=0$
Degree of saturation of the wetting fluid (S_{wM})			$\frac{\partial S_{wM}}{\partial n}=0$	$\frac{\partial S_{wM}}{\partial n}=0$
Wetting fluid pressure (p_{wM})	Upper	Natural (Neumann)	Variation of value	Variation of value
Degree of saturation of the wetting fluid (S_{wM})			$\frac{\partial S_{wM}}{\partial n}=0$	$\frac{\partial S_{wM}}{\partial n}=0$
Wetting fluid pressure (p_{wM})	Left side	Natural (Neumann)	$\frac{\partial p_{wM}}{\partial n}=0$	$\frac{\partial p_{wM}}{\partial n}=0$
Degree of saturation of the wetting fluid (S_{wM})			$\frac{\partial S_{wM}}{\partial n}=0$	$\frac{\partial S_{wM}}{\partial n}=0$

The values of boundary conditions are defined based on the premises regarding both the reproduction of drying and wetting tests and the equilibrium condition related to the initial conditions of the problem discussed in Section 4.1.

When specifically referring to the boundary condition of the upper part of the domain, the values are varied, with the intention of verifying the effect of this boundary condition on the overall behavior of the theoretical soil sample.

Then, the simulations are conducted. Firstly, the drying simulation results are shown. Then, the results which correspond to the wetting simulations are presented. Capillary pressure and degree of saturation data for position ($x=0,5$; $y=0,9$) of the domain are assessed.

For the drying trajectory, the values of the boundary condition of the upper part of the contour of the domain were varied gradually from an initial, established value, to a maximum value for which the simulation may still be carried out without losses on the quality of the results. A relationship between the limitation observed in laboratory for this type of test and this sensitivity analysis can be established. It corresponds to a flux to which the sample has its water saturation degree reduced to approximately its residual value. The referred results are shown in Table 6.8.

Table 6.8 - Sensitivity analysis of the Neumann boundary condition for drying simulations on the theoretical bimodal soil sample.

$\frac{\partial p_{wM}}{\partial n}$	**Final p_{cM} and p_{cm} (ε=0,0012)**	**Final p_{cM} and p_{cm} (ε=0,0072)**
$-1{,}00 \cdot 10^{-1}$	22,70 kPa	138,00 kPa
$-1{,}00 \cdot 10^{0}$	150,00 kPa	1410,00 kPa
$-1{,}50 \cdot 10^{0}$	353,00 kPa	2087,00 kPa
$-1{,}80 \cdot 10^{0}$	581, 00 kPa	3050,00 kPa
$-1{,}90 \cdot 10^{0}$	683,00 kPa	3320,00 kPa
$-2{,}00 \cdot 10^{0}$	761,00 kPa	3630,00 kPa
$-2{,}10 \cdot 10^{0}$	930,00 kPa	3960,00 kPa
$-2{,}20 \cdot 10^{0}$	1080,00 kPa	-

As noticed, the absolute values for the natural boundary condition are higher for the simulations carried out with the value ε=0,0072 for the homogenization parameter. It can be inferred that the highest values of capillary pressure were reached with the simulations performed with the highest value for the homogenization parameter (ε=0,0072). If the values of capillary pressure and natural boundary conditions for both cases are compared, it can be verified that the same value for the boundary condition in both cases represent different values of capillary pressure. Analyzing the results, it can be noticed that the value of capillary pressure correspondent to the natural boundary condition of $-1{,}00 \cdot 10^{0}$ for the simulation with ε =0,0012 is 150 kPa. For the simulation with ε =0,0072, the capillary pressure value for the same boundary condition is 1410 kPa, 9,4 times greater than in the first case.

This behavior could be interpreted as a verification of the extents of the values for simulation for each case. For that purpose, the simulations were made so as to reach the maximum value of natural boundary condition (understood here as a measure of wetting fluid flow rate) and capillary pressure the sample could be subjected to.

Analyzing the results found in these cases, one can assume that the limit for the simulation made with ε=0,0072 is much higher than for the simulation with ε=0,0012. Higher values of capillary pressure can be reached without attaining the maximum value for the natural boundary condition when the homogenization parameter is greater. This can be pointed out as a significant advantage in the simulations of drainage of the sample.

This behavior tendency might be explained due to the fact that ε=0,0012 corresponds to the homogenization parameter calculated value. Its calculation is made with the values of radius of the micro and macropores of the sample. The size of the micropores is significantly small, which makes more difficult the removal of water from them. Besides that, one should remind that the radii values of the micro and macropores are retrieved from the PSD curve (Figure 6.2). The values of size of the pores in the PSD curve are shown in a logarithmic scale. If the reading of values were made differently, it could be defined other values of radii, even in a different order of magnitude, implying on a different value for the calculated homogenization parameter.

Other results of these simulations are analyzed. The values of degree of saturation achieved with the simulation are compared to the values which correspond to the original SWCC of the entire sample. The value of degree of saturation of the entire sample is calculated with a weighted average based on Equations (4.3) and (4.4). The values used for the calculation of the volume fraction average weight parameters of the macro and microscale are shown in Table 6.9. The calculated value for w_M is 0,6313 and for w_m is 0,8721 in this set of simulations.

Table 6.9 - Data for calculation of w_M and w_m for drying of the theoretical bimodal sample.

Parameter	Macroscale	Microscale	Total
Degree of saturation of the wetting fluid (S_{wi})	54,90%	99,99%	88,61%
Porosity (ϕ_i)	20,00%	42,86%	50,00%

The results of the values of degree of saturation calculated with the described procedure are compared to the values retrieved from the SWCC of the entire sample. The value of capillary pressure achieved with the simulation is used for the verification of the correspondent degree of saturation. The referred results are represented in Figure 6.5 and Figure 6.6 and summarized in Table 6.10.

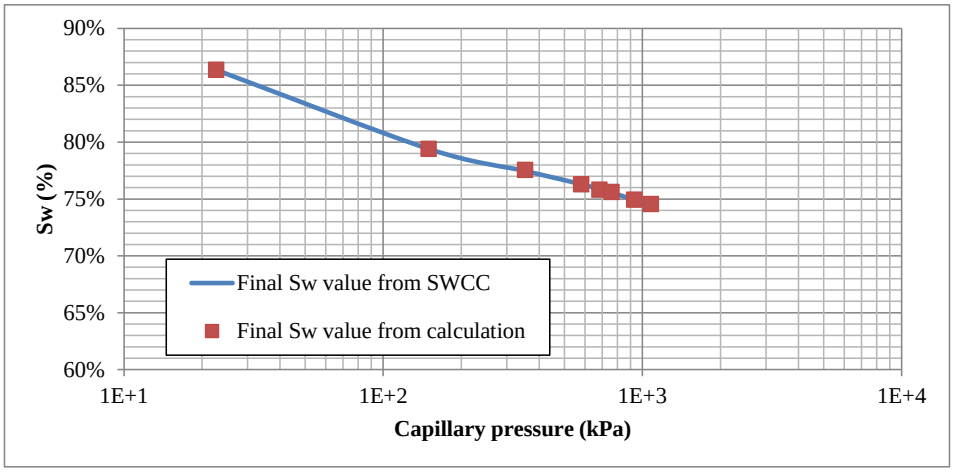

Figure 6.5 - Final S_w value of the entire theoretical bimodal soil sample (SWCC versus calculated value) for the drying trajectory simulations - ε= 0,012.

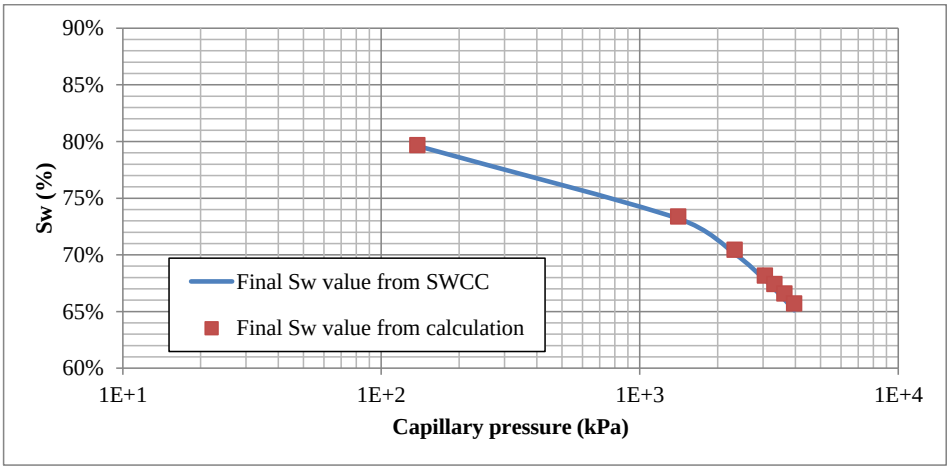

Figure 6.6 - Final S_w value of the entire theoretical bimodal soil sample (SWCC versus calculated value) for the drying trajectory simulations - ε= 0,072.

Table 6.10 - Results of S_w of the entire theoretical bimodal soil sample for drying.

ε	$\frac{\partial p_{wM}}{\partial n}$	**Final S_{wM}**	**Final S_{wm}**	**Final S_w (SWCC)**	**Final S_w (calculated)**	$\frac{S_w^{calc} - S_w^{data}}{S_w^{data}} \times 100\%$
0,0012	$-1{,}00 \cdot 10^{-1}$	46,0000%	99,9860%	86,3433%	86,3579%	0,02%
	$-1{,}00 \cdot 10^{0}$	19,0000%	99,7990%	79,3978%	79,3998%	0,00%
	$-1{,}50 \cdot 10^{0}$	13,0000%	99,3400%	77,4578%	77,5415%	0,11%
	$-1{,}80 \cdot 10^{0}$	10,0000%	98,6900%	76,2980%	76,2980%	0,00%
	$-1{,}90 \cdot 10^{0}$	9,0000%	98,3800%	75,8684%	75,8137%	-0,07%
	$-2{,}00 \cdot 10^{0}$	9,0000%	98,1200%	75,5573%	75,6194%	0,08%
	$-2{,}10 \cdot 10^{0}$	8,0000%	97,5500%	74,9148%	74,9408%	0,03%
	$-2{,}20 \cdot 10^{0}$	8,0000%	97,0200%	74,3667%	74,5446%	0,24%

0,0072	$-1{,}00\cdot10^{-1}$	20,0000%	99,8200%	79,6077%	79,6680%	0,08%
	$-1{,}00\cdot10^{0}$	7,0000%	95,8000%	73,1993%	73,3801%	0,25%
	$-1{,}50\cdot10^{0}$	5,8451%	93,1778%	70,8947%	71,1283%	0,33%
	$-1{,}80\cdot10^{0}$	5,0000%	89,5000%	67,8008%	68,1656%	0,54%
	$-1{,}90\cdot10^{0}$	5,0000%	88,5000%	66,9772%	67,4181%	0,66%
	$-2{,}00\cdot10^{0}$	5,0000%	87,4000%	66,0568%	66,5958%	0,82%
	$-2{,}10\cdot10^{0}$	5,0000%	86,2000%	65,1071%	65,6988%	0,91%

As it can be noticed, the estimate of degree of saturation of the entire sample made via Equation (4.4) is appropriate. Verifying this determination procedure is extremely significant, given that the possibility of evaluating the degree of saturation of each scale and of the entire sample may be useful for the hydraulic behavior prediction of bimodal soils.

It is important to highlight that this methodology of calculation for the degree of saturation of the entire soil sample uses the MIP technique as basis, with the PSD curve data being input for the model. This is extremely significant in terms of improving the type of results that can be retrieved from the PSD curve. This methodology allows the use of the PSD curve data to its extent, and provides interesting results for the hydraulic behavior understanding of a multiscale porous medium.

Also, it should be addressed that in this particular set of simulations, only some values of degree of saturation were defined. This is justified due to the fact that there are limitations related to the numerical model and software used for the simulations. The boundary condition used for representing the drainage of the sample corresponds to flux of the wetting fluid. A more elaborated approach for drying the sample would be the thermodynamic, which is not comprised in the mathematical model proposed in the present research. This could a suggestion of improvement in this model for further research on that domain.

At the same time, it can be verified that the results are more accurate (associated error is smaller) for the cases in which when the homogenization parameter is ε= 0,012. This tendency could be justified by the fact that, for this value of ε, the drainage of the sample is less pronounced; less water can be drained from the pores for the values of capillary pressure reached. As mentioned, when using ε=0,0012, the pattern of distribution of the micropores is such that the difference of size between the macro and microscale is more significant, and it affects the hydraulic behavior of the entire soil sample, making the drainage of sample more difficult if compared to the case of the simulations made with ε=0,0072. Since the values of

capillary pressure are lower, a less extreme flow simulation is verified, and it should correspond to lower error in the obtained results.

Nonetheless, the accuracy of the achieved results for both values of homogenization parameter is remarkable and the importance of these results should be pointed out as significant for the representation of the hydraulic behavior of bimodal porous media.

Then, taking into consideration that the most extreme drainage situation was achieved with the highest value for the homogenization parameter, ε=0,0072, the results shown and discussed here correspond to it. For the same reason, the highest possible value for the natural boundary condition is chosen for the performed drying simulation. The values used for fluid characterization are shown in Table 6.4 and the SWCC parameters of the macro and microscale curves are presented in Table 6.5. The input values that correspond to the proposed drying simulation are summarized in Table 6.11.

Table 6.11 - Input data for the theoretical bimodal soil sample drying trajectory simulation.

Parameter	**Value**
Homogenization parameter value (ε)	0,0072
Intrinsic permeability of the macroscale (K_M)	$4{,}83 \cdot 10^{-10}$ m²
Porosity of the macroscale (ϕ_M)	20,00%
Intrinsic permeability of the microscale (K_m)	$3{,}75 \cdot 10^{-14}$ m²
Porosity of the microscale (ϕ_m)	42,86%
Boundary condition of the upper part of the domain	$-2{,}10 \cdot 10^{0}$

The main results of the drying trajectory simulation are summarized and presented in Table 6.12. There is information related to the values of degree of saturation of each scale of the sample, and the minimum achieved value of degree of saturation within the sample in each scale is informed. Also, the highest value of capillary pressure, which corresponds to the minimum degree of saturation value, is presented.

Table 6.12 - Theoretical bimodal soil sample drying trajectory simulation results.

Evaluated variable	**Initial value**	**Final value**
Degree of saturation of the wetting fluid in the macroscale (S_{wM})	54,90%	5,00%
Degree of saturation of the wetting fluid in the microscale (S_{wm})	99,99%	86,20%
Capillary pressure of the macro and microscale (p_{cM} and p_{cm})	15 kPa	3960 kPa

It can be inferred from the presented results that during the drying trajectory test simulation, the degree of saturation of the wetting phase decreases more significantly on the macroscale if compared to the microscale. This can be verified with the values of degree of saturation expected for the final value of capillary pressure for the sample.

In a drying trajectory test, it is easier to verify the reduction of the volume of water within the larger pores than within the smaller pores. Higher values of capillary pressure would be required to significantly dry the micropores. When analyzing the SWCC for the macroscale in contrast to the microscale (Figure 6.3), this tendency is confirmed, given that the residual value of degree of saturation for the macroscale is reached within the range of 10000 kPa order of magnitude for the capillary pressure. For this same range of value, the microscale still has a degree of saturation higher than 40%.

This is comparable to the hydraulic behavior verified in typical bimodal tropical soils, as the case of the soil samples studied and used as reference for the present research.

It is important to highlight that the continuity of the both wetting and non-wetting fluid phases is a premise of the simulations performed in the present research, as mentioned Section 5.1. Therewith, the formation of bubbles for a specific range of capillary pressure is not expected neither for the wetting nor the non-wetting fluid.

For the wetting trajectory, the followed simulation procedure was the same used for the drying trajectory simulations.

The results for the sensitivity analysis of the Neumann boundary condition for the wetting trajectory simulation for the theoretical bimodal soil sample are shown in Table 6.13.

Table 6.13 - Sensitivity analysis of the Neumann boundary condition for wetting simulations on the theoretical bimodal soil sample.

$\frac{\partial p_{wM}}{\partial n}$	**Final p_{cM} and p_{cm} (ε=0,0012)**	**Final p_{cM} and p_{cm} (ε=0,0072)**
$1{,}00 \cdot 10^{-3}$	9990,30 kPa	9988,20 kPa
$1{,}00 \cdot 10^{-2}$	9902,00 kPa	9878,00 kPa
$1{,}00 \cdot 10^{-1}$	9050,00 kPa	8820,00 kPa
$1{,}00 \cdot 10^{0}$	3200,00 kPa	1700,00 kPa
$1{,}20 \cdot 10^{0}$	2400,00 kPa	800,00 kPa
$1{,}30 \cdot 10^{0}$	2090,00 kPa	390,00 kPa
$1{,}50 \cdot 10^{0}$	1600,00 kPa	-
$2{,}00 \cdot 10^{0}$	700,00 kPa	-

In this set of simulations, the absolute values for the natural boundary condition are higher for the simulations carried out with the smallest value for the homogenization parameter (ε =0,0012), correspondent to the theoretical value, calculated via Equation (5.1). Also, the lowest values of capillary pressure achieved are observed in the simulations performed with the highest value for the homogenization parameter (ε =0,0072).

Again, this behavior could be analyzed for the verification of the extents of possibility of each simulation with the variation of the value of the referred boundary condition. The numerical procedure was made following the premise of reaching the maximum value of natural boundary condition (understood here as a measure of fluid flow rate), with the capillary pressure going to its lowest range it could be without compromising the results in terms of representativeness of the studied phenomenon.

Analyzing specifically the results found in these cases, one can assume that the limit for the simulation made with ε =0,0072 is much higher than for the simulation with ε =0,0012. The lowest values of capillary pressure can be reached without attaining the maximum value for the natural boundary condition when the homogenization parameter is greater. This is an advantage in the simulations in which with the lowest values of capillary pressure are achieved, with the degree of saturation of the soil taken to the highest possible values.

As made for the drying trajectory simulation analyses, the values of degree of saturation achieved with the simulation are compared to the values correspondent to the original SWCC of the entire sample. The value of degree of saturation of the entire sample is calculated with a weighted average based on the Equations (4.3) and (4.4).

The values used for the calculation of the volume fraction average weight parameters of the macro and microscale are shown in Table 6.14.

Table 6.14 - Data for calculation of w_M and w_m for wetting of the theoretical bimodal sample.

Parameter	Macroscale	Microscale	Total
Degree of saturation of the wetting fluid (S_{wi})	3,21%	70,37%	52,42%
Porosity (ϕ_i)	20,00%	42,86%	50,00%

The value for w_M is 0,6686 and for w_m is 0,8547 for this set of simulations. Then, the calculation of the degree of saturation of the entire sample is made via Equation (4.4), with the macro and microscale degree of saturation final values. The input data for the calculation and its results are represented in Figure 6.7 and Figure 6.8 and summarized in Table 6.15.

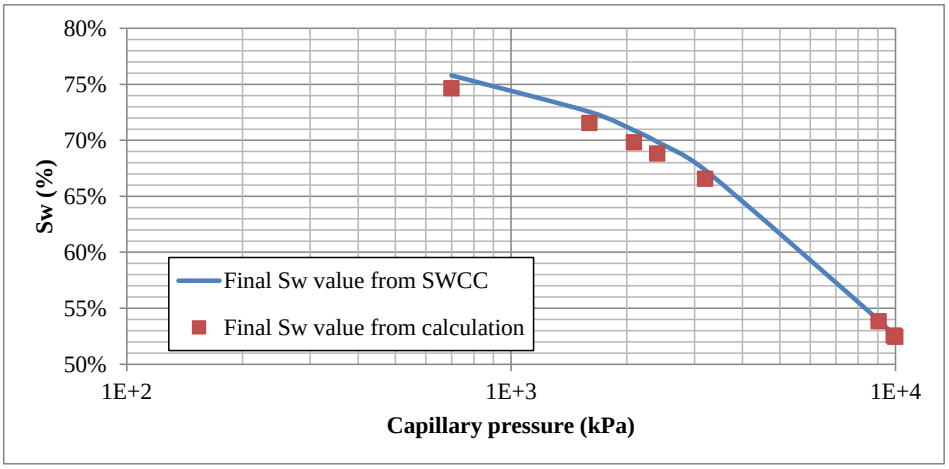

Figure 6.7 - Final S_w value of the entire theoretical bimodal soil sample (SWCC *versus* calculated value) for the wetting trajectory simulations - ε= 0,012.

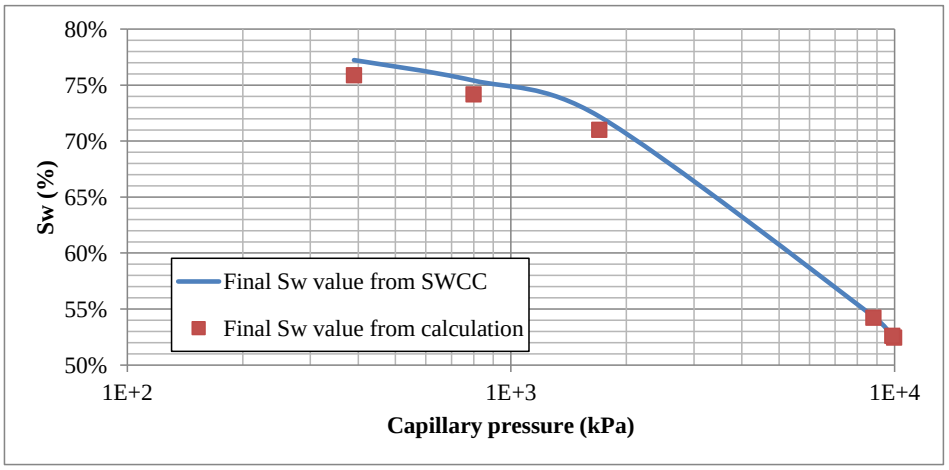

Figure 6.8 - Final S_w value of the entire theoretical bimodal soil sample (SWCC *versus* calculated value) for the wetting trajectory simulations - ε= 0,072.

Table 6.15 - Results of S_w of the entire theoretical bimodal soil sample for wetting.

ε	$\frac{\partial p_{wM}}{\partial n}$	**Final S_{wM}**	**Final S_{wm}**	**Final S_w (SWCC)**	**Final S_w (calculated)**	$\frac{S_w^{calc} - S_w^{data}}{S_w^{data}} \times 100\%$
0,0012	$1{,}00 \cdot 10^{-3}$	3,2148%	70,3920%	52,4276%	52,4306%	0,01%
	$1{,}00 \cdot 10^{-2}$	3,2246%	70,5610%	52,5636%	52,5570%	-0,01%
	$1{,}00 \cdot 10^{-1}$	3,2700%	72,2851%	53,9345%	53,8323%	-0,19%
	$1{,}00 \cdot 10^{0}$	4,9300%	89,0500%	67,3408%	66,5585%	-1,16%
	$1{,}20 \cdot 10^{0}$	5,5100%	91,9200%	69,8639%	68,8163%	-1,50%
	$1{,}30 \cdot 10^{0}$	5,8400%	93,1700%	70,8847%	69,8203%	-1,50%
	$1{,}50 \cdot 10^{0}$	6,6200%	95,2500%	72,5421%	71,5528%	-1,36%
	$2{,}00 \cdot 10^{0}$	9,5500%	98,4100%	75,7995%	74,6514%	-1,51%

0,0072	$1{,}00 \cdot 10^{-3}$	3,2150%	70,3955%	52,4308%	52,4332%	0,00%
	$1{,}00 \cdot 10^{-2}$	3,2273%	70,6090%	52,6007%	52,5929%	-0,01%
	$1{,}00 \cdot 10^{-1}$	3,3570%	72,7800%	54,3240%	54,2181%	-0,19%
	$1{,}00 \cdot 10^{0}$	6,3300%	94,6000%	72,1996%	70,9990%	-1,66%
	$1{,}20 \cdot 10^{0}$	8,8500%	98,0000%	75,4058%	74,1638%	-1,65%
	$1{,}30 \cdot 10^{0}$	12,0000%	99,2000%	77,2375%	75,8854%	-1,75%

Accurate results were found with the estimation of degree of saturation made via calculation. When comparing the simulation and the calculation results, it is proven that Equation (4.4) is adequate for the determination of the degree of saturation of the entire sample with the information of degree of saturation of each scale of the sample. As mentioned, this is particularly significant for hydraulic behavior prediction analyses.

Again, the importance of applying this calculation methodology for the degree of saturation of the entire soil sample using the PSD curve data as input for the model is addressed. Its significance in terms of the results achieved is remarkable and pointed out as one of the contributions of the present research.

The accuracy of the achieved results is considered appropriate and it is pointed out as significant for the representation of the hydraulic behavior of bimodal porous media.

Considering the sensitivity analyses made for the natural boundary condition, the results correspondent to the homogenization parameter of ε=0,0072 are the ones shown and discussed in the present section. For the same reason, the highest possible value for the natural boundary condition is chosen for the performed wetting simulation. The values used for fluid characterization are shown in Table 6.4 and the SWCC parameters of the macro and microscale curves are presented in Table 6.5. The input values that correspond to the proposed drying simulation are summarized in Table 6.16.

Table 6.16 - Input data for the theoretical bimodal soil sample wetting trajectory simulation.

Parameter	**Value**
Homogenization parameter value (ε)	0,0072
Intrinsic permeability of the macroscale (K_M)	$4{,}83 \cdot 10^{-10}$ m²
Porosity of the macroscale (ϕ_M)	20,00%
Intrinsic permeability of the microscale (K_m)	$3{,}75 \cdot 10^{-14}$ m²
Porosity of the microscale (ϕ_m)	42,86%
Boundary condition of the upper part of the domain	$1{,}30 \cdot 10^{0}$

The main results of the wetting trajectory simulation are summarized and presented in Table 6.17. There is information related to the values of degree of saturation of each scale of the sample, and the maximum achieved value of degree of saturation within the sample in each scale is informed. Also, the lowest value of capillary pressure, which corresponds to the maximum degree of saturation value, is presented.

Table 6.17 - Theoretical bimodal soil sample wetting trajectory simulation results.

Evaluated variable	**Initial value**	**Final value**
Degree of saturation of the wetting fluid in the macroscale (S_{wM})	3,21%	12,00%
Degree of saturation of the wetting fluid in the microscale (S_{wm})	70,37%	99,20%
Capillary pressure of the macro and microscale (p_{cM} and p_{cm})	10000 kPa	390 kPa

From the results, it can be inferred that the degree of saturation of the wetting phase increases significantly on both scales. This can be explained with a comparative analysis of the expected degree of saturation values for the final value of capillary pressure.

In a wetting trajectory test, when the wetting fluid is injected, the value of capillary pressure decreases. For the initial value of capillary pressure in this particular simulation, 10000 kPa, the degree of saturation of the macroscale was low (3,21%) and as the volume of wetting fluid gradually increases, the larger pores of the sample are progressively filled. At the same time, the initial value of degree of saturation (70,37%) of the microscale and the hydraulic behavior of the microscale have to be taken into account.

As the microscale initial degree of saturation was already high, even though the microscale was not fully saturated, it was still possible to fill the micropores with wetting fluid. The wetting fluid that already partially filled the micropores of the sample simplified the process of transfer of wetting fluid to the micropores, making it possible to saturate it. Also, the capillary pressure value at the end of the simulation (390 kPa) was appropriate to saturate the micropores. Nonetheless, this value of capillary pressure was still significant for the saturation of the macropores. This justifies the observed tendency of increase of degree of saturation on both scales, whereas the saturation of the micropores taking place first.

With this stage of simulations and its correspondent results, it was possible to verify the overall behavior tendency of the proposed numerical model.

6.1.4 SENSITIVITY ANALYSES FOR THE SOIL-WATER CHARACTERISTIC CURVE PARAMETERS

The final set of simulations proposed for the theoretical bimodal soil sample is made for the evaluation of the influence of each parameter of the SWCC on the hydraulic behavior of the porous medium. The sensitivity analyses were made by varying the values of the residual degree of saturation ($S_{res_{wi}}$), parameter a_i (non-wetting fluid entry pressure value) and parameter n_i (inclination of the curve) for both macro and microscale. The values used for the sensitivity analyses are presented in Table 6.18.

Table 6.18 - Values for the SWCC parameters sensitivity analyses of the theoretical sample.

SWCC parameters	**Values**	
Residual degree of saturation of the macroscale ($S_{res_{wM}}$)	1,00%	Initial value
	4,00%	
Residual degree of saturation of the microscale ($S_{res_{wm}}$)	4,00%	Initial value
	10,00%	
	40,00%	
Parameter a_M (macroscale)	5 kPa	Initial value
	25 kPa	
	50 kPa	
	500 kPa	
Parameter a_m (microscale)	5000 kPa	Initial value
	500 kPa	
	10000 kPa	
	50000 kPa	
Parameter n_M (macroscale)	1,50	Initial value
	1,40	
	1,60	
Parameter n_m (microscale)	1,40	Initial value
	1,30	
	1,50	

The verification of the effect of the variation of these parameters was made by analyzing the differences observed in the overall format of the SWCC for each case. Then, the numerical simulations were performed so as to assess the observed in the first step. The

simulations were made only for cases in which a significant difference of the format of the SWCC was verified. The results of these simulations were compared and analyzed using the initial SWCC curve as basis, and the effects of the parameter variation were discussed.

The simulations were made for the drying trajectory. This test was preferred due to the numerical stability it shows during the simulations. Also, the value of natural boundary condition applied to the upper part of the domain was chosen based on the representativeness of the results of the test for the different values of the parameters of the SWCC for the sensitivity analyses. The initial conditions of the variables were the same used for the simulations shown in Section 6.1.3, making it possible to compare the results from the initial curve to the results for the modified curves. The input data for the sensitivity analyses are shown in Table 6.19 and Table 6.20.

Table 6.19 - SWCC parameters sensitivity analyses input data.

Variable	**Macroscale**	**Microscale**
Homogenization parameter value	0,0072	
Porosity (ϕ_i)	20,00%	42,86%
Intrinsic permeability (K_i)	$4{,}83 \cdot 10^{-10}$ m²	$3{,}75 \cdot 10^{-14}$ m²
Initial fluid pressure value of the wetting phase (p_{wi})	100 kPa	100 kPa
Capillary pressure (p_{ci})	15 kPa	15 kPa
Degree of saturation of the wetting fluid (S_{wi})	54,90%	99,99%

Table 6.20 - SWCC parameters sensitivity analyses boundary conditions.

Variable	**Boundary**	**Condition**	**Drying simulation**
Wetting fluid pressure (p_{wM})	Bottom	Essential (Dirichlet)	p_{wM}=100 kPa
Degree of saturation of the wetting fluid (S_{wM})		Essential (Dirichlet)	S_{wM}=54,90%
Wetting fluid pressure (p_{wM})	Right side	Natural (Neumann)	$\frac{\partial p_{wM}}{\partial n} = 0$
Degree of saturation of the wetting fluid (S_{wM})		Natural (Neumann)	$\frac{\partial S_{wM}}{\partial n} = 0$
Wetting fluid pressure (p_{wM})	Upper	Natural (Neumann)	$-1{,}5 \cdot 10^{0}$
Degree of saturation of the wetting fluid (S_{wM})		Natural (Neumann)	$\frac{\partial S_{wM}}{\partial n} = 0$

Wetting fluid pressure (p_{wM})	Left side	Natural (Neumann)	$\frac{\partial p_{wM}}{\partial n} = 0$
Degree of saturation of the wetting fluid (S_{wM})		Natural (Neumann)	$\frac{\partial S_{wM}}{\partial n} = 0$

The sensitivity analyses basically involved varying the values of the parameters for both macro and microscale of the SWCC. Even though this implies on changing the format of the entire sample SWCC, the values used for the initial condition of the problem were the same for all performed simulation, with no verification of the referred equilibrium condition of the degree of saturation *versus* capillary pressure. This choice was made so the simulations performed throughout the sensitivity analyses results could be appropriately compared to the initial SWCC drying trajectory results, and the hydraulic behavior change properly addressed.

The results of these analyses are presented as follows: the results for the residual degree of saturation are in Section 6.1.4.1; the results for the parameter a_i are in Section 6.1.4.2; and the results for the parameter n_i are in Section 6.1.4.3.

So as to standardize the presentation of results, in all graphic representations, the SWCC used as basis for comparison of results corresponds to the one traced as a red line. In each set of analyses, other colors are used for the tracing of the updated SWCC.

6.1.4.1 SENSITIVITY ANALYSIS OF THE RESIDUAL DEGREE OF SATURATION

The first verifications made were for the macroscale residual degree of saturation. For this parameter, only one value above the initial was verified, as shown in Table 6.18; this is justified by the fact that the initial value, 1,00%, is extremely low, and it would not significantly affect the overall hydraulic behavior of the sample. At the same time, the highest possible value acceptable for the macroscale residual degree of saturation is 4,00%, because it corresponds to the microscale residual degree of saturation. It would not be adequate to have the macroscale residual degree of saturation higher than the one defined for the microscale, thereby representing a limit to it. The variation made for the macroscale residual degree of saturation is shown in Figure 6.9.

As noticed, the difference between the curves is not significant; there is no change on the format of the updated SWCC (blue line) in comparison to the initial SWCC (red line. With that, no simulations were carried out for the verification of the influence of this parameter in terms of the response of the numerical model.

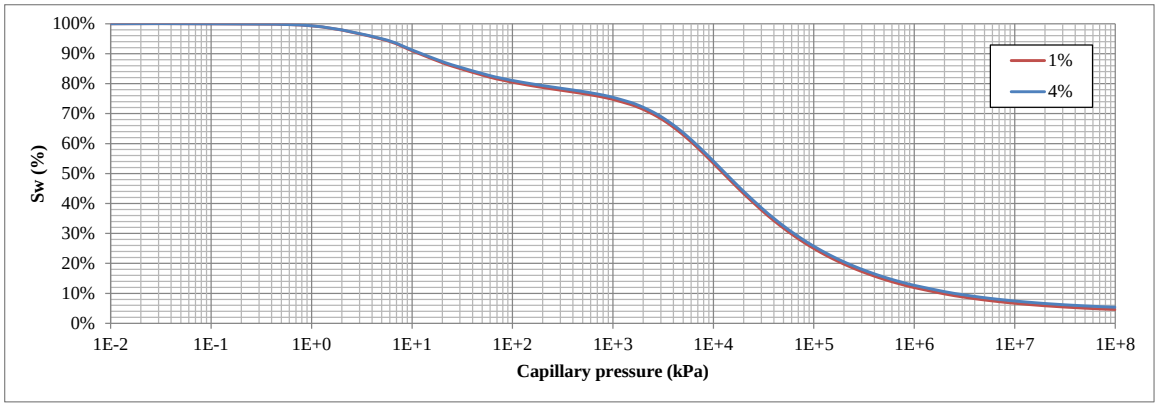

Figure 6.9 - Sensitivity analysis for $S_{res_{wM}}$ of the SWCC of the theoretical soil sample.

Then, the residual degree of saturation for the microscale was analyzed. Two different values were evaluated; 10,00% and 40,00%; all above the initial value (4,00%). Given it is already low, decreasing it would not affect the hydraulic behavior of the sample significantly. The variation made for the microscale residual degree of saturation is shown in Figure 6.10.

There is a significant change in the format of the SWCC when the microscale residual degree of saturation is increased by one order of magnitude (green line; $S_{res_{wm}}$=40,00%); if not, the SWCC stays similar (blue line; $S_{res_{wm}}$=10,00%) to the initial curve. Considering this, the simulation was performed for $S_{res_{wm}}$=40,00%, with referring results in Table 6.21.

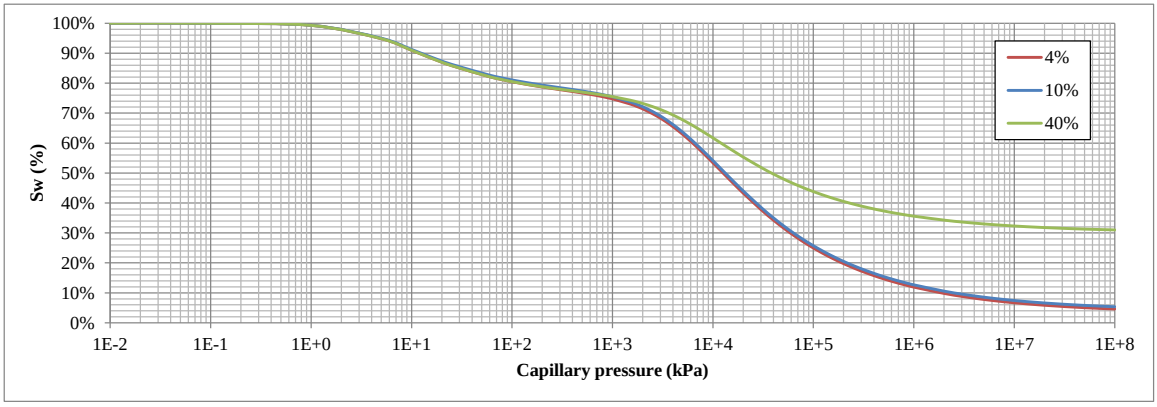

Figure 6.10 - Sensitivity analysis for $S_{res_{wm}}$ of the SWCC of the theoretical soil sample.

Table 6.21 - Results for $S_{res_{wm}}$=40,00% of the SWCC for the theoretical bimodal soil sample.

Evaluated value	**Initial theoretical sample**	**$S_{res_{wm}}$=40,00%**	**Difference**
Initial S_{wM}	54,9000%	54,9000%	-
Final S_{wM}	5,8451%	5,9007%	0,9512%

Initial S_{wm}	99,9919%	99,9919%	-
Final S_{wm}	93,1778%	95,8505%	2,8684%
Initial p_c	15 kPa	15 kPa	-
Final p_c	2087 kPa	2040 kPa	-2,2520%
Initial S_w (SWCC)	88,6050%	88,6050%	-
Final S_w (SWCC)	70,8947%	71,0514%	0,2210%
Initial S_w (calculated)	88,6100%	88,6100%	-
Final S_w (calculated)	71,1283%	73,1402%	2,8286%

It can be inferred from the results that the macroscale drainage occurs in the same way observed for the initial theoretical bimodal soil sample. The changes in the SWCC due to the variation of the residual degree of saturation do not affect the macroscale hydraulic behavior.

There is a significant amount of it in the micropores. With that, when the residual degree of saturation is increased, less wetting fluid can be removed from the micropores of the sample. In terms of the draining test, a higher value of degree of saturation for the micropores is then expected, also affecting the degree of saturation of the entire sample, which should be greater. This is proven when verifying that the degree of saturation of the microscale and entire sample are greater than the initial theoretical sample observed values.

6.1.4.2 SENSITIVITY ANALYSIS OF THE PARAMETER a

The second set of verifications for the sensitivity analysis of the SWCC of the theoretical bimodal soil sample consisted on varying the value of the parameter *a*. This parameter physically represents the value of capillary pressure required for initiating the process of drainage of a fully saturated soil sample. As the parameter *a* is higher, a higher value of capillary pressure is required for the desaturation of the sample.

The values for evaluation of the influence of this parameter on the hydraulic behavior of the sample were chosen so as to change the format of the SWCC significantly. For the macroscale, three values above the initial value of a_M were chosen; 25, 50 and 500. The goal was to reach values in different order of magnitude from the initial value and from each other. The variation of SWCC with the changes in the parameter a_M is shown in Figure 6.11.

As it can be observed, the format of the curve significantly changes with the variation of a_M. As its value is increased, the sinuosity of the curve given by the bimodal distribution of

pores of the soil sample is no longer verified; this influences the pattern of distribution of fluids within the soil sample, and its overall hydraulic behavior.

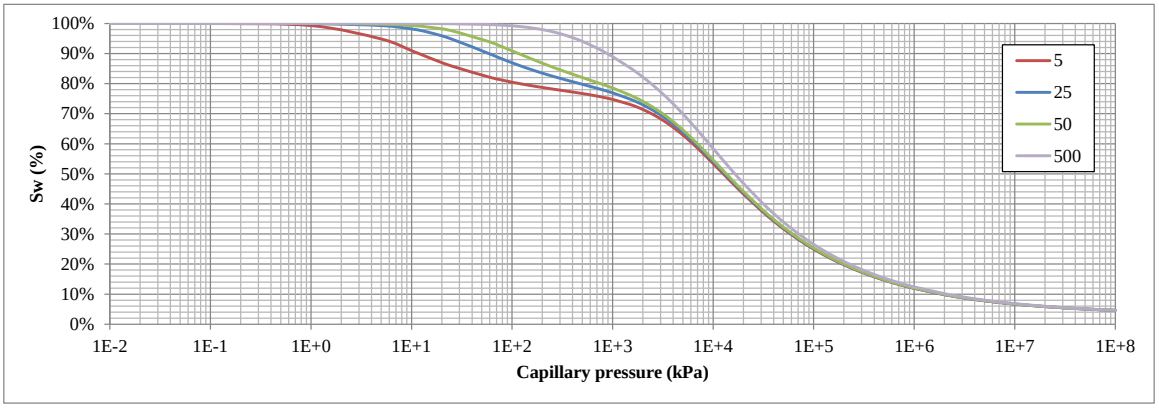

Figure 6.11 - Sensitivity analysis for a_M of the SWCC of the theoretical bimodal soil sample.

Only the attempts made with a_M = 25 kPa and 50 kPa were possible. When the value of a_M = 500 kPa was used, the numerical model was not able to achieve a solution for the problem due to numerical instabilities. It is possible to observe from the curves represented in Figure 6.11 that this value for the parameter a_M is extremely high, which makes the curve slope gentle for the initial value of capillary pressure established for the simulation (15 kPa). In mathematical terms, this generates difficulties regarding the calculation of the derivative term of the degree of saturation in relation to the capillary pressure (required in the proposed formulation). These difficulties make the proper calculation of the variables of the problem unviable, given they could compromise the physical representation of the studied phenomenon. For that reason, only the simulations made with a_M = 25 kPa and for a_M = 50 kPa were carried out. Their results are shown in Table 6.22 and Table 6.23, respectively.

Table 6.22 - Results for a_M = 25 kPa of the SWCC for the theoretical bimodal soil sample.

Evaluated value	**Initial theoretical sample**	**a_M=25 kPa**	**Difference**
Initial S_{wM}	54,9000%	54,9000%	-
Final S_{wM}	5,8451%	12,4534%	113,0571%
Initial S_{wm}	99,9919%	99,9919%	-
Final S_{wm}	93,1778%	94,0381%	0,9233%
Initial p_c	15 kPa	15 kPa	-
Final p_c	2087 kPa	1866 kPa	-10,5894%

Initial S_w (SWCC)	88,6050%	88,6050%	-
Final S_w (SWCC)	70,8947%	71,6359%	1,0455%
Initial S_w (calculated)	88,6100%	88,6100%	-
Final S_w (calculated)	71,1283%	73, 4402%	3,2503%

Table 6.23 - Results for a_M = 50 kPa of the SWCC for the theoretical bimodal soil sample.

Evaluated value	**Initial theoretical sample**	**a_M=50 kPa**	**Difference**
Initial S_{wM}	54,9000%	54,9000%	-
Final S_{wM}	5,8451%	17,0143%	191,0866%
Initial S_{wm}	99,9919%	99,9919%	-
Final S_{wm}	93,1778%	93,8847%	0,7587%
Initial p_c	15 kPa	15 kPa	-
Final p_c	2087 kPa	1905 kPa	-8,7207%
Initial S_w (SWCC)	88,6050%	88,6050%	-
Final S_w (SWCC)	70,8947%	71,5043%	0,8599%
Initial S_w (calculated)	88,6100%	88,6100%	-
Final S_w (calculated)	71,1283%	74,4773%	4,7084%

As expected, with higher values of a_M, it is more difficult to drain wetting fluid out of the macropores of the sample. As a_M is increased, the required capillary pressure value to drain wetting fluid from within the macropores of the sample is higher than in the initial sample conditions. Considering that the boundary condition was kept the same for all cases, higher values of capillary pressure within the sample are not expected. With that, the same tendency is observed in both cases: higher values of degree of saturation for the macroscale and for the entire sample are registered, and lower values of capillary pressure are reached.

Nevertheless, it is important to remind that the majority of the sample voids is composed by micropores (the porosity of the sample is 50,00%; the microscale porosity, 42,86%, and the macroscale porosity, 20,00%). This could justify the fact that the final value of degree of saturation of the sample is not greatly increased, even though the drainage of the sample was compromised with the changes of the parameter a_M; given most of the wetting fluid is stored in the micropores, the microscale hydraulic behavior is dominant over the overall hydraulic behavior tendency of the sample, making any variation of the parameters related to the macroscale represent subtle changes on the entire sample degree of saturation.

Finally, it is also important to highlight the fact that the hydraulic behavior tendency of the microscale is not affected by the changes in the parameter a_M, proving that it influences majorly the macroscale. Considering this for analysis of the general behavior of bimodal is extremely interesting, given that the macroscale is usually the one that it is primarily addressed in most soil hydraulic behavior models.

Next, the evaluation of the SWCC was made for the variation of the parameter a_m. Here, three values for the referred were verified: 500, 10000, and 50000. Again, the purpose was to reach a different order of magnitude from the initial value and from each other. In this case, it was possible to use a value of a_m lower than the initial. The variation of the format of the SWCC made with the changes in a_m is shown in Figure 6.12.

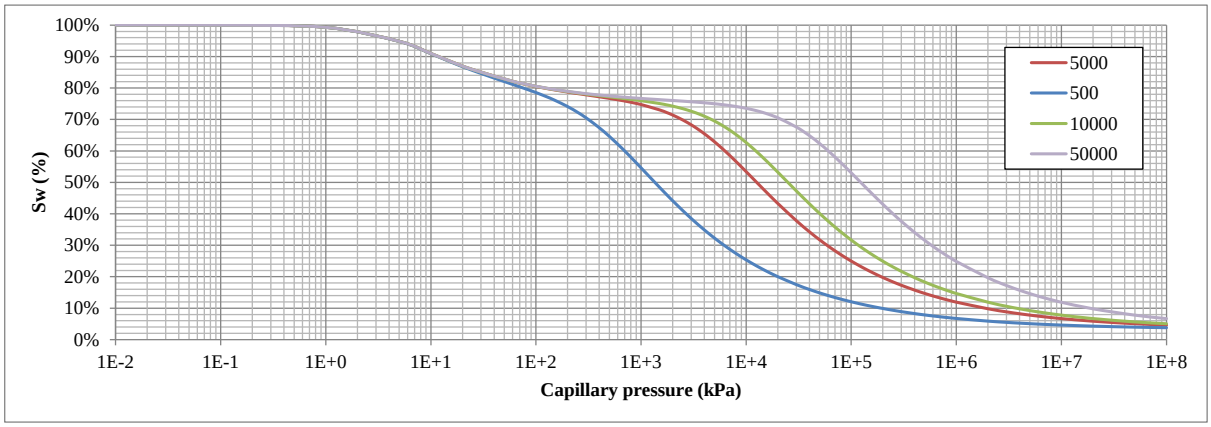

Figure 6.12 - Sensitivity analysis for a_m of the SWCC of the theoretical bimodal soil sample.

The parameter a_m physically represents the value of capillary pressure required for the initiating the process of drainage of the micropores of the soil sample. As it is lowered, it should become easier to remove wetting fluid from the micropores; a lower value of capillary pressure is required in this case; at the same time, if it is increased, it should become more difficult to remove the wetting fluid from the micropores, given the value of capillary pressure should be higher for that purpose. This tendency can be observed in Figure 6.12.

For the value of a_m = 500 kPa, the format of the curve changes to a condition that almost destroys the microscale plateau. In terms of it physical representativeness, it should depict the case in which the soil presents a quasi monomodal pore distribution; for the values of capillary pressure used as condition for the analysis, it means the micropores of the sample would be drained almost as quickly as the macropores, generating high hydraulic gradients values, and, consequently, numerical instabilities in the numerical model.

When the value of a_m = 50000 kPa was used, higher capillary pressure values are required to remove wetting fluid from the micropores. In terms of the representativeness of the studied phenomenon, this could generate difficulties regarding the calculation of the variables of the problem. The capillary pressure value required to drain the microscale would be in a different order of magnitude if compared to the one required to do the same with the macroscale, The drainage of the micropores would be difficult for the values of capillary pressure reached with the conditions established for the solution of the problem. This is observed for a_m = 50000 kPa, and it justifies the difficulty of solving the problem in this case.

It can be inferred that there is an optimal range for the order of magnitude of the parameter a_m. The value of the parameter a_m should be around 3 orders of magnitude higher than the value of the parameter a_M, with values larger than that being avoided for optimal results when numerically verifying the hydraulic behavior of the soil sample.

Nonetheless, it is still possible to carry out the numerical solution of the problem with the value of a_m = 10000 kPa. The results of these simulations are shown in Table 6.24.

Table 6.24 - Results for a_m = 10000 kPa of the SWCC for the theoretical bimodal soil sample.

Evaluated value	**Initial theoretical sample**	**a_m=10000 kPa**	**Difference**
Initial S_{wM}	54,9000%	54,9000%	-
Final S_{wM}	5,8451%	5,9332%	1,5072%
Initial S_{wm}	99,9919%	99,9919%	-
Final S_{wm}	93,1778%	97,2748%	4,3970%
Initial p_c	15 kPa	15 kPa	-
Final p_c	2087 kPa	2013 kPa	-3,5458%
Initial S_w (SWCC)	88,6050%	88,6050%	-
Final S_w (SWCC)	70,8947%	71,1417%	0,3484%
Initial S_w (calculated)	88,6100%	88,6100%	-
Final S_w (calculated)	71,1283%	74,2131%	4,3370%

Similarly to the observed in the macroscale, the microscale hydraulic behavior is affected with the change in the parameter a_m. In this case, it can be seen that the macroscale hydraulic behavior is not affected by the parameter a_m, as expected. This parameter only affects the drainage condition of the micropores of the sample. For higher values of a_m, the values of capillary pressure required for draining the micropores are expected to be higher. In practical terms, it means that for the conditions established for the proposed analysis, less wetting fluid should be drained out of the micropores. Therewith, given a_m = 10000 kPa is

larger than the initial condition established for the theoretical soil sample, the expectation is confirmed and it is indeed more difficult to drain the wetting fluid out of the micropores in this particular case. Even though the capillary pressure value reached with the simulation (2013 kPa) is close to the one reached for the initial simulation used as basis of comparison for the evaluation of the results (2087 kPa), it still was not possible to drain the micropores equally in both cases, with the degree of saturation of the microscale for the initial condition as 93,1778%, and 97,2748% for the simulation with a_m = 10000 kPa.

6.1.4.3 SENSITIVITY ANALYSIS OF THE PARAMETER n

Finally, the parameter n_i is assessed for its influence on the format of the SWCC of the soil sample. This parameter changes the slope of the curve for each scale, which affects the values of capillary required for draining the sample. The variation of the format of the SWCC made with the changes in the parameter n_M is shown in Figure 6.13.

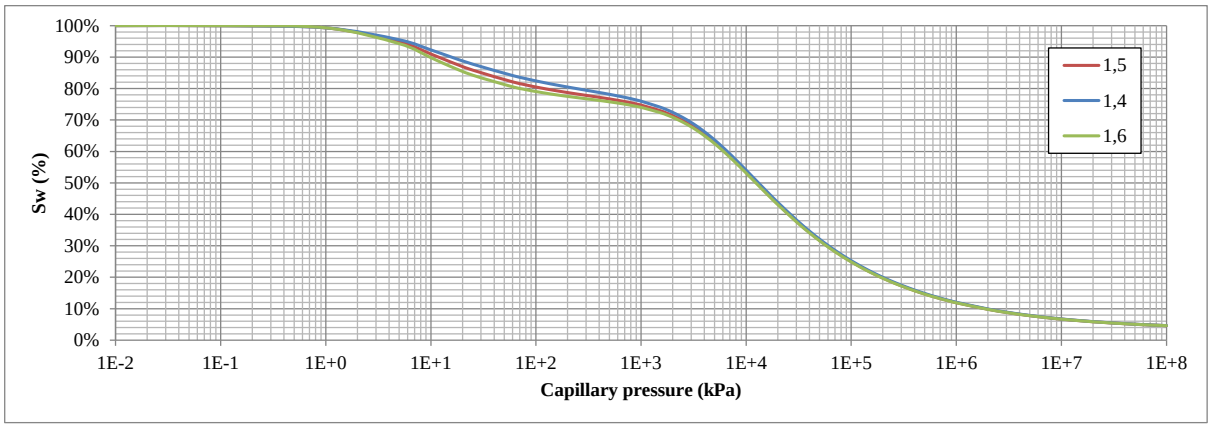

Figure 6.13 - Sensitivity analysis for n_M of the SWCC of the theoretical bimodal soil sample.

It can be verified that as the value of the parameter n_M increases, the macroscale portion of the SWCC becomes steeper. Nonetheless, the effect of varying this parameter was not considered extremely significant and, therefore, no simulations were carried out for the verification of the influence of this parameter in terms of the response of the numerical model. Then, the variation of the format of the SWCC with the changes in the parameter n_m is analyzed based on its representation shown in Figure 6.14.

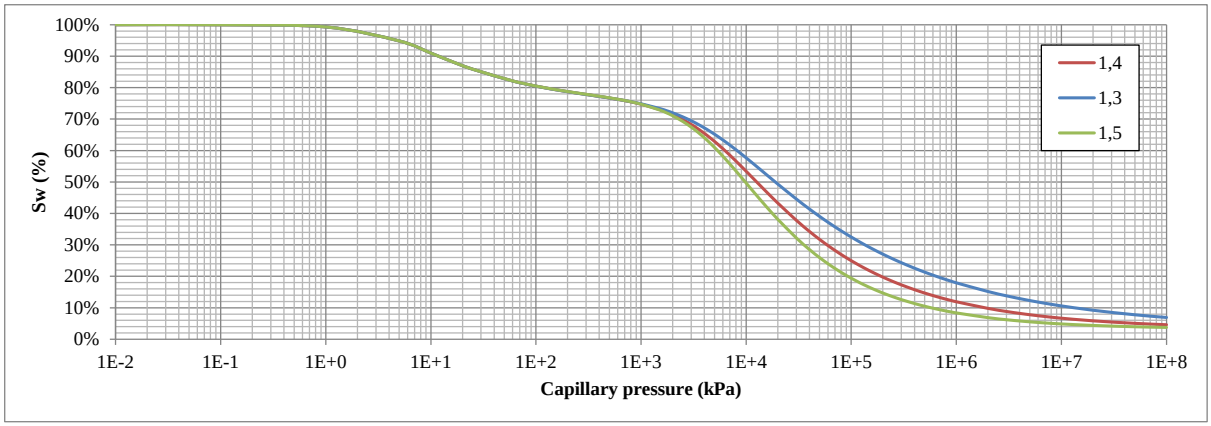

Figure 6.14 - Sensitivity analysis for n_m of the SWCC of the theoretical bimodal soil sample.

The variation of the parameter n_m affects more significantly the format of the microscale portion of the SWCC and, therefore, it is expected to change significantly the overall behavior of the soil sample. When the value of the parameter n_m is decreased, the microscale portion of the SWCC becomes less steep, and, therefore, only higher values of capillary pressure are expected to drain the micropores in comparison to the higher values of n_m. On the other hand, when the value of the parameter n_m is increased, the microscale portion of the curve becomes steeper, and this should make the drainage of the micropores of the sample easier, given lower values of capillary pressure are then required for that purpose.

The verification of the influence of the parameter n_m is made with the simulations for n_m = 1,3 and 1,5. The results of the simulations for n_m = 1,3 are shown in Table 6.25.

Table 6.25 - Results for n_m = 1,3 of the SWCC for the theoretical bimodal soil sample.

Evaluated value	**Initial theoretical sample**	**n_m=1,3**	**Difference**
Initial S_{wM}	54,9000%	54,9000%	-
Final S_{wM}	5,8451%	5,8587%	0,2327%
Initial S_{wm}	99,9919%	99,9919%	-
Final S_{wm}	93,1778%	94,0598%	0,9466%
Initial p_c	15 kPa	15 kPa	-
Final p_c	2087 kPa	2075 kPa	-0,5750%
Initial S_w (SWCC)	88,6050%	88,6050%	-
Final S_w (SWCC)	70,8947%	70,9346%	0,0563%
Initial S_w (calculated)	88,6100%	88,6100%	-
Final S_w (calculated)	71,1283%	71,7910%	0,9317%

The drainage of the microscale portion of the sample was more difficult in this case, as expected. For the same boundary conditions used for the initial SWCC format, it was not possible to drain the micropores of the sample as much with n_m=1,3. The value of the final degree of saturation at the monitored point in the sample was 0,9466% greater than the one achieved with the initial condition of sample. The capillary pressure was not sufficient to drain the sample as significantly as it was for the initial condition of sample, even though almost the same value is reached (2087 kPa for the initial condition; 2075 kPa with n_m=1,3).

Again, it is important to highlight that the behavior of the macroscale is not affected by the microscale parameter variation; the drainage of the macropores is the same observed for the initial condition of the sample. Also, the degree of saturation of the entire sample is changed due to the influence on the microscale hydraulic behavior; given the degree of saturation of the microscale is higher, it is also possible to verify that the degree of saturation of the entire sample is higher than in the initial condition of sample.

Finally, the results of the simulations for n_m=1,5 are shown in Table 6.26.

Table 6.26 - Results for n_m = 1,5 of the SWCC for the theoretical bimodal soil sample.

Evaluated value	**Initial theoretical sample**	**n_m=1,5**	**Difference**
Initial S_{wM}	54,9000%	54,9000%	-
Final S_{wM}	5,8451%	5,8236%	-0,3678%
Initial S_{wm}	99,9919%	99,9919%	-
Final S_{wm}	93,1778%	92,5704%	-0,6519%
Initial p_c	15 kPa	15 kPa	-
Final p_c	2087 kPa	2106 kPa	0,9104%
Initial S_w (SWCC)	88,6050%	88,6050%	-
Final S_w (SWCC)	70,8947%	70,8315%	-0,0892%
Initial S_w (calculated)	88,6100%	88,6100%	-
Final S_w (calculated)	71,1283%	70,6688%	-0,6460%

As it can be seen from the format of the curve shown in Figure 6.14, the value of capillary pressure required to lower the degree of saturation of the micropores is lower than the one verified for the initial condition of the sample. In practical terms, it means that for the same boundary conditions, more wetting fluid drainage was expected with the parameter n_m higher than in the initial condition of the sample, as proven with the performed simulation. Even a subtle difference in this parameter affected the degree of saturation of the microscale, and, therefore, of the entire sample, making the drainage of the sample more significant.

In an overall evaluation of the influence of the parameters of the SWCC for the hydraulic behavior of a bimodal soil sample, it can be established that:

- The variation of the parameters on each scale affects most significantly the hydraulic behavior of the referred scale, and does not influence the other scale. This information is particularly valuable in cases in which the bimodal soil structure is observed, because for the appropriate description of the hydraulic phenomena of the sample, it would be of paramount importance the consideration of the multiscale approach.
- The accuracy of the parameters is quite significant for the performance of the numerical model. Therewith, it is important to verify the input data used to determine the SWCC of the studied soil sample, as well as the initial conditions of the evaluated problem.

6.2 SIMULATION OF FLOW IN BIMODAL TROPICAL SOILS

These simulations are made for the evaluation of the hydraulic behavior of real bimodal soils. More specifically, the data for two different soil samples provided by Otálvaro (2013) were used for this stage of the research.

Otálvaro (2013) made an experimental research of the hydraulic behavior of bimodal soils. The studied soil samples were collected in Taguatinga, Distrito Federal, and they are composed by a tropical, lateritic soil, with high contents of clay minerals.

The soil characterization was made by the author, with physical and chemical analyses so as to better evaluate the structure of the studied soil. According to the Unified Soil Classification System (USCS), the soil was classified as ML. With more laboratory tests run by Otálvaro (2013), it was observed there were silt and clay aggregations (sand grain-sized aggregations) in the samples, as typically observed in Brazilian lateritic soils. Given the local-specific features and the results of the tests run in this soil, it can be classified as a compacted residual soil with bimodal structure. Previous studies (Guimarães, 2002; Delgado, 2002; Silva, 2007) also indicated this type of structure for the soil of this region.

Otálvaro (2013) prepared the soils samples by manual disaggregation, followed by their compaction for different conditions of moisture content and applied compaction energy. Two samples, PN28 and NP24, were chosen for the study. PN28 refers to the soil sample with moisture content of 28% and compacted with standard Proctor energy (600 kN-m/m^3). NP24 refers to the soil sample with moisture content of 24% and compacted with lower energy (240 kN-m/m^3). It is important to highlight that the bimodal soil structure remains present in the

samples even after compaction. According to Otálvaro et al. (2016), the bimodal structure could explain the particularities of the hydro-mechanical behavior of this soil.

Then, tests regarding the structural arrangement of the soil were carried out: Scanning Electronic Microscopy (SEM) and MIP. Otálvaro et al. (2016) discuss the possibility of using this type of experimental result as input of models for reproduction of physical phenomena that are influenced by the double structure of the soil. Also, the SWCC of the sample was retrieved from experimental procedures made by the referred author.

The results of the tests run by Otálvaro (2013) were used as basis for definition of the input data for the simulations and comparison for further analyses made. In Sections 6.2.1 and 6.2.2, these results are presented and discussed.

6.2.1 HOMOGENIZATION PARAMETER SENSITIVITY ANALYSIS

6.2.1.1 DEFINITION OF THE BIMODAL SOIL SAMPLES PARAMETERS

The first step was determining the intrinsic permeability of each scale of pores within the samples. As known, there is a direct correlation between the size and the distribution of the pores of the sample and the permeability of the medium. The mathematical definition of the premises of García-Bengochea et al. (1979) was shown in Equation (2.9).

The determination of the diameter of the pores of the sample and the definition of the void ratio are based on the results of the MIP tests performed by Otálvaro (2013). At first, it is possible to relate the required pressure for the intrusion of mercury in the pores of the soil sample and size of the pores with Washburn's equation, defined in Equation (2.1). Then, the non-wetting fluid void ratio is calculated with the collected data of intruded volume of mercury with Equation (2.4). Finally, the void ratio parameter for the wetting fluid phase is calculated as expressed in Equation (2.3).

It is important to highlight that the total void ratio of the sample was calculated during the tests of characterization of the soil performed by Otálvaro (2013), based on the values of void volume and solids volume of each sample. Also, the MIP procedure of the referred research was made not only for intrusion, but also for extrusion of mercury from the pores. All the values of pressure, for both intrusion and extrusion procedures, were collected, analyzed and used as basis for the definition of parameters proposed in the present research.

The next step for the definition of the intrinsic permeability is to determine the pore size range that represents each scale of the problem, macro and micropores. Delage &

Lefebvre (1984) suggest a procedure based on the data of wetting fluid void ratio (e_w) and diameter of the pores (D). They are plotted in a graphic and the curve is analyzed: the value of the largest pore diameter of the extrusion portion of the curve is used as basis for the definition of the limit between macro and micropores.

The value of wetting fluid void ratio (e_w) correspondent to the largest pore diameter of the extrusion portion of the curve is used as reference for the definition of the limit value of diameter between macro and microscale. The results of this step of the analysis are shown in Figure 6.15 and Figure 6.16 for soil samples PN28 and NP24, respectively.

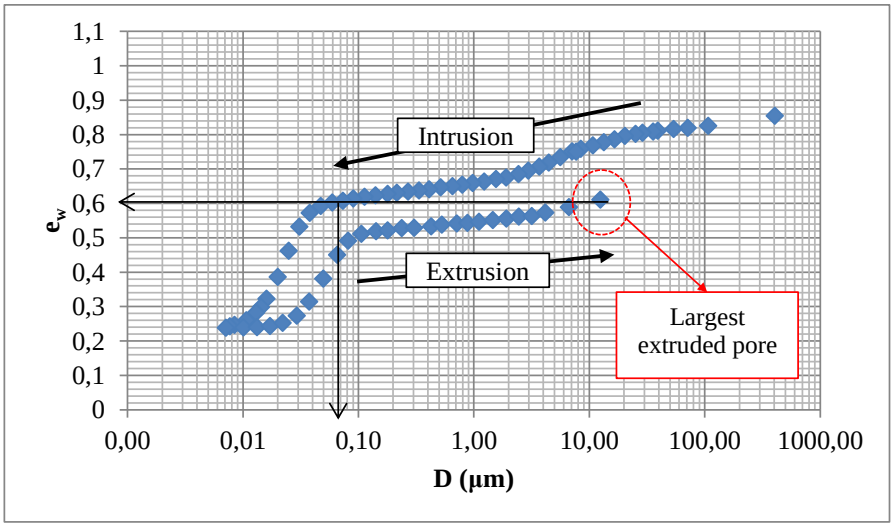

Figure 6.15 – e_w versus diameter of the pores curve for the PN28 sample.

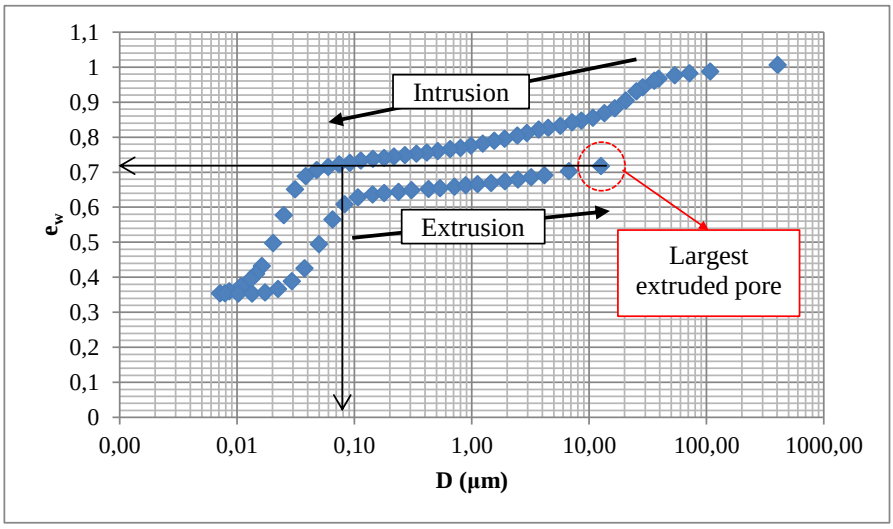

Figure 6.16 - e_w versus diameter of the pores curve for the NP24 sample.

Then, the procedure for definition of macro and microscale porosity is:

- Definition of the microscale void ratio based on the definition of limit value between macro and microscale. The wetting fluid void ratio corresponds to the void ratio of the microscale (e_m), following the procesure established by Delage & Lefebvre (1984);
- Definition of the macroscale void ratio based on the definition of microscale void ratio and total void ratio of the sample and depicted in Equation (2.7);
- Determination of the porosity of macro and microscale (ϕ_M and ϕ_m, respectively).

For the PN28 soil sample, the limit value of pore diameter that establishes the limit between the macro and micropores of the sample is 0,09 µm. This value of diameter is equivalent to a wetting fluid void ratio of 0,61.

For the NP24 soil sample, the limit value of pore diameter that establishes the limit between the macro and micropores of the sample is 0,07 µm. This value of diameter is equivalent to a wetting fluid void ratio of 0,72.

The value of total void ratio of each sample had been defined beforehand, as a result of the soil characterization tests performed by Otálvaro (2013). As mentioned, the values of void ratio defined in the latter step are used for calculation of the porosity of the sample. The porosity of soil sample can be calculated based on the values of void ratio as depicted in Equation (2.10). All values of void ratio and porosity are organized in Table 6.27.

Table 6.27 - Void ratio values for PN28 and NP24 soil samples.

Evaluated index	**PN28**	**NP24**
Total void ratio (e)	0,85	1,01
Limit diameter D	0,09 µm	0,07 µm
Limit value of e_w: microscale void ratio (e_m)	0,61	0,72
Macroscale void ratio (e_M)	0,24	0,29
Total porosity (ϕ)	46,08%	50,14%
Microscale porosity (ϕ_m)	37,93%	41,76%
Macroscale porosity (ϕ_M)	19,58%	22,40%

After the definition of limit diameter, non-wetting fluid void ratio and porosity for each scale of the sample (macro and microscale), the PSD value is calculated, following Equation (2.2). With the values of PSD calculated, it is possible to plot the PSD curve, which depicts the relationship between the values of PSD and the diameter of the pores of the sample. The PSD curves for PN28 and NP24 are shown in Figure 6.17 and Figure 6.18, respectively.

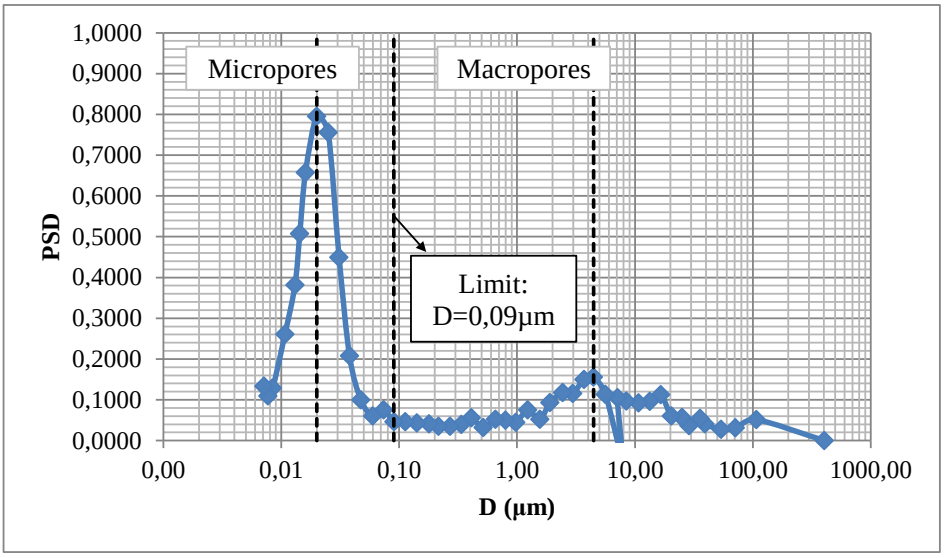

Figure 6.17 - PSD curve for PN28 sample.

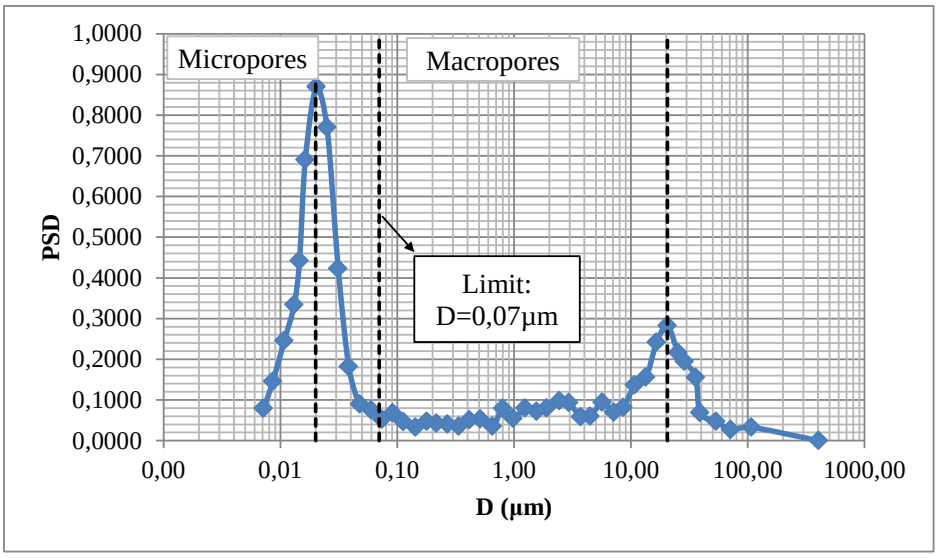

Figure 6.18 - PSD curve for NP24 sample.

Based on the PSD curve, the average values of the macro and micropores diameter of each sample can be defined. These values are used for the definition of the homogenization parameter ε (Equation (5.1)):

- Macropore diameter average value for PN28: 4,46 µm
- Micropore diameter average value for PN28: 0,02 µm
- Macropore diameter average value for NP24: 20,52 µm
- Micropore diameter average value for NP24: 0,02 µm

Finally, the intrinsic permeability of each scale is calculated with Equation (2.11). The values used for the calculation and the final value of intrinsic permeability for PN28 and NP24 are shown in Table 6.28. The intrinsic permeability values calculated here are used as input parameters of the set of simulations shown in Sections 6.2.1.2 and 6.2.2.

Table 6.28 - Intrinsic permeability calculation parameters for PN28 and NP24 samples.

Sample	Calculation parameter	Macroscale	Microscale	Total
PN28	Porosity (ϕ_t)	19,58%	37,93%	46,08%
	$\sum_{1}^{i} f(r_i) r_i^2$	$2{,}82 \cdot 10^{-10}$	$6{,}88 \cdot 10^{-16}$	$2{,}82 \cdot 10^{-10}$
	Intrinsic permeability (K_i)	$6{,}90 \cdot 10^{-12}$ m²	$3{,}26 \cdot 10^{-17}$ m²	$1{,}62 \cdot 10^{-11}$ m²
NP24	Porosity (ϕ_t)	22,40%	41,76%	50,14%
	$\sum_{1}^{i} f(r_i) r_i^2$	$3{,}75 \cdot 10^{-10}$	$5{,}93 \cdot 10^{-16}$	$3{,}75 \cdot 10^{-10}$
	Intrinsic permeability (K_i)	$1{,}05 \cdot 10^{-11}$ m²	$3{,}10 \cdot 10^{-17}$ m²	$2{,}35 \cdot 10^{-11}$ m²

6.2.1.2 RESULTS OF THE NUMERICAL ANALYSES

The homogenization parameter ε is part of the hydraulic behavior mathematical model (Chapter 5). This parameter should be calibrated for the bimodal soils samples that are used in the different numerical simulation analyses proposed in this research.

For this purpose, a set of simulations is proposed. These simulations are permeability tests, and they follow the procedure described in Section 4.1.

The value of hydraulic conductivity of the medium is used as measurement for comparison of the behavior of the medium and for the proper adjustments of the homogenization parameter ε. Then, the first step was the calculation of the equivalent hydraulic conductivity for Region 1. In order to consider both macro and microscales, the equivalent hydraulic conductivity is calculated with the values of total intrinsic permeability, shown in Table 6.28, and fluid properties, shown in Table 4.1. Using Equation (4.2), the equivalent hydraulic conductivity is calculated. The results are shown in Table 6.29.

Finally, the simulations were conducted and their results are summarized in Table 6.30 for PN28 and Table 6.31 for NP24.

Table 6.29 - Equivalent hydraulic conductivity calculation parameters for PN28 and NP24.

Calculation parameter	**PN28**	**NP24**
Intrinsic permeability (K_t)	$1{,}62 \cdot 10^{-11}$ m²	$2{,}35 \cdot 10^{-11}$ m²
Water specific mass (ρ_w)	1,00 g/cm³	1,00 g/cm³
Water viscosity (μ_w)	$1{,}00 \cdot 10^{-6}$ kPa.s	$1{,}00 \cdot 10^{-6}$ kPa.s
Gravity (g)	10 m/s²	10 m/s²
Equivalent hydraulic conductivity (k_{wt})	$1{,}58 \cdot 10^{-4}$ m/s	$2{,}29 \cdot 10^{-4}$ m/s

Table 6.30 - Homogenization parameter calibration data for PN28 soil sample.

ε	q_{wM} [m³/s]/[m]	q_{wm} [m³/s]/[m]	q_{wt} [m³/s]/[m]	q_{wc} [m³/s]/[m]	$h_{y=1,0001m}$ [m]	k_{wc} [m/s]
0,10000	$6{,}853 \cdot 10^{-4}$	$3{,}238 \cdot 10^{-7}$	$6{,}856 \cdot 10^{-4}$	$6{,}856 \cdot 10^{-4}$	0,068546	$6{,}90 \cdot 10^{-5}$
0,01000	$6{,}850 \cdot 10^{-4}$	$3{,}237 \cdot 10^{-5}$	$7{,}174 \cdot 10^{-4}$	$7{,}174 \cdot 10^{-4}$	0,071727	$7{,}23 \cdot 10^{-5}$
0,00900	$6{,}850 \cdot 10^{-4}$	$3{,}996 \cdot 10^{-5}$	$7{,}250 \cdot 10^{-4}$	$7{,}250 \cdot 10^{-4}$	0,072481	$7{,}30 \cdot 10^{-5}$
0,00700	$6{,}85 \cdot 10^{-4}$	$6{,}603 \cdot 10^{-5}$	$7{,}509 \cdot 10^{-4}$	$7{,}509 \cdot 10^{-4}$	0,07507	$7{,}57 \cdot 10^{-5}$
0,00500	$6{,}844 \cdot 10^{-4}$	$1{,}293 \cdot 10^{-4}$	$8{,}137 \cdot 10^{-4}$	$8{,}137 \cdot 10^{-4}$	0,081356	$8{,}20 \cdot 10^{-5}$
0,00300	$6{,}828 \cdot 10^{-4}$	$3{,}585 \cdot 10^{-4}$	$1{,}041 \cdot 10^{-3}$	$1{,}041 \cdot 10^{-3}$	0,104106	$1{,}05 \cdot 10^{-4}$
0,00200	$6{,}798 \cdot 10^{-4}$	$8{,}029 \cdot 10^{-4}$	$1{,}483 \cdot 10^{-3}$	$1{,}483 \cdot 10^{-3}$	0,148239	$1{,}50 \cdot 10^{-4}$
0,00199	$6{,}797 \cdot 10^{-4}$	$8{,}109 \cdot 10^{-4}$	$1{,}491 \cdot 10^{-3}$	$1{,}491 \cdot 10^{-3}$	0,149036	$1{,}51 \cdot 10^{-4}$
0,00195	$6{,}795 \cdot 10^{-4}$	$8{,}443 \cdot 10^{-4}$	$1{,}524 \cdot 10^{-3}$	$1{,}524 \cdot 10^{-3}$	0,152345	$1{,}55 \cdot 10^{-4}$
0,00193	$6{,}794 \cdot 10^{-4}$	$8{,}617 \cdot 10^{-4}$	$1{,}541 \cdot 10^{-3}$	$1{,}541 \cdot 10^{-3}$	0,154076	$1{,}57 \cdot 10^{-4}$
0,00191	$6{,}792 \cdot 10^{-4}$	$8{,}797 \cdot 10^{-4}$	$1{,}559 \cdot 10^{-3}$	$1{,}559 \cdot 10^{-3}$	0,155862	$1{,}58 \cdot 10^{-4}$
0,00190	$6{,}792 \cdot 10^{-4}$	$8{,}889 \cdot 10^{-4}$	$1{,}568 \cdot 10^{-3}$	$1{,}568 \cdot 10^{-3}$	0,156775	$1{,}59 \cdot 10^{-4}$
0,00189	$6{,}791 \cdot 10^{-4}$	$8{,}982 \cdot 10^{-4}$	$1{,}577 \cdot 10^{-3}$	$1{,}577 \cdot 10^{-3}$	0,157703	$1{,}60 \cdot 10^{-4}$
0,00100	$6{,}638 \cdot 10^{-4}$	$3{,}136 \cdot 10^{-3}$	$3{,}800 \cdot 10^{-3}$	$3{,}800 \cdot 10^{-3}$	0,379914	$3{,}95 \cdot 10^{-4}$

Table 6.31 - Homogenization parameter calibration data for NP24 soil sample.

ε	q_{wM} [m³/s]/[m]	q_{wm} [m³/s]/[m]	q_{wt} [m³/s]/[m]	q_{wc} [m³/s]/[m]	$h_{y=1,0001m}$ [m]	k_{wc} [m/s]
0,10000	$1{,}039 \cdot 10^{-3}$	$3{,}068 \cdot 10^{-7}$	$1{,}039 \cdot 10^{-3}$	$1{,}039 \cdot 10^{-3}$	0,103919	$1{,}05 \cdot 10^{-4}$
0,01000	$1{,}039 \cdot 10^{-3}$	$3{,}067 \cdot 10^{-5}$	$1{,}069 \cdot 10^{-3}$	$1{,}069 \cdot 10^{-3}$	0,106923	$1{,}08 \cdot 10^{-4}$
0,00500	$1{,}038 \cdot 10^{-3}$	$1{,}226 \cdot 10^{-4}$	$1{,}160 \cdot 10^{-3}$	$1{,}160 \cdot 10^{-3}$	0,116015	$1{,}17 \cdot 10^{-4}$
0,00400	$1{,}037 \cdot 10^{-3}$	$1{,}914 \cdot 10^{-4}$	$1{,}228 \cdot 10^{-3}$	$1{,}228 \cdot 10^{-3}$	0,122823	$1{,}24 \cdot 10^{-4}$
0,00300	$1{,}036 \cdot 10^{-3}$	$3{,}397 \cdot 10^{-4}$	$1{,}375 \cdot 10^{-3}$	$1{,}375 \cdot 10^{-3}$	0,137499	$1{,}39 \cdot 10^{-4}$
0,00200	$1{,}031 \cdot 10^{-3}$	$7{,}611 \cdot 10^{-4}$	$1{,}792 \cdot 10^{-3}$	$1{,}792 \cdot 10^{-3}$	0,179193	$1{,}82 \cdot 10^{-4}$
0,00160	$1{,}027 \cdot 10^{-3}$	$1{,}184 \cdot 10^{-3}$	$2{,}211 \cdot 10^{-3}$	$2{,}211 \cdot 10^{-3}$	0,221051	$2{,}26 \cdot 10^{-4}$
0,00158	$1{,}026 \cdot 10^{-3}$	$1{,}214 \cdot 10^{-3}$	$2{,}240 \cdot 10^{-3}$	$2{,}240 \cdot 10^{-3}$	0,223999	$2{,}29 \cdot 10^{-4}$
0,00157	$1{,}026 \cdot 10^{-3}$	$1{,}229 \cdot 10^{-3}$	$2{,}256 \cdot 10^{-3}$	$2{,}256 \cdot 10^{-3}$	0,225515	$2{,}31 \cdot 10^{-4}$
0,00156	$1{,}026 \cdot 10^{-3}$	$1{,}245 \cdot 10^{-3}$	$2{,}271 \cdot 10^{-3}$	$2{,}271 \cdot 10^{-3}$	0,22706	$2{,}32 \cdot 10^{-4}$
0,001555	$1{,}026 \cdot 10^{-3}$	$1{,}253 \cdot 10^{-3}$	$2{,}279 \cdot 10^{-3}$	$2{,}279 \cdot 10^{-3}$	0,227844	$2{,}33 \cdot 10^{-4}$
0,00155	$1{,}026 \cdot 10^{-3}$	$1{,}261 \cdot 10^{-3}$	$2{,}287 \cdot 10^{-3}$	$2{,}287 \cdot 10^{-3}$	0,228635	$2{,}34 \cdot 10^{-4}$
0,00150	$1{,}025 \cdot 10^{-3}$	$1{,}345 \cdot 10^{-3}$	$2{,}370 \cdot 10^{-3}$	$2{,}370 \cdot 10^{-3}$	0,236976	$2{,}43 \cdot 10^{-4}$
0,00100	$1{,}008 \cdot 10^{-3}$	$2{,}976 \cdot 10^{-3}$	$3{,}985 \cdot 10^{-3}$	$3{,}985 \cdot 10^{-3}$	0,398384	$4{,}15 \cdot 10^{-4}$

In the latter results, the value of the appropriate homogenization parameter is highlighted. For the PN28 soil sample, the homogenization parameter ε is 0,00191. For the NP24 soil sample, the homogenization parameter ε is 0,00158.

The homogenization parameter can be calculated via Equation (5.1) with the data collected from the PSD curves of each sample (Figure 6.17 and Figure 6.18). The calculation parameters and theoretical ε for each sample are resumed in Table 6.32. Then, a comparison of the numerical and the theoretical values of ε is made and shown in Table 6.33.

Table 6.32 - Theoretical homogenization parameter ε for PN28 and NP24.

Calculation parameter	**PN28**	**NP24**
Macropore diameter average value (μm)	4,46	20,52
Micropore diameter average value (μm)	0,02	0,02
ε	0,0045	0,0010

Table 6.33 - Calibrated and theoretical homogenization parameter ε for PN28 and NP24.

Homogenization parameter ε	**PN28**	**NP24**
Calibrated ε (via numerical simulation)	0,0019	0,0016
Theoretical ε (via Equation (5.1))	0,0045	0,0010

It can be seen that they are in the same order of magnitude. Therewith, the calibration of the homogenization parameter is validated and appropriate for the goals of the research.

6.2.2 DRYING AND WETTING SIMULATIONS IN BIMODAL SOIL SAMPLES

In this set of simulations, the verification of the hydraulic behavior of the bimodal soil samples was made. Drying and wetting tests were carried out for the PN28 and the NP24 soil samples following the same methodology used for the theoretical bimodal soil sample, presented in Section 4.1. At first, the definition of input data for the drying and wetting simulations is made, and they are summarized in Section 6.2.2.1; then, the simulations results and discussion are presented in Section 6.2.2.2.

6.2.2.1 INPUT DATA FOR THE NUMERICAL MODEL

Based on the numerical analyses already made for calibration of the parameters of the model for these soil samples (Section 6.2.1), the input data for the drying and wetting simulations are presented in Table 6.34 for PN28 and in Table 6.35 for NP24 soil samples.

Table 6.34 - Input data for the drying and wetting tests for the PN28 soil sample.

Variable	Drying	Wetting
Homogenization parameter value (ε)	0,0045	
Intrinsic permeability of the macroscale (K_M)	$6{,}90 \cdot 10^{-12}$ m²	
Porosity of the macroscale (ϕ_M)	19,58%	
Intrinsic permeability of the microscale (K_m)	$3{,}26 \cdot 10^{-17}$ m²	
Porosity of the microscale (ϕ_m)	37,93%	
Wetting fluid pressure of the macroscale (p_{wM})	100 kPa	100 kPa
Wetting fluid pressure of the microscale (p_{wm})	100 kPa	100 kPa
Capillary pressure of the macro and microscale (p_{cM} and p_{cm})	4001 kPa	100000 kPa
Degree of saturation of the wetting fluid of the macroscale (S_{wM})	11,98%	10,23%
Degree of saturation of the wetting fluid of the microscale (S_{wm})	99,56%	38,46%

Table 6.35 - Input data for the drying and wetting tests for the NP24 soil sample.

Variable	Drying	Wetting
Homogenization parameter value (ε)	0,0016	
Intrinsic permeability of the macroscale (K_M)	$1{,}05 \cdot 10^{-11}$ m²	
Porosity of the macroscale (ϕ_M)	22,40%	
Intrinsic permeability of the microscale (K_m)	$3{,}10 \cdot 10^{-17}$ m²	
Porosity of the microscale (ϕ_m)	41,76%	
Wetting fluid pressure of the macroscale (p_{wM})	100 kPa	100 kPa
Wetting fluid pressure of the microscale (p_{wm})	100 kPa	100 kPa
Capillary pressure of the macro and microscale (p_{cM} and p_{cm})	2500 kPa	100000 kPa
Degree of saturation of the wetting fluid of the macroscale (S_{wM})	13,43%	10,40%
Degree of saturation of the wetting fluid of the microscale (S_{wm})	99,97%	49,39 %

Then, the values of boundary conditions are defined. They are based on the initial equilibrium condition addressed in Section 4.1. When specifically referring to the boundary condition of the upper part of the domain, the values are varied with the intention of tracking different values of degree of saturation and capillary pressure. With that, the suitability of the

proposed methodology for the definition of the SWCC from the input data retrieved from the MIP test results for each analyzed soil sample is verified. The boundary conditions of the PN28 and the NP24 soil samples are shown in Table 6.36 and Table 6.37, respectively.

Table 6.36 - Boundary conditions for the drying and wetting trajectories simulations for the PN28 soil sample.

Variable	Boundary	Condition	Drying	Wetting
Wetting fluid pressure (p_{wM}) Degree of saturation of the wetting fluid (S_{wM})	Bottom	Essential (Dirichlet)	p_{wM}=100 kPa S_{wM}=11,98%	p_{wM}=100 kPa S_{wM}=10,23%
Wetting fluid pressure (p_{wM}) Degree of saturation of the wetting fluid (S_{wM})	Right side	Natural (Neumann)	$\frac{\partial p_{wM}}{\partial n}=0$ $\frac{\partial S_{wM}}{\partial n}=0$	$\frac{\partial p_{wM}}{\partial n}=0$ $\frac{\partial S_{wM}}{\partial n}=0$
Wetting fluid pressure (p_{wM}) Degree of saturation of the wetting fluid (S_{wM})	Upper	Natural (Neumann)	Variation of value $\frac{\partial S_{wM}}{\partial n}=0$	Variation of value $\frac{\partial S_{wM}}{\partial n}=0$
Wetting fluid pressure (p_{wM}) Degree of saturation of the wetting fluid (S_{wM})	Left side	Natural (Neumann)	$\frac{\partial p_{wM}}{\partial n}=0$ $\frac{\partial S_{wM}}{\partial n}=0$	$\frac{\partial p_{wM}}{\partial n}=0$ $\frac{\partial S_{wM}}{\partial n}=0$

Table 6.37 - Boundary conditions for the drying and wetting trajectories simulations for the NP24 soil sample.

Variable	Boundary	Condition	Drying	Wetting
Wetting fluid pressure (p_{wM}) Degree of saturation of the wetting fluid (S_{wM})	Bottom	Essential (Dirichlet)	p_{wM}=100 kPa S_{wM}=13,43%	p_{wM}=100 kPa S_{wM}=10,40%
Wetting fluid pressure (p_{wM}) Degree of saturation of the wetting fluid (S_{wM})	Right side	Natural (Neumann)	$\frac{\partial p_{wM}}{\partial n}=0$ $\frac{\partial S_{wM}}{\partial n}=0$	$\frac{\partial p_{wM}}{\partial n}=0$ $\frac{\partial S_{wM}}{\partial n}=0$
Wetting fluid pressure (p_{wM}) Degree of saturation of the wetting fluid (S_{wM})	Upper	Natural (Neumann)	Variation of value $\frac{\partial S_{wM}}{\partial n}=0$	Variation of value $\frac{\partial S_{wM}}{\partial n}=0$

Wetting fluid pressure (p_{wM}) Degree of saturation of the wetting fluid (S_{wM})	Left side	Natural (Neumann)	$\frac{\partial p_{wM}}{\partial n} = 0$ $\frac{\partial S_{wM}}{\partial n} = 0$	$\frac{\partial p_{wM}}{\partial n} = 0$ $\frac{\partial S_{wM}}{\partial n} = 0$

Also, the SWCC for the macro and microscale and the entire soil sample are required for the proposed set of simulations. The definition of the SWCC for each scale and for the entire sample for both cases was made based on the data of the MIP tests. The results of these tests were shown in Figure 6.15 (PN28 sample) and Figure 6.16 (NP24 sample) in Section 6.2.1.1. The curves were retrieved from the data of the MIP tests via Equation (2.8), for the calculation of the degree of saturation of the sample, and Equation (2.1), for the calculation of the capillary pressure. These curves are shown in Figure 6.19 and Figure 6.20, for PN28 and NP24 soil samples, respectively.

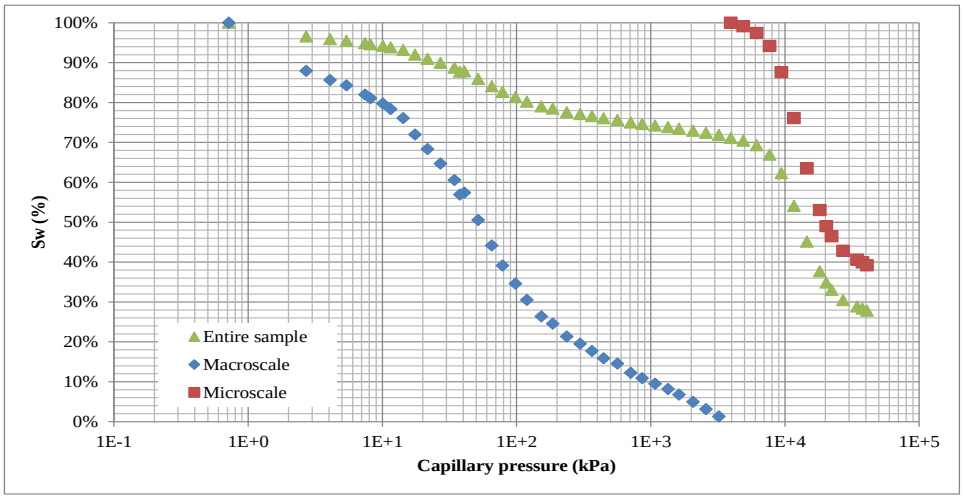

Figure 6.19 - SWCC from the data of the MIP test for the PN28 soil sample.

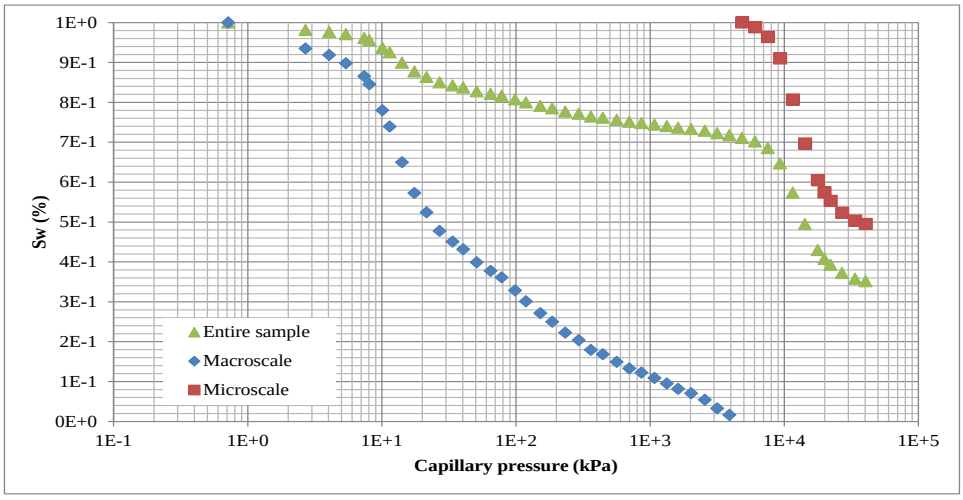

Figure 6.20 - SWCC from the data of the MIP test for the NP24 soil sample.

The approximation of the data to the van Genuchten approach of the SWCC was made via Equation (5.26). They are represented in Figure 6.21 and Figure 6.22 for PN28 and NP24 soil samples, respectively, with the parameters detailed in Table 6.38.

It is important to highlight that the parameter *m* of the macroscale for the NP24 soil sample was defined as 0,35; it did not followed the calculation previewed with Equation (2.6). This adjustment was required for better performance of the numerical model, avoiding numerical instabilities related to the slope of the macroscale portion of the curve.

The referred data of each sample corresponds to the input data of the numerical model defined for the set of simulations proposed at this stage of the research. With these definitions, it was possible to proceed to the drying and wetting trajectory simulations. The simulation methodology followed here was the same used in Section 6.1.3.2 for the theoretical bimodal soil sample.

Table 6.38 - Parameters of the SWCC of the macro and microscale of the PN28 soil sample.

Sample	**SWCC parameters**	**Macroscale**	**Microscale**
PN28	Residual degree of saturation ($S_{res_{wi}}$)	10,00%	38,40%
	Parameter a_i	13,56 kPa	12049,47 kPa
	Parameter n_i	1,67	4,24
	Parameter m_i	0,40	0,76
NP24	Residual degree of saturation ($S_{res_{wi}}$)	10,00%	49,36%
	Parameter a_i	9,34 kPa	12158,17 kPa
	Parameter n_i	1,67	4,64
	Parameter m_i	0,35	0,78

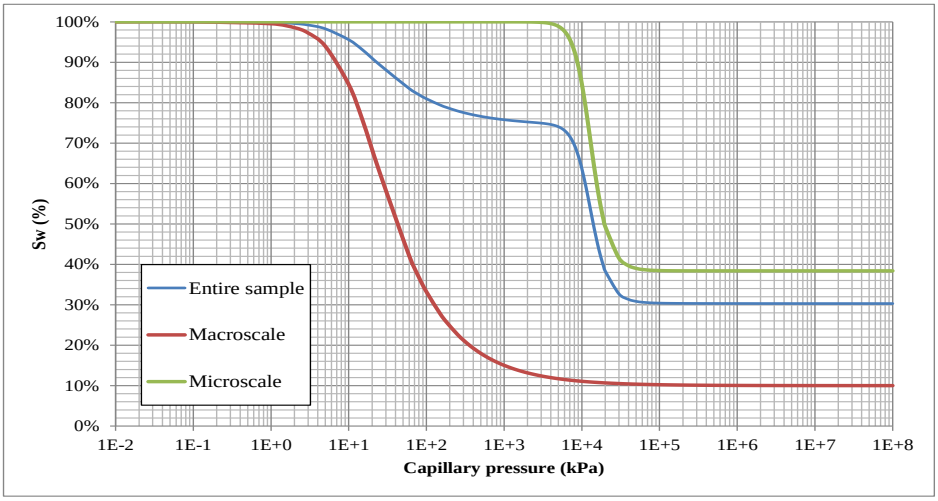

Figure 6.21 - SWCC approximated curve for PN28 sample.

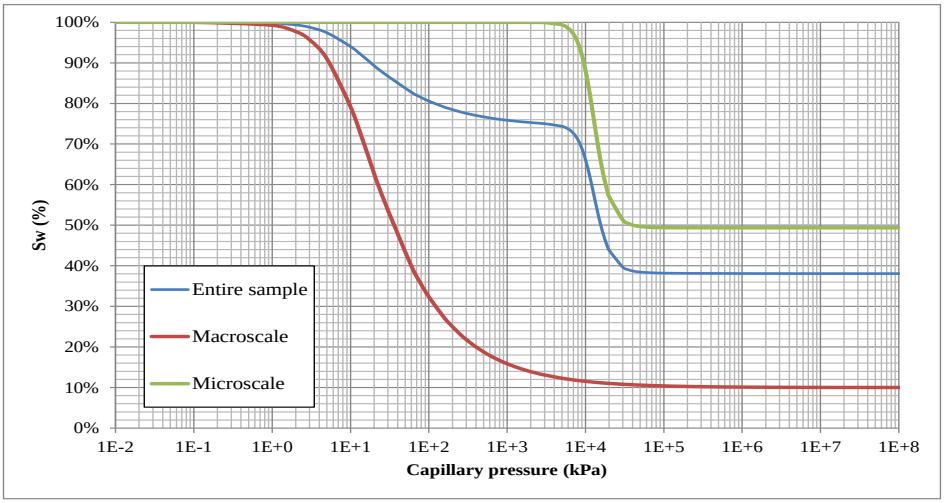

Figure 6.22 - SWCC approximated curve for NP24 sample.

6.2.2.2 RESULTS OF THE DRYING AND WETTING TRAJECTORY SIMULATIONS

The drying and wetting tests were performed for the NP24 and PN28 soil samples with the purpose of verifying the accuracy of the proposed methodology for bimodal soil samples. The simulations were made so as to reproduce the drainage and the wetting of each sample, with retrieval of the results for comparison with the SWCC of the samples. The results shown in this section of the research make reference to the position ($x=0,5$; $y=0,9$) of the sample.

The values of degree of saturation achieved with the simulation are compared to the values which correspond to the original SWCC of the entire sample. The value of degree of saturation of the entire sample is calculated with a weighted average using Equation (4.3) and (4.4). The volume fraction average weight parameters for the PN28 and the NP24 soil samples are presented in Table 6.39.

Table 6.39 - w_M and w_m for drying and wetting of the PN28 and NP24 soil samples.

Sample	**Parameter**	**Drying test**	**Wetting test**
PN28	Volume fraction average weight of the macroscale (w_M)	0,6705	0,6705
	Volume fraction average weight of the microscale (w_m)	0,8687	0,8687
NP24	Volume fraction average weight of the macroscale (w_M)	0,6425	0,6425
	Volume fraction average weight of the microscale (w_m)	0,8561	0,8561

The results of degree of saturation for the drying and wetting trajectory tests are respectively shown in Table 6.40 for the PN28 sample and in Table 6.41 for the NP24

sample. The results are plotted over the SWCC for their comparison to the SWCC curve of Otálvaro (2013). They are represented in Figure 6.23 and Figure 6.24 for both samples.

Table 6.40 - Results of degree of saturation of the PN28 soil sample for drying and wetting.

Test	$\frac{\partial p_{wM}}{\partial n}$	**Final S_{wM}**	**Final S_{wm}**	**Final p_c**	**Final S_w (SWCC)**	**Final S_w (calc.)**	$\frac{S_w^{calc} - S_w^{data}}{S_w^{data}} \times 100\%$
Drying	$-1{,}00 \cdot 10^{-4}$	13,4241%	99,9739%	2507,42	75,1345%	75,1347%	0,0003%
	$-1{,}00 \cdot 10^{-3}$	13,3789%	99,9709%	2565,06	75,1194%	75,1197%	0,0003%
	$-1{,}00 \cdot 10^{-2}$	13,0011%	99,9256%	3142,03	74,9785%	74,9789%	0,0005%
	$-1{,}50 \cdot 10^{-2}$	12,8352%	99,8833%	3463,04	74,9006%	74,9011%	0,0006%
	$-1{,}70 \cdot 10^{-2}$	12,7755%	99,8618%	3591,56	74,8682%	74,8687%	0,0007%
	$-1{,}80 \cdot 10^{-2}$	12,7469%	99,8500%	3655,84	74,8515%	74,8520%	0,0007%
Wetting	$1{,}00 \cdot 10^{-4}$	10,3972%	49,3836%	99978,97	38,1963%	38,1948%	-0,0038%
	$1{,}00 \cdot 10^{-3}$	10,3977%	49,3838%	99748,98	38,1966%	38,1951%	-0,0038%
	$1{,}00 \cdot 10^{-2}$	10,4032%	49,3860%	97449,22	38,1996%	38,1982%	-0,0039%
	$1{,}50 \cdot 10^{-2}$	10,4063%	49,3872%	96171,69	38,2015%	38,2000%	-0,0039%
	$1{,}70 \cdot 10^{-2}$	10,4075%	49,3878%	95660,71	38,2022%	38,2007%	-0,0039%
	$2{,}00 \cdot 10^{-2}$	10,4095%	49,3886%	94894,26	38,2033%	38,2019%	-0,0039%
	$3{,}00 \cdot 10^{-2}$	10,4160%	49,3916%	92339,70	38,2074%	38,2059%	-0,0039%
	$5{,}00 \cdot 10^{-2}$	10,4301%	49,3988%	87231,92	38,2166%	38,2151%	-0,0040%
	$1{,}00 \cdot 10^{-1}$	10,4718%	49,4291%	74473,20	38,2502%	38,2486%	-0,0043%
	$4{,}00 \cdot 10^{-1}$	11,5232%	88,0323%	10025,64	66,0949%	66,0747%	-0,0305%

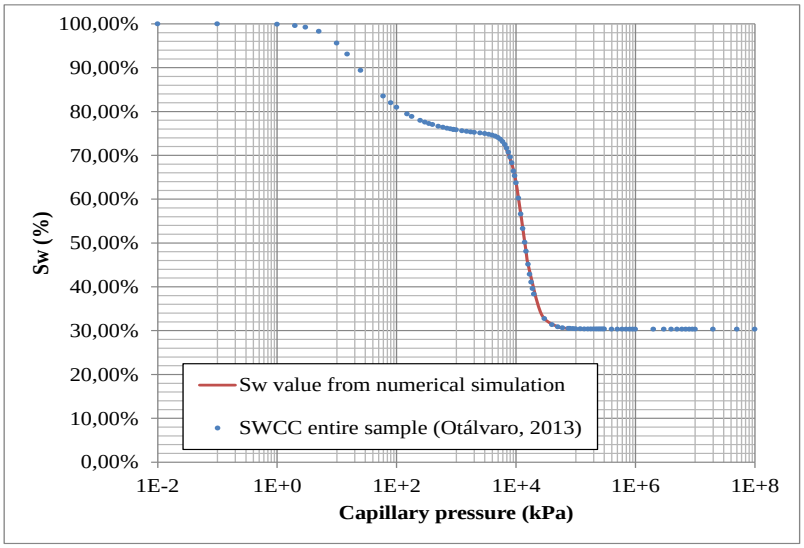

Figure 6.23 - Numerical simulation results compared to the SWCC for PN28 sample.

Table 6.41 - Results of degree of saturation of the NP24 soil sample for drying and wetting.

Test	$\frac{\partial p_{wM}}{\partial n}$	Final S_{wM}	Final S_{wm}	Final p_c	Final S_w (SWCC)	Final S_w (calc.)	$\frac{S_w^{calc} - S_w^{data}}{S_w^{data}} \times 100\%$
Drying	$-1{,}00 \cdot 10^{-4}$	13,4241%	99,9739%	2507,42	75,1345%	75,1347%	0,0003%
	$-1{,}00 \cdot 10^{-3}$	13,3789%	99,9709%	2565,06	75,1194%	75,1197%	0,0003%
	$-1{,}00 \cdot 10^{-2}$	13,0011%	99,9256%	3142,03	74,9785%	74,9789%	0,0005%
	$-1{,}50 \cdot 10^{-2}$	12,8352%	99,8833%	3463,04	74,9006%	74,9011%	0,0006%
	$-1{,}70 \cdot 10^{-2}$	12,7755%	99,8618%	3591,56	74,8682%	74,8687%	0,0007%
	$-1{,}80 \cdot 10^{-2}$	12,7469%	99,8500%	3655,84	74,8515%	74,8520%	0,0007%
Wetting	$1{,}00 \cdot 10^{-4}$	10,3972%	49,3836%	99978,97	38,1963%	38,1948%	-0,0038%
	$1{,}00 \cdot 10^{-3}$	10,3977%	49,3838%	99748,98	38,1966%	38,1951%	-0,0038%
	$1{,}00 \cdot 10^{-2}$	10,4032%	49,3860%	97449,22	38,1996%	38,1982%	-0,0039%
	$1{,}50 \cdot 10^{-2}$	10,4063%	49,3872%	96171,69	38,2015%	38,2000%	-0,0039%
	$1{,}70 \cdot 10^{-2}$	10,4075%	49,3878%	95660,71	38,2022%	38,2007%	-0,0039%
	$2{,}00 \cdot 10^{-2}$	10,4095%	49,3886%	94894,26	38,2033%	38,2019%	-0,0039%
	$3{,}00 \cdot 10^{-2}$	10,4160%	49,3916%	92339,70	38,2074%	38,2059%	-0,0039%
	$5{,}00 \cdot 10^{-2}$	10,4301%	49,3988%	87231,92	38,2166%	38,2151%	-0,0040%
	$1{,}00 \cdot 10^{-1}$	10,4718%	49,4291%	74473,20	38,2502%	38,2486%	-0,0043%
	$4{,}00 \cdot 10^{-1}$	11,5232%	88,0323%	10025,64	66,0949%	66,0747%	-0,0305%

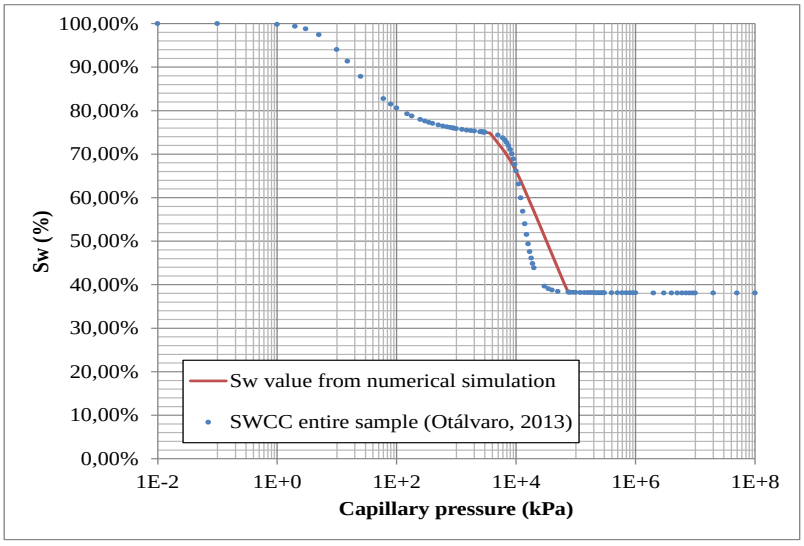

Figure 6.24 - Numerical simulation results compared to the SWCC for NP24 sample.

It is possible to infer from the results that the proposed simulation methodology for verification of hydraulic behavior of bimodal soil samples is appropriate to reproduce the values of capillary pressure and degree of saturation of the medium.

The numerical simulation results are sufficiently accurate in comparison to SWCC. MIP test results were used as input data for the proposed numerical model, and they were

proven adequate for the definition of format of the SWCC. A unique methodology has been established, as the results experimentally obtained by Otálvaro (2013) are numerically reproduced with the mathematical model proposed in the present research.

It is important to highlight that some limitation was encountered in the employed procedure for the wetting simulation. For some values of the natural boundary condition of the wetting fluid phase pressure, it was not possible to proceed with the analyses due to numerical error. This difficulty is associated to the values of capillary pressure that were achieved, that correspond to values higher than the limit for reaching the macroscale residual degree of saturation (in case of the drying trajectory) and lower than the limit for reaching the complete saturation of the micropores (in case of the wetting trajectory).

One possibility for addressing this condition and minimizing the encountered issue could be the addition of a thermodynamic approach in the mathematical model, which would permit the definition of boundary conditions that would more accurately represent the drainage and the wetting of the sample when compared to the real laboratory test.

Another option could be proceed to a second set of analyses, with continuation of the wetting of the sample. When the maximum wetting limit is reached with the initial and boundary conditions used as shown in the performed simulations, the results of the numerical analysis could be used as input data for a new set of simulations; the degree of saturation of each scale reached at the end of the wetting simulation could be used as initial condition for a new round of simulations. Then, the wetting of the sample could be carried out and taken to higher values of degree of saturation, with almost complete saturation of the macroscale.

Finally, the significance of the achieved results resides on the fact that the format of the SWCC is reproduced. The presented results suggest that the MIP test could be made for a given soil sample and, from its results, the SWCC of the sample could be defined via numerical simulation. This is one of the main contributions of this research, given it could simplify the tests made in laboratory for hydraulic behavior analysis of bimodal samples.

6.3 SUMMARY

In Chapter 6, the results of the simulations previewed for the verification of the proposed numerical model are presented and discussed.

At first, the Stage 2a of simulations was conducted for verification of validity the model for accurately representing the hydraulic behavior of a bimodal medium.

The definition of the parameters of the theoretical bimodal soil sample was the first step (shown in Section 6.1.1). The SWCC for the entire theoretical sample was determined, and from the capillary pressure data, the diameter of the pores of the sample was defined. Then, the PSD curve was delineated and from its data, the intrinsic permeability and the porosity of the macroscale and the microscale portion of the sample were determined.

These primary data were used as input for the homogenization parameter sensitivity analysis made for the theoretical bimodal soil sample. The homogenization parameter was defined based on the equivalent hydraulic conductivity value of the entire sample with the simulation of a permeability test, as shown in Section 6.1.2. The order of magnitude of the homogenization parameter ε calculated and the one determined via numerical simulation is the same, assessing that the numerical model should be appropriate for the research proposal.

Then, the parametric analyses for drying and wetting trajectories simulations were performed as shown in Section 6.1.3. The degree of saturation of each scale and the capillary pressure were evaluated so as to assess the hydraulic behavior of the sample when subjected to drying and to wetting trajectories. A sensitivity analyses was made for the natural boundary condition used as reference for the outlet/inlet of wetting fluid for drying/wetting the sample, respectively. After defining the appropriate value of this boundary condition, the simulations of the drying and wetting tests were conducted.

Using the results of the simulations as input, a methodology of calculation for the degree of saturation of the entire soil sample was suggested using the MIP technique as basis. To summarize, the PSD curve was used as input data and the results achieved from this procedure were accurate enough to point it out as one of the major contributions of the present research. The effect of each scale for the overall hydraulic behavior of the sample is remarkable and it is specifically addressed with the proposed mathematical model for both simulation and verification of results. It proves the multiscale approach is interesting for the development of hydraulic models for multiscale porous medium, such as bimodal soils.

Finally, the last set of simulations for the theoretical bimodal soil sample was conducted, with sensitivity analyses for the parameters of the SWCC. The residual degree of saturation and the parameters *a* and *n* of the curve were varied for macro and microscale so as to assess their influence on each scale and the overall hydraulic behavior of the sample.

It was inferred from the results that each scale is affected by the parameters specifically related to it, with minimal influence of the parameters of the other scale on its particular

hydraulic behavior. This justifies once more the significance of using multiscale hydraulic models to accurately assess the behavior of multiscale porous media such as bimodal soils.

Also, it was noticed that the parameters evaluated in this stage of the research could significantly affect the hydraulic behavior of the medium. This indicates that the accuracy in the determination of the input data for the numerical simulation is of paramount importance.

The Stage 2b of simulations was then performed with the purpose of verifying the accuracy of the model when comparing the numerical results to the ones achieved by Otálvaro (2013) with laboratory tests performed in bimodal soil samples. The referred tests provided the data used for simulation. Following the procedure used for the theoretical bimodal soil sample, the hydraulic behavior of the PN28 and the NP24 samples of Otálvaro (2013) were studied with the homogenization parameter sensitivity analysis and drying and wetting trajectories simulations.

In the homogenization parameter sensitivity analysis, the order of magnitude of the calculated and the value of ε achieved with the set of simulations is the same, proving the model to be appropriate for hydraulic behavior prediction of the bimodal media.

Then, the drying and wetting trajectories simulations were performed. The results achieved with the numerical simulations made it possible to reproduce the SWCC of the PN28 and NP24 soil samples obtained by Otálvaro (2013) using the MIP test results as input data. This proves it is possible to retrieve the hydraulic properties and characteristics of the bimodal medium using the distribution of pores as reference for the definition of input data for the numerical model. This methodology is innovative in terms of assessing flow and storage conditions of the medium considering the influence of macro and microscale retrieved from the MIP test.

7 CONCLUSIONS AND SUGGESTIONS FOR FURTHER RESEARCH

The main goal of the present research was to evaluate the hydraulic behavior of multiscale porous media. For that matter, a mathematical model was proposed for the consideration of the different scales that can be observed in tropical soils, with a bimodal pattern of pore size distribution, and fractured rocks, with a solid matrix and well-defined pattern of fractures within the geologic formation.

In this mathematical model, the main concern was to properly represent the definition of scales of the medium; it was assumed that in each scale, fluid flow and storage may take place, and, therefore, the conservation of mass of each scale should be represented.

The definition of the flow equation for each scale implies on the necessity of a coupling term, physically representing the transfer of mass between scales. This term is mathematically described in the proposed formulation and its influence on the overall hydraulic behavior of the medium is the main topic of research of this thesis, being the main contribution presented here for multiscale mathematical approach models when verifying its application to bimodal soil samples.

It is important to emphasize that the referred flow conditions are defined with an adaptation of the boundary condition of the microscale, transforming it into the mass transferred to the macroscale fluid flow. Therewith, it is not necessary to address the microscale boundary conditions of flow, being the conditions restrictedly employed for the macroscale flow equation.

At the same time, for the appropriate description of the phenomenon, it is important to guarantee that the macro and microscale flow equations are in the same scale for evaluation of the overall hydraulic behavior of the medium. Therewith, an upscaling procedure is employed, with the adjustment of the differentiation operator of the microscale flow equation. A homogenization parameter ε is used as a mathematical tool to transform the small scale terms and make the equations appropriate for the evaluation of the overall flow and storage conditions of the studied medium. After the adapted homogenization procedure, the equations are in the same scale and can finally be used for simulation.

Firstly, the simulations were made for a theoretical bimodal soil sample. The main goal with this step was to assess the accuracy of the model. A permeability test was carried out for the calibration of the homogenization parameter ε. Then, drying and wetting trajectory tests

were performed, so as to verify the extent of the limits of the model in terms of reproducing what can be observed experimentally in typical bimodal soil samples. Finally, sensitivity analyses were made for the parameters of the soil-water characteristic curve of the sample for each scale of the model.

The accuracy of the model was assessed; the performed numerical simulations adequately suited the objectives of this stage of the research. It was possible to verify the influence of the microstructure in the overall hydraulic behavior of the medium, guaranteeing that the model is appropriate for reproduction of some particularities of hydraulic behavior of multiscale media.

Also, it is important to highlight that the transfer term works as an inlet/outlet term in both equations, and implies on fluid being transferred from the microscale to the macroscale. This is proven by the fact that, in the studied case, most of the wetting fluid is stored within the micropores of the sample, and it influences significantly the overall hydraulic behavior of the medium.

Finally, the degree of influence of each parameter of the SWCC was assessed and it was verified that the variation of the parameters on each scale affects most significantly the hydraulic behavior tendency of the referred scale, with small influence on the other scale.

Then, the model was used for retro analyses of the experimental research made by Otálvaro (2013). Three sets of numerical simulations were carried out for two soil samples, PN28 and NP24: permeability tests for the calibration of the homogenization parameter ε, drying and wetting trajectory tests.

It was possible to retrieve the data from the MIP test and use it as input for the numerical model. The porosity and the permeability of each scale are calculated from the MIP test results provided by Otálvaro (2013). Then, the drying and wetting trajectories simulations are carried out and their results are used for prediction of the SWCC of the sample.

From these results, a methodology for calculation of the degree of saturation of the sample was proposed. The final degree of saturation of the macro and microscale, after drying or wetting the sample, are used for the definition of the final degree of saturation of the entire sample. The values of degree of saturation of the entire sample in each stage of the drying and wetting tests, combined to the final value of capillary pressure of the sample, are used for the determination of the SWCC of the entire soil sample. It was verified that the numerical results match the SWCC experimentally found by Otálvaro (2013).

This is one of the main contributions of this research. With the proposed mathematical model, it was possible to reproduce the hydraulic behavior of the bimodal medium, and accurately define the SWCC from MIP test results. In terms of application of these results, the laboratory tests performed in bimodal samples could be optimized, with only testing the sample with the MIP procedure and using its data for the prediction of the SWCC via numerical simulation.

The formulation here presented was tested extensively for bimodal soil hydraulic behavior verification; nonetheless, its generic approach is addressed. With proper adaptation of the homogenization parameter, this model could be adopted for fractured media, as mentioned and mathematically shown. This is highlighted as one of its advantages, being pointed out as one of the contributions of the present research.

7.1 RECOMMENDATION FOR FURTHER RESEARCH

Some aspects have not been studied during this research and are suggested as themes for future work. This includes some themes which are beyond the scope of research of this doctoral thesis and some difficulties faced during the development of the stages of this study. The suggestions made for further research are believed to being appropriate to contribute to the improvement of the results achieved with the model proposed in this doctoral thesis.

These suggestions are:

- Adapt the parameter *s* of the transfer term of the flow equations for the generalization of the geometry of the medium;
- Test anisotropic conditions of flow for the macroscale, so as to assess different geometric patterns for fractured media;
- Adapt the conditions of transfer of mass of the microscale to the macroscale, with changes to the boundary conditions of the microscale, and, therefore, of the entire studied porous medium;
- Consider thermodynamic condition for the study of fluid flow, improving the boundary conditions implemented for the solution of the problem; and,
- Implement different mechanical constitutive models for the study of hydromechanical behavior of the macro and microstructure of the sample.

REFERENCES

Alonso, E.E, Gens, A., Josa, A. (1990). A constitutive model for partly saturated soil. *Géotechnique.*Vol. 40(3): 405-430.

Alonso, E. E., Pinyol, N. M., Gens, A. (2013). Compacted soil behaviour: initial state, structure and constitutive modelling. *Géotechnique*. Vol. 63 (6): 463-478.

Alonso, E. E.; Romero, E., Hoffmann, C. (2011). Hydromechanical behaviour of compacted granular expansive mixtures: experimental and constitutive study. *Géotechnique*. Vol. 61 (4):329-344.

Alonso, E. E. , Vaunat, J. Gens , A. (1999). Modelling the mechanical behavior of expansive clays. *Engineering Geology*. Vol. 54 (199): 173-183.

Auriault, J.-L., Boutin, C., Geindreau, C. (2009). Homogenization of coupled phenomena in heterogeneous media. ISTE Ltd., London, UK. 476 p.

Arbogast, T. (1992). Gravitational forces in dual-porosity systems – I. Model derivation by homogenization. *Transport in Porous Media*. Vol. 13: 179-203.

Arbogast, T., Douglas Jr., J., Hornung, U. (1990). Derivation of the double porosity model of single phase flow via homogenization theory. *SIAM Journal of Mathematical Analysis*. Vol. 21, n. 4: 823-836.

Arson, C. & Pereira , J-M. (2013). Influence of damage on pore size distribution and permeability of rocks. *International Journal for Numerical and Analytical Methods in Geomechanics*. Vol. 37: 810-831.

Baca, R. G., Arnett, R. C., Langford, C. W. (1984). Modeling of fluid flow in fractured-porous rock masses by finite-element techniques. *International journal for numerical methods in fluids*. Vol. 4: 337-348.

Bagherieh, A. R., Khalili, N., Habibagahi, G., Ghahramani, A. (2009). Drying response and effective stress in a double porosity aggregated soil. *Engineering Geology*. Vol. 105: 44-50.

Bai, M., Elsworth, D., Roegiers, J.-C. (1993). Multiporosity/multipermeability approach to the simulations of naturally fractured reservoirs. *Water resources research*. Vol. 29, n. 6: 1621-1633.

Barenblatt, G. I. & Zheltov, Y. P. (1960). Basic flow equations of homogeneous fluids in fissured rocks. *Akademiia nauk SSSR*. Vol. 132: 545-548.

Bear, J. (1993). *Modeling flow and contaminant transport in fractured rocks*. In: Bear, J., Tsang, C.-F., Marsily, G. de. *Flow and contaminant transport in fractured rock*. Academic Press Inc., 1st ed. 1-37.

Beavis, F. C. (1985). *Engineering geology*. Blackwell scientific publications, 1st ed. 231 p.

Belytschko, T. & Black, T. (1999). Elastic crack growth in finite elements with minimal remeshing. *International Journal for numerical methods in engineering*. Vol. 45: 601-620.

Bensoussan, A., Lions, J.-L., Papanicolaou, G. (1978). *Asymptotic analysis for periodic structures – studies in mathematics and its applications*. North-Holland Publishing Company, Amsterdam, Holland. 700 p.

Biot, M. A. (1941). General theory of three-dimensional consolidation. Journal of Applied Physics. Vol. 12: 155-164.

Buenfil, C.M.B. (2007). *Caracterización Experimental del Comportamiento Hidromecánico de uma Arcilla Compactada*. Tese de doutorado, Departamento de Engenharia de Terreno e Cartografia, Universidade Politécnica da Catalunia, Barcelona, 466 p.

Borbiaux, B., Basquet, R., Daniel, J. M., Hu, L. Y., Jenni, S., Lange, A., Rasolofosaon, P. (2005). Fractured reservoirs modelling: a review of the challenges and some recent solutions. *EAGE, first break*. Vol. 23: 33-40.

Borges, C. R. (2014). *Estudo microestrutural do comportamento hidromecânico do solo de Brasília – DF*. Tese de Doutorado, Publicação G.TD-102/14, Departamento de Eng. Civil e Ambiental, Universidade de Brasília, Brasília, DF, 112 p.

Carter, M. & Bentley, S. P. (1991). *Correlations of Soil Properties.* Pentech Press, London, UK. 130 p.

Castro, A. O. S. (2004). *Seleção de poços de petróleo para operação de fraturamento hidráulico: uma abordagem comparativa entre sistemas fuzzy-genético e neuro-fuzzy*. Tese de Doutorado, Programa de Engenharia de Produção, Universidade Federal do Rio de Janeiro, COPPE, Rio de Janeiro, RJ. 172 p.

Chen, Z., Huan, G., Ma, Y. (2006). *Computational methods for multiphase flow in porous media*. SIAM, Computational & Science Engineering. 549 p.

Chen, Z. (2013). Implementation of the XFEM for hydraulic fracture problems. *Proceedings of the 13th International Conference on Fracture*. Beijing, China, 1-10.

Choo, J., White, J. A., Borja, R. I. (2016). Hydromechanical Modeling of Unsaturated Flow in Double Porosity Media. *International Journal of Geomechanics*. Vol. 16, n. 6. 18 p.

Dake, L. P. (1978). *Fundamentals of reservoir engineering*. Elsevier Inc., The Hague, Netherlands, 1st ed. 437 p.

Daux, C., Moës, N., Dolbow, J., Sukumar, N., Belytschko, T. (2000). Arbitrary branched and intersecting cracks with the extended finite element method. *International Journal for numerical methods in engineering*. Vol. 48: 1741-1760.

Delgado, A. K. C. (2002). *Influência da sucção no comportamento de um perfil de solo tropical compactado*. Dissertação de Mestrado, Publicação G.DM-093A/02, Departamento de Eng. Civil e Ambiental, Universidade de Brasília, Brasília, DF, 200p.

Delage, P., Audiguier M., Cui, Y. J., Howatt, M. D. (1996). Microstructure of a compacted silt. *Canadian Geotechnique Journal*. Vol. 33: 150-158.

Delage, P. & Lefebvre, G. (1984). Study of the structure of a sensitive Champlain clay and of its evolution during consolidation. *Canadian Geotechnical Journal*. Vol. 21: 21-35.

Diamond, S. (1970). Pore size distributions in clays. *Clays and Clay Minerals*. Vol. 18: 7-23.

Diodato, D. M. (1994). *A compendium of fracture flow models*. Center for environmental restoration systems, energy systems division, Argonne National Laboratory. 88 p.

Duarte, C. A. (2014). Recent developments in the generalized finite element method for 3-D hydraulic fracture propagation and interactions. *Workshop on computational geomechanics*. University of Pittsburg. 46 f.

Feuerharmel, C., Gehling, W., Bica, A. (2006). The Use of Filter-Paper and Suction-Plate Methods for Determining the Soil-Water Characteristic Curve of Undisturbed Colluvium Soils. *Geotechnical Testing Journal*. Vol. 29, n. 5: 419-425.

Fredlund, D G. & Rahardjo, H. (1993). *Soil Mechanics for Unsaturated Soils*. John Wiley & Sons, Inc., Hoboken, New Jersey, United States of America. 544 p.

FlexPDE (2006). *FlexPDE Samples*. Available in: FlexPDE 5.0.9.

Franciss, F. O. (2010). *Fractured Rock Hydraulics*. Taylor & Francis, London, UK. 179 p.

Garcia-Bengochea, I., Lovell, C. W., Altschaeffl, A. G. (1979). Pore distribution and permeability of silty clays. *Journal of Geotechnical and Engeneering Division*. VOl. 105(GT7): 839-856.

Gordeliy, E. & Peirce, A. (2012). Coupling schemes for modeling hydraulic fracture propagation using the XFEM. *Computational methods in applied mechanics and engineering*. Vol. 253: 305-322.

Gong, B. (2007). *Effective models of fractured systems*. Doctorate dissertation. Department of energy resources engineering. Standford University. 151 p.

Griffiths, F. J. & Joshi, R. C. (1989). Changes in pore size distribution due to consolidation of clays. *Géotechnique*. Vol. 39 (1): 159-167.

Grigarten, E. (1998). Fracnet: stochastic simulation of fractures in layered systems. *Computer & Geosciences*. Vol. 24, n. 8: 729-736.

Guimarães, R. C. (2002). *Análise das Propriedades e Comportamento de um Perfil de Solo Laterítico Aplicada ao Estudo do Desempenho de Estacas Escavadas*. Dissertação de Mestrado, Publicação G.DM-090A/02, Departamento de Eng. Civil e Ambiental, Universidade de Brasília, Brasília, DF, 183p.

King, H. (2014). *Geoscience news and information – Shale*. Available in: http://geology. com/rocks/shale.shtml

Hoek, E. & Brown, E.T. (1997). Practical estimates of rock mass strength. *International journal of rock mechanics and mining sciences*. Vol. 34, n. 8: 1165-1186.

Juanes, R., Samper, J., Molinero, J. (2002). A general and efficient formulation of fractures and boundary conditions in the finite element method. *International Journal for numerical methods in engineering*. Vol. 54: 1751-1774.

Jung, J., Ahmad, J., Kanniken, M. F. (1981). Finite element analysis of dynamic crack propagation. *Failure prevention and reliability conference*. Hartford, Connecticut. 22 p.

Kazemi, H., Merill Jr., L. S., Porterfield, K. L., Zeman, P. R. (1976). Numerical simulation of water-oil flow in naturally fractured reservoirs. *Society of Petroleum Engineers Journal*. SPE 5719, vol. 16, n. 06: 317-326.

Khristianovic, S. A. & Zheltov, Y. P. (1955). Formation of vertical fractures by means of highly viscous fluids. *Proceedings of the 4th World Petroleum Congress*. Vol. 2: 579-586.

Koliji, A., Vulliet, L., Laloui L. (2010). Structural characterization of unsatured aggregated soil. *Canadian Geotechnique Journal*. Vol. 47: 297-311.

Kosugi, K. & Hopmans, J. W. (1998). Scaling Water Retention Curves for Soils with Lognormal Pore-Size Distribution. *Soil Science Society of America Journal*. Vol. 62: 1496-1505.

Lemonier, P. & Borbiaux, B. (2010). Simulation of Naturally Fractured Reservoirs - State of the Art - Part 2 - Matrix-Fracture Transfers and Typical Features of Numerical Studies. Oil & Gas Science and Technology – Rev. IFP. Vol. 65, n. 2: 263-286.

Mascarenha, M. M. A. (2008). *Influência da microestrutura no comportamento hidromecânico de uma argila siltosa não saturada incluindo pequenas deformações*. Tese de Doutorado, Publicação G.TD-056/08, Departamento de Eng. Civil e Ambiental, Universidade de Brasília, Brasília, DF, 158 p.

Matthai, S. K., Mezentsev, A., Belayneh, M. (2005). Control-volume finite-element two-phase flow experiments with fractured rock represented by unstructured 3D hybrid meshes. *Proceedings of the SPE Reservoir Simulation Symposium*. SPE 93341.

Mitchell, J. K. & Soga, K. (2005). *Fundamentals of Soil Behavior*. John Wiley & Sons, Inc., Hoboken, New Jersey, United States of America. 3rd ed. 592 p.

Moës, N., Gravouil, A., Belytschko, T. (2002). Non-planar 3D crack growth by the extended finite element and level sets – Part I: Mechanical Model. *International Journal for numerical methods in engineering*. Vol. 53: 2549-2568.

Nelson, R. (2001). *Geologic analysis of naturally fractured reservoirs*. Gulf Professional Publishing, 2nd ed. 352 p.

Nordgren, R. P. (1972). Propagation of a vertical hydraulic fracture. *Society of Petroleum Engineers Journal*. SPE 3009-PA, vol. 12, n. 4: 306-314.

Olson, J. E. (1993). Joint pattern development: effects of subcritical crack growth and mechanical crack interaction. *Journal of geophysical research*. Vol. 98, n. B7: 12251-12265.

Otálvaro, I. F. (2013). *Comportamento hidromecânico de um solo tropical compactado*. Tese de Doutorado, Publicação G.TD-082/13, Departamento de Eng. Civil e Ambiental, Universidade de Brasília, Brasília, DF, 122 p.

Otálvaro, I. F., Cordão Neto, M. P., Delage, P., Caicedo, B. (2016). Relationship between soil structure and water retention properties in a residual compacted soil. *Engineering Geology*, Vol. 205: 73-80.

Palmer, I. D. & Carroll, H. B. (1982). Three-dimensional hydraulic fracture propagation in the presence of stress variation. *Proceedings of the SPE/DOE/GRI unconventional gas recovery symposium*. SPE/DOE10849. p. 870-878.

Penumadu, D. & Dean, J. (2000). Compressibility effect in evaluating the pore-size distribution of kaolin clay using mercury intrusion porosimetry. *Canadian Geotechnical Journal*. Vol. 37: 393-405.

Pereira, J-M. & Arson, C. (2013). Retention and permeability properties of damaged porous rocks. *Computers and Geotechnics*. Vol. 48: 272-282.

Perkins, T. K. & Kern, L. R. (1961). Widths of Hydraulic Fractures. *Journal of Petroleum Technology*. Vol. 13, n. 9: 937-949.

Prapaharan, S., Altschaeffl, A. G., Dempsey, B. J. (1985). Moisture curve of a compacted clay: mercury intrusion method. *Journal of Geotechnical Engineering*. Vol. 111(9): 1139-1143.

Riley, M. S. (2004). An algorithm for generating rock fracture patterns: mathematical analysis. *Mathematical geology*. Vol. 36, n. 6:683-702.

Romero, E. (1999). *Characterisation and Thermo Hydro-mechanical Behaviour of Unsaturated Boom Clay: An Experimental Study*. Tese de Doutorado, Departamento de Engenharia de Terreno e Cartografia, Universidade Politécnica da Catalunia, Barcelona. 405 p.

Romero, E. & Simms, P. H. (2008). Microstructure Investigation in Unsaturated Soils: A Review with Special Attention to Contribution of Mercury Intrusion Porosimetry and Environmental Scanning Electron Microscopy. *Geotechnical and Geological Engineering.* Vol. 26(6): 705-727.

Romero, E., Vecchia, G. D., Jommi, C. (2011). An insight into the water retention properties of compacted clayey soils. *Géotechnique*. Vol. 61 (4): 313-328.

Rosa, A. J., Carvalho, R. de S., Xavier, J. A. D. (2006). *Engenharia de reservatórios de petróleo*. Interciência, 1 ed. 808 p.

Sabathier J.C., Bourbiaux B., Cacas M.C., Sarda S. (1998). A New Approach of Fractured Reservoirs. *Society of Petroleum Engineers International Petroleum Conference and Exhibition*. Paper SPE 39825. Villahermosa, Mexico, March 3-5.

Salimi, H. (2010). *Physical aspects in upscaling of fractured reservoirs and improved oil recovery prediction*. Doctorate thesis. Faculty of Civil Engineering and Geosciences, Section of Petroleum Engineering, Delft University of Technology.

Settari, A. & Cleary, M. P. (1986). Development and testing of a pseudo-three-dimensional model of hydraulic fracture geometry. *SPE Production Engineering*. p. 449-466.

Silva, J. P. (2007). *Estudos Preliminares para Implantação de Trincheiras de Infiltração*. Dissertação de Mestrado, Publicação G.DM - 154 /07, Departamento de Eng. Civil e Ambiental, Universidade de Brasília, Brasília, DF, 155p.

Silva, M. T. M. G. (2009). *Metologia para Determinação de Parâmetros para Solos não Saturados Utilizando Ensaios com Umidade Conhecida*. Dissertação de Mestrado, Publicação G.DM - 182/09, Departamento de Eng. Civil e Ambiental, Universidade de Brasília, Brasília, DF, 98 p.

Simms, P. H. & Yanful, E. K. (2001). Measurement and estimation of pore shrinkage and pore distribution in a clayey till during soil-water characteristic curve tests. *Canadian Geotechnical Journal*. Vol. 38: 741-754.

Simms, P. H. & Yanful, E. K. (2002). Predicting soil-water characteristic curves of compacted plastic soils from measured pore-size distributions. *Géotechnique*. Vol. 52 (4): 269-278.

Simms, P. H. & Yanful, E. K. (2004). A discussion of the application of mercury intrusion porosimetry for the investigation of soils, including an evaluation of its use to estimate volume change in compacted clayey soils. *Géotechnique.* Vol. 54 (6): 421-426.

Simunek, J., Jarvis, N. J., van Genuchten, M. Th., Gardenas, A. (2003). Review and comparison of models for describing non-equilibrium and preferential flow and transport in the vadose zone. *Journal of Hydrology*. Vol. 272: 14-35.

Sivakumar, V., Sivakumar, R., Boyd, J., Mackinnon, P. (2010). Mechanical behaviour of unsaturated kaolin (with isotropic and anisotropic stress history). Part 1: wetting and compression behaviour. *Géotechnique*. Vol. 60 (8): 581-594.

Stephenson, M. (2013). Shale gas: BGS research. *British Geological Survey*. 2 p.

Sukumar, N., Moës, N., Moran, B., Belytschko, T. (2000). Extended finite element method for three-dimensional crack modeling. *International Journal for numerical methods in engineering*. Vol. 48: 1549-1570.

Szymkiewicz, A. (2013). *Modelling water flow in unsaturated porous media - Accouting for nonlinear permeability and material heterogeneity*. Springer, Berlin, Germany. 237 p.

Thomas, L. K., Dixon, T. N., Pierson, R. G. (1983). Fractured reservoir simulation. *Society of Petroleum Engineers Journal*. SPE 9305, vol. 23: 42-54.

Uleberg, K. & Kleppe, J. (1996). Dual porosity, dual permeability formulation for fractured reservoir. *Presented at the Norwegian University of Science and Technology (NTNU), Trondheim RUTH Seminar, Stavanger*.

van Genuchten, M. T. (1980). A closed-form equation for predicting the hydraulic conductivity of unsaturated soils. *Soil Science Society of America Journal*, Vol. 44: 892-898.

Vargas, C. A. L. (2001). *Modelo probabilístico de distribuição tridimensional de descontinuidades em maciços rochosos fraturados*. Tese de Doutorado, Publicação G.TD-008A/01, Departamento de Eng. Civil e Ambiental, Universidade de Brasília, Brasília, DF, 253 p.

Warren, J. E. & Root, P. J. (1963). The behavior of naturally fractured reservoirs. *Society of Petroleum Engineers Journal*. Vol. 3: 245-255.

Weber, N., Siebert, P., Willbrand, K., Feinendegen, M., Clauser, C., Fries, T. P. (2013). *Chapter 35 - The XFEM with an explicit-implicit crack description for hydraulic fracture problems*. In: Bunger, A. P., McLennan, J., Jeffrey, R. *Effective and suistanable hydraulic fracturing*. InTech, 1st ed. 711-724.

Zhang, X. & Sanderson, D. (2002). *Numerical modeling and analysis of fluid flow and deformation of fractured rock masses*. Elsevier Science, Oxford.

Zhang, B., Liu, W. I., Liu, X. (2006). Scale-dependent nature of the surface fractal dimension for bi- and multi-disperse porous solids by mercury porosimetry. *Applied Surface Science*. Vol. 253:1349-1355.